THE CROSS-SHORE DISTRIBUTION OF GRAIN SIZE IN THE LONGSHORE TRANSPORT ZONE

by

CHRISTOPH SOLTAU

A thesis submitted in fulfilment of the requirements for
the degree of

MASTER OF SCIENCE

DEPARTMENT OF CIVIL ENGINEERING
UNIVERSITY OF STELLENBOSCH

Supervisor: D.E. Bosman

December 2009

Declaration

By submitting this work electronically, I declare that the work contained therein is my own, original work, that I am the owner of the copyright thereof (unless to the extent explicitly otherwise stated) and that I have not previously in its entirety or in part submitted it for obtaining any qualification.

Abstract

Calculation of longshore sediment transport rates is a typical part of coastal engineering work. One of the important inputs to such calculations is the sediment grain size. A single, representative grain size is typically required. The inter-tidal beach is the most convenient and common area from which grain size data can be obtained. Yet only a fraction of the longshore transport occurs at the beach, with the bulk of the transport occurring in the surf zone, where sampling is difficult. Sediment transport calculations can be improved if the representative grains size is also characteristic of this area. A better understanding how the grain size in the longshore transport zone compares to the beach grain size is required.

A review of relevant literature indicates that limited attention has been given to quantifying the grain size in the longshore transport zone. No previous investigations were found that tried to link the longshore transport zone grain size to that found on the beach. A comprehensive analysis of beach and longshore transport zone grain sizes was therefore undertaken and is described in this thesis.

Beach grain sizes were compared to those in the longshore transport zone for three different locations around the world: Published grains size information, together with detailed wave and profile data, was obtained from the US Army Field Research Facility at Duck; a second data set was obtained from measurements done at Bogenfels in Namibia; a third dataset was compiled from sampling undertaken by the author in Table Bay, South Africa. A total of 189 samples were collected at four sampling lines in Table Bay between September 2005 and September 2006. Samples were collected across the entire profile from the primary dune to a water depth of 10 m. Samples were collected by grab in the offshore, and by swimming and diving in the surf zone. The location of the four Table Bay sampling lines was chosen so as to obtain data from beaches with different wave and grain size characteristics. Together with the Duck and Bogenfels data, data from six different beaches was therefore available for study.

A settling tube was used to determine the grain sizes. Verification of the settling tube analyses against conventional sieving indicated a good comparison. However, the settling tube proved unsuitable for processing of samples with coarse to very coarse material, for which sieving was conducted instead.

The grain size at the mid-tide level has been used to characterise the beach. The limits of the longshore transport zone were defined by calculating the cross-shore distribution of longshore transport with the Unibest model. Simpler methods, such as the depth of closure, either overestimated or underestimated it, depending on which wave condition was used in the depth of closure formula.

It was found that the beaches with steeper mid-tide beach slopes, such as Bogenfels and northern Table Bay, had coarser median grain sizes than more gently sloping beaches such as found in the south of Table Bay. On energetic beaches, the mid-tide beach grain sizes were significantly coarser than those in the surf zone, by more than twice. At less exposed locations, such as Duck and the central Table Bay beaches, this difference was less. At sheltered locations, such as the southern sampling lines in Table Bay, the mid-tide beach grain sizes are virtually the same as those found in the surf zone. The surf similarity parameter was used to compare the characteristics of the different sites. This parameter was defined using the average wave height seaward of breaking, and the mid-tide beach slope. The ratio between the longshore transport zone grain size and the mid-tide beach grain size was found to be similar to the inverse of the surf similarity parameter for the six beaches that were studied.

These findings have led to an improved understanding of the grain size in the longshore transport zone and allow a better characterisation of the representative grain size to use for sediment transport calculations.

Opsomming

In kusingenieurswese word langstrandse sedimentvervoer (langsvervoer) gereeld bereken. Belangrike invoer vir sulke berekeninge is die verteenwordigende korrelgrootte van die sand. Die sandkorrelgrootte van die benatte strand is die maklikste om te bepaal, al vind net ‘n klein gedeelte van die langsvervoer op die benatte strand plaas. Die grootste gedeelte van die langsvervoer kom in die brandersone voor, waar dit moeilik is om monsters te neem. Sedimentvervoerberekeninge kan verbeter word as die korrelgrootte ook hierdie sone verteenwoordig. Dit is dus van belang om te verstaan hoe die korrelgrootte van die benatte strand met die gemiddelde korrelgrootte oor die algehele langsvervoersone vergelyk.

‘n Literatuursoektog dui aan dat min aandag al gegee is aan hoe die korrelgrootte op die benatte strand met dié in die langsvervoersone vergelyk. ‘n Ontleding van sandkorrelgroottes op die benatte strand en in die langsvervoersone is dus onderneem en word in die tesis uiteengesit.

Strandkorrelgroottes word met dié in die langsvervoersone vergelyk vir drie verskillende gebiede in die wereld : (1) Gepubliseerde data oor korrelgroottes, sowel as strandhellings en golwe, is van die Field Research Facility by Duck in die VSA verkry ; (2) ‘n tweede stel data is van opmetings by Bogenfels in Namibie verkry; (3) die derde stel data is saamgestel deur die skrywer tydens opmetings in Tafelbaai, Suid-Afrika. ‘n Totaal van 189 monsters is tussen September 2005 en September 2006 by vier verskillende opmetingslyne in Tafelbaai geneem. Monsters is geneem van die duin tot in 10 m waterdiepte. In dieper water is grypmonsters geneem, terwyl dié in the brandersone verkry is deur te duik. Die posisie van die vier Tafelbaaise opmetingslyne is gekies om strande met verskillende golftoestande en korrelgroottes te dek. Tesame met die data van Duck en Bogenfels is dus ses datastelle vir ontleding beskikbaar.

‘n Valbuis is gebruik om die korrelgroottes te bepaal. Die valbuismetode het goed met gewone sifresultate vergelyk, behalwe vir monsters met baie growwe korrels. Hiervoor is sifwerk gebruik.

Die korrelgrootte van die benatte strand is gebruik om die strand te karakteriseer. Die grense van die langsvervoersone is bepaal deur die dwarsstrandse verdeling van die langsvervoer met die Unibest-model te bereken. Eenvoudiger metodes, soos die berekening van die sluitingsdiepte, het minder betroubare resultate gelewer.

Daar is gevind dat steiler benatte strande, soos Bogenfels en Noord-Tafelbaai se strande, groter gemiddelde korrelgroottes as platter benatte strande, soos dié in suidelike Tafelbaai, het. Op blootgestelde strande is die benatte strand se korrelgrootte tot meer as twee keer groter as dié in die brandersone. By gedeeltelik beskutte strande, soos Duck en Sentraal-Tafelbaai se strande, was die verskil minder. Op beskutte strande, soos die Suid-Tafelbaai se strande, is gevind dat die benatte strand se korrelgrootte amper dieselfde as dié in die brandersone is. Die brandergelyksoortigheidsfaktor is gebruik om die verskillende strande te vergelyk. Die golfhoogtes net buite die branderlyn en die benatte strandhelling is gebruik om die veranderlike te bereken. Daar is gevind dat by die ses strande wat ondersoek is, die verhouding van die korrelgrootte in die langsvervoersone en dié van die benatte strand ongeveer gelyk aan die omgekeerde brandergelyksoortigheidsfaktor is.

Die bevindings het tot ‘n beter begrip van die wisseling van die korrelgroottes in die langsvervoersone gelei. Gevolglik kan ‘n akkurater verteenwoordigende sandkorrelgrootte bepaal word.

Acknowledgments

This thesis has been a long time in the making. It has weathered the tests of a growing family, career changes and alternating bursts of enthusiasm and lack of motivation. I wish to thank my supervisor, Mr Eddie Bosman, for maintaining the belief that I would finish, and for his constructive comments on draft manuscripts. I am also grateful to a number of ex-colleagues at the CSIR who, through their humble encouragement, made me believe that it was a possible task.

On a less esoteric level, I appreciated the assistance of Mr Alistair Adonis and Mr Warren Joubert during the field sampling in Table Bay. This was undoubtedly the most enjoyable part of this study. I am also indebted to Mr Godfrey Moses, who helped me work through a mass of samples by conducted selected sieving analyses.

Mr Don Stauble provided an initial impetus for this thesis when he kindly sent me a copy of his analyses of the Duck data, for which I am grateful. I also wish to acknowledge the US Army Corps of Engineers Field Research Facility at Duck, who make all their information and data available on the internet. Namdeb Diamond Corporation are acknowledged for providing the data from Bogenfels.

CONTENTS

FIGURES

TABLES

APPENDICES

Appendix 1: Soltau, C., 2005. Towards Predicting Nearshore Grain Size. Proceedings of Fifth International Conference on Coastal Dynamics, Barcelona, Spain. ASCE. 2005.

Appendix 2: Grain Size Data from Bogenfels Beach.

Appendix 3: Grain Size Data Collected in Table Bay.

Chapter 1: Introduction

1.1 Background

Longshore sediment transport is one of the dominant processes along a sandy coastline. Waves approaching the shoreline at an oblique angle generate an alongshore directed current. The breaking action of the waves causes sediment to be suspended which can then be transported by this current. Fine particles can be suspended from the seabed more readily than coarse ones, leading to higher transport rates for finer sediment under the same wave breaking conditions.

This effect of particle size on longshore transport rate has long been recognised and incorporated into the equations that coastal engineers use to calculate longshore transport rates. This can be seen in the following simplified equation for longshore sand transport proposed by Van Rijn (2002):

$$Q_{t,mass} = K_o \, K_{swell} \, K_{grain} \, K_{slope} \, (H_{s,br})^{2.5} \, V_{eff,L} \qquad (1.1)$$

Where: $Q_{t,mass}$ = longshore sand transport (in kg/s, dry mass);

K_o = a dimensionless coefficient (Van Rijn suggests a value of 42);

K_{swell} = correction factor for swell waves;

K_{grain} = particle size correction factor = $D_{50,ref}/D_{50}$, where $D_{50\ is}$ the median grain size and $D_{50,ref}$ is a reference size = 0.2 mm;

K_{slope} = $(\tan_b/\tan_{bref})^{0.5}$ is a bed slope correction factor, where $\tan_b$ is the actual bed slope and $\tan_{bref}$ is a reference slope = 0.01;

$H_{s,br}$ = significant wave height at breaking (in m);

$V_{eff,L}$ = effective, tidal and wave-induced) longshore velocity in the middle of the surf zone (in m/s).

While a number of factors can be seen to affect the longshore transport rate, particularly the wave height at breaking, the effect of grain size is clearly present in the factor K_{grain}: in Equation 1.1, a two-fold increase of the grain size leads to a two fold *decrease* in longshore transport rate. According to Van Rijn (2002), the longshore transport rate is thus a direct function of the grain size, all other factors remaining constant. Obtaining an accurate value for the longshore transport rate clearly requires the correct grain size information.

However, providing this important input data can be difficult in practice – it may be easy to sample the grain sizes on the beach, but obtaining data from the dynamic surf zone area is difficult: On most Southern African beaches the surf zone is a region of intense wave breaking, turbulence and strong currents, making it virtually inaccessible, as illustrated in Figure 1.1 below. It will be shown in subsequent chapters that much of the longshore transport activity occurs in the surf zone.

Figure 1.1: An energetic day in the Table Bay surf zone

How would one determine the grain size from such a surf zone, and thus the longshore transport zone? Obtaining data from this zone requires much patience to wait for calm seas and/or specialised (expensive) equipment that can readily operate in this difficult environment. Frequently, coastal engineers have little to spare of either. Reliance may therefore be placed on only limited sampling, typically only the dry beach, or rough estimates of the appropriate grain size. The result is that a degree of uncertainty is introduced to longshore transport calculations and extensive calibration of transport equations may be required. This effort could be reduced if the grain size in the longshore transport zone is better understood.

In contrast to the surf zone, it is generally easy to sample the grain sizes of the inter-tidal and upper beach – samples can be collected under all but the most extreme wave and tide

conditions. If we have a better understanding of the relationship between the grain size found on the beach and that found in the longshore transport zone, is it possible to use only samples of the beach sand, together with an understanding of the beach characteristics, to give us the input information for longshore transport calculations?

Figure 1.2: The inter-tidal beach face can be sampled without getting your feet wet

Knowledge of a relation between the grain size on the dry or inter-tidal beach and that in the more active surf zone would assist coastal engineers in using the appropriate, representative grain size in the derivation of e.g. longshore transport rates.

1.2 Aim

The aim of this thesis research is to investigate the relation between the grain size in the longshore transport zone and that on the inter-tidal beach and to address the questions:

- Is such a relation the same at all beaches?
- Does it vary for beaches that have different wave energy, or have different grain sizes, or are steeper or flatter in slope?

1.3 Methodology

The approach followed in investigating these questions has been to use measured data. This required field data of sediment grain sizes of the beach and longshore transport zone. A field measurement campaign was undertaken to obtain grain size data from typical South African beaches at four sites in Table Bay, Cape Town. A further dataset was obtained from the US Army Corps of Engineers Waterways Experiment Station at Duck, USA. A third dataset was obtained from a commercial project undertaken by the author at Bogenfels, Namibia. These three datasets form the basis of this thesis work.

1.4 Thesis structure

Chapter 2 outlines and describes the background to the key concepts and definitions used in this study. These include definition of the relevant beach zones, grain size parameters and discretisation of the longshore transport area.

Existing information on the cross-shore distribution of grain sizes was researched through a literature survey, and is described in Chapter 3. The literature review includes information of use to the field sampling, such as articles on where on a beach profile the samples should be taken and what sampling techniques or equipment are commonly used. Information on methods that have been applied to predict cross-shore changes in grain size was also sought and is described.

Chapter 4 provides a description of the field measurement campaign undertaken for this thesis to obtain cross-shore grain size samples at selected locations within Table Bay. The sample processing and analysis methods are briefly described, together with details of analysis instruments and procedures.

Chapter 5 presents a comprehensive discussion and analysis of the three cross-shore grain size datasets (Table Bay, Duck and Bogenfels) that were obtained. The relation between the particle size on the beach and that in the longshore transport zone is developed for each dataset. Key findings from the data are summarised.

Conclusions and recommendations are presented in Chapter 6.

The research presented in this thesis developed from initial work presented by the author at the Coastal Dynamics 2005 conference held in Barcelona, Spain, in 2005. The conference paper is attached as Appendix 1. The grain size datasets from Bogenfels and Table Bay have not previously been published and they are therefore presented in a summarised form in Appendices 2 and 3 respectively.

Chapter 2: Definition of Relevant Beach and Nearshore Parameters and Concepts

2.1 The cross-shore profile

A beach profile represents a vertical cross-section through the beach, perpendicular to the shoreline. A schematic of the beach system is shown in Figure 2.1. Only sandy beaches are considered in this study.

Four hydrodynamic zones (Figure 2.1(a)) can be defined on the beach:

- An offshore area of deeper water, where wave shoaling occurs as waves move into shallower water;
- The breaker zone, which varies in location according to individual wave heights, the tide and bathymetry changes;
- A surf zone of variable width, consisting of broken waves/whitewater/rollers, and where waves may re-form and break again;
- The swashzone where waves run up the beach face.

Longshore currents and transport may occur from the breaker zone to the swash zone.

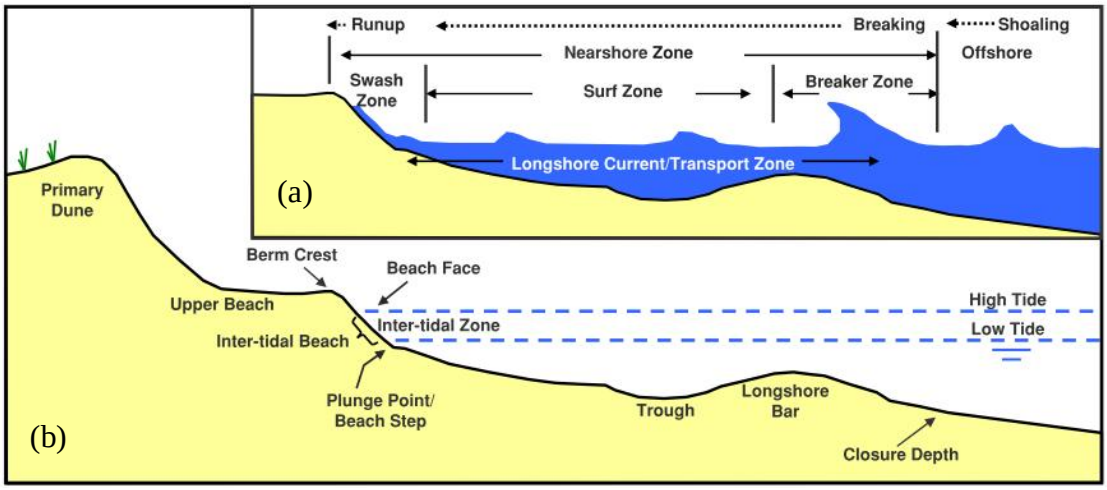

Figure 2.1: Schematic of a beach profile showing typical terms used in this study

While specific terms used to describe the different zones may vary between countries and institutions, the general separation of zones is common. The terms given in Figure 2.1 are considered fairly generic and will therefore be used in this study.

Depending on beach and wave characteristics, not all the zones may be present. For example, under surging wave conditions there may be no surf zone because the wave breaks directly onto the beach face.

The characteristics of the seabed profile are related to the hydrodynamic zones described above. The seabed profile usually steepens where waves shoal. At the breaking point a longshore bar and trough may be present. The longshore bar is frequently also referred to as the nearshore bar. Secondary bars may occur in the surf zone, particularly if waves are reforming and breaking a second (or third) time. The beach profile may also not have a bar, and instead have a progressive slope towards the shore.

A beach step, or shore parallel gully, may be present at the lower end of the beach face. This is often associated with collapsing or surging wave breaking just prior to runup and is usually found just below the low-water mark. The beach face itself may have a distinctly steeper slope than the adjoining nearshore profile, or there may be a gentle transition in slope. The latter is more common under spilling wave conditions.

A berm may be present at the crest of the beach face, coinciding with a typical high tide runup level. It is usually only under very high tide and wave conditions that the wave runup will reach beyond this point and to the toe of the primary dune.

2.2 A method to compare beaches

Beaches can vary considerably from location to location. The beach may be steep or gently sloping, waves may be large and break powerfully, or they may be small and break in a dissipative manner, or just surge onto the beach. A quantitative method of describing beaches and comparing them is therefore of use. A number of methods exist (see, e.g. Woodroffe, 2002), one of which is the surf similarity parameter, sometimes also called the Irribarren number. It is denoted by ξ. This is a useful parameter for describing the overall surf zone. It relates the beach slope to the typical wave conditions, in the form:

$$\xi = \frac{\tan\beta}{\left(H_b / L_o\right)^{0.5}}$$

Where: tanβ is here taken as the mid-tide beach slope (dimensionless)

H_b is here taken as the nearshore wave height prior to breaking (m)

L_o is the deepwater wavelength (m)

It is widely used in coastal engineering, for example in the calculation of wave runup on beaches or structures. It inherently relates the wave steepness to the slope of the beach or structure. Depending on its application, the parameters used may represent the local conditions, such as the breaking wave height, or offshore conditions. In this thesis, the nearshore wave height prior to breaking will be used and tanβ will be taken as the mid-tide beach slope.

2.3 The cross-shore distribution of longshore sediment transport

This study deals with the grain sizes in that area of the beach and nearshore profile where longshore transport occurs. It is therefore relevant to obtain an understanding of where on the cross-shore profile this transport occurs.

2.3.1 Information from literature

A summary of investigations of the cross-shore distribution of the longshore transport is presented in the Coastal Engineering Manual (CEM, 2006, p. III-2-35). This summary lists methods that were employed to investigate the longshore sediment transport distribution, including: observation of the movement of fluorescent tracers, sediment traps, measurements of suspended sediment concentrations, and direct trapping using temporary groynes. These were employed both in the field and at laboratory scale. The investigations yielded widely ranging, and sometimes conflicting, results. A summary of the findings of these studies is as follows (CEM, 2006, p. II-2-40):

- Significant levels of transport may occur at and above the mean water level, due to energy in the wave runup;
- About 10 to 30 percent of the total transport occurs seaward of the breaker zone;
- Maximum local transport has been noted within the shoreward half of the surf zone as often as within the seaward half;
- Greater transport is often associated with shallower depths and breaking waves (i.e. at breakpoint bars and at the shoreline);
- The shape of the transport distributions is very variable.

Differences in transport distribution were also noted for different types of wave breaking. It would appear that spilling breakers result in the transport distribution being spread over a greater part of the surf zone, while plunging breakers result in a more peaked distribution, occurring close to the plunge point. This is logical when one considers the high local

turbulence associated with plunging waves as opposed to the more continuous, low level, turbulence associated with spilling breakers.

What is clear from the investigations is that the distribution of transport varies as wave conditions change and as the beach and nearshore profile changes. Measurement of the distribution is thus clearly difficult due to temporal and spatial changes.

2.3.2 A simplified assessment using closure depth

A simplified way of determining the longshore transport zone may be of use. Hallermeier (1981) investigated the seaward limit of effective profile change resulting from wave action, termed the *closure depth*, h_c, with the intention of defining the limits of *cross-shore* sediment transport. While it is thus not directly related to *longshore* transport, it does serve as a useful parameter in defining the seaward limit of sediment movement by wave action. It is also readily related to the common parameters of wave height and period.

Birkemeier (1985) improved and simplified Hallermeier's work by applying it to measurements of profile change at Duck in the USA. (This same profile data set was measured during the cross-shore grain size sampling described by Stauble (1992), and which is analysed in Chapter 5). Birkemeier's closure depth h_c is relative to mean low water (MLW) and is given by the following equation:

$$h_c = 1.75H_e - 57.9\left(\frac{H_e^2}{gT_e^2}\right) \qquad (2.1)$$

where: H_e is the effective significant wave height (the height exceeded only 12 hours per year).

T_e is the associated wave period.

g is the acceleration due to gravity.

H_e can be determined from:

$$H_e = \overline{H} + 5.6\sigma_H \qquad (2.2)$$

where: $\overline{H}$ is the annual mean significant wave height and σ_H is its standard deviation.

Birkemeier (1985) also proposed a simplified formulation for the closure depth (h_c) that was independent of the wave period, as follows:

$$h_c = 1.57 H_e \quad (2.3)$$

This last equation provides us with a simple means of demarcating the seaward boundary to which notable sediment movement due to wave action occurs on the cross-shore profile. In this thesis, Birkemeier's method will be used as an initial guideline in defining the area of longshore transport.

2.3.3 Calculated distributions of longshore transport

The cross-shore distribution of longshore current can be calculated in a numerical longshore transport models. While the accuracy of such models is a function of the input data and the model's theoretical basis, they provide the opportunity to rapidly simulate many wave conditions and different beach and nearshore profile shapes.

For illustration purposes the UnibestCL+ model (WL|Delft, 2005) was used to obtain an indication of the cross-shore distribution of longshore transport. The longshore transport module of this numerical model calculates the cross-shore changes in wave height and direction, the energy dissipation, and the resulting longshore current, flux and sediment transport. Three idealised test cases were simulated, with input conditions to the model summarised in Table 2.1. A simple regular wave input condition was used. Figure 2.2 presents the longshore transport distributions for the three schematised profiles investigated:

1. A linear sloping beach and nearshore (1:50 slope) – upper figure;
2. A simple concave nearshore slope – middle figure;
3. A profile with a single nearshore bar/trough feature – lower figure.

Table 2.1: Parameters used for calculation of longshore sediment transport distribution

Wave Height (at 10m depth, seaward point of profile)	1.8 m
Wave Period	12 s
Wave Direction (at 10m depth, seaward point of profile)	10° from shore normal
Transport equation	Bijker (1968)
D_{50} grain size*	0.25 mm
Breaker index γ	0.8

* In the model this is assumed representative of the entire cross-shore region

In Figure 2.2 the beach and nearshore profiles are represented by the solid lines, with the dashed lines indicating the calculated cross-shore distributions of longshore transport corresponding to each profile.

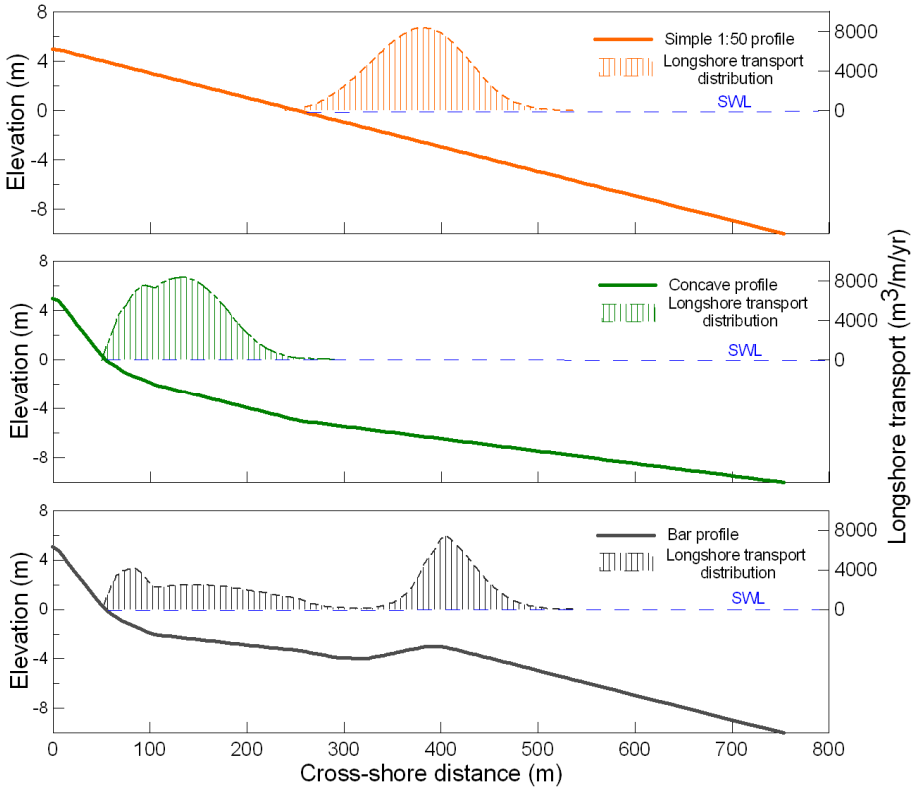

Figure 2.2: Examples of calculated cross-shore distributions of longshore sediment transport

In the case of the linear profile, breaking occurs at a single position, determined by the breaker index, γ, defined as the wave height at breaking divided by the water depth at breaking (a value of 0.8 was used in the calculations). The distribution has a single peak distributed around the breaking point. The concave profile exhibits two peaks almost merged together. The first, most seaward, peak is likely at the initial breaking point, while the second is close to shore and reflects the final breaking action. The barred profile has a sharper peak in approximately the same position as the linear profile. However, the peak is narrower, indicating that not all energy is dissipated in the initial breaking. There are two further peaks, the first of these a gradual increase leading to the last peak occurring close to shore. The latter is similar, though of lower magnitude, to the second (swash-zone) peak found for the concave upward profile. (It must be borne in mind that these calculations have assumed the grain size to be the same everywhere on the cross-shore profile.)

At a higher (or lower) state of the tide, less (or more) energy would be dissipated on the bar and the distribution would be different for these schematised profiles. They are of course also influenced by the accuracy with which the Unibest model simulates the processes. For this investigation this has been assumed to be satisfactory.

2.3.4 Discussion

The distribution of transport is clearly quite dependent on the profile, and is related to the location of wave breaking. It can thus vary considerably between different beaches, as was clearly shown by the exercise conducted in Figure 2.2, but also at the same beach it will vary as wave conditions change and even as tidal changes cause the location of breaking to shift. This has implications on the sand being transported by the longshore current – if a certain size of sand is only present at a particular location on the profile (e.g. say coarse sand occurs just landward of the bar) this material may be transported under only certain conditions. It might not be subject to longshore transport for the remainder of the time.

This would seem to suggest that "dynamic" consideration of the cross-shore distribution of *sediment size* is required, with changes occurring wave-by-wave, together with continuous estimation of the distribution of longshore transport, in order to estimate the appropriate particle size being transported. However, such an approach is immensely complicated and impractical for the purposes of this study and will not be pursued in this study. Supporting this decision is the action of cross-shore transport: longshore transport is not a solitary process, cross-shore movement of sediment occurs continually under wave action as well. Cross-shore sediment transport will therefore be considered a "smearing" factor that allows us to consider the area of longshore transport *in general*, and avoid over-complications (and over-simplifications).

To consider only that area of the cross-shore profile where longshore transport occurs under *average* wave conditions is not realistic either: CEM (1998, p. II-2-31) suggests that it is quite likely that a large proportion of the annual longshore transport occurs under infrequent episodic conditions. These conditions could be a combination of a storm wave condition with only a small approach angle to the beach, or a moderate wave condition at a very oblique approach angle to the beach. From the previous part of the discussion, it is clear that for these two situations the transport would not occur over exactly the same part of the cross-shore profile. Areas of the profile with different grain size could therefore be involved for the two cases.

From the above analysis it is clear that the processes involved in longshore transport, and determining its cross-shore distribution, are quite involved. Ideally, the representative grain size used in longshore transport rate calculations should be based on some weighted mean size related to the relative cross-shore distribution of longshore transport.

2.4 Grain size parameters

A number of descriptive terms are used to define commonly used grain size parameters and concepts. Those relevant to this thesis are outlined in this section.

2.4.1 Size classification

Two descriptive grain size classification scales are commonly used. These are the ASTM or Unified Soils classification and the Wentworth classification. These are given in Table 2.2. The main differences between the two are that the Wentworth system has a greater number of classification bands. It is important to note that the same term means quite different grain sizes in the two systems. Sand described as “coarse” could therefore have typical size of 2.0 to 4.75 mm (Unified Soils) or 0.5 to 1.0 mm (Wentworth). It is thus important to state which system is being referred to when describing particle size. In this study, grain sizes will generally be described in numerical units. The Wentworth classification scale is used in this study where descriptive terms are applied.

Table 2.2: Classification of sediment particle sizes (CEM, 2004)

Table III-1-2
Sediment Particle Sizes

ASTM (Unified) Classification[1]	U.S. Std. Sieve[2]	Size in mm	Phi Size	Wentworth Classification[3]
Boulder		4096.	-12.0	
		1024.	-10.0	Boulder
	12 in. (300 mm)	256.	-8.0	
Cobble		128.	-7.0	Large Cobble
		107.64	-6.75	
		90.51	-6.5	Small Cobble
	3 in. (75 mm)	76.11	-6.25	
		64.00	-6.0	
		53.82	-5.75	
		45.26	-5.5	Very Large Pebble
Coarse Gravel		38.05	-5.25	
		32.00	-5.0	
		26.91	-4.75	
		22.63	-4.5	Large Pebble
	3/4 in. (19 mm)	19.03	-4.25	
		16.00	-4.0	
		13.45	-3.75	
		11.31	-3.5	Medium Pebble
		9.51	-3.25	
Fine Gravel	2.5	8.00	-3.0	
	3	6.73	-2.75	
	3.5	5.66	-2.5	Small Pebble
	4 (4.75 mm)	4.76	-2.25	
	5	4.00	-2.0	
Coarse Sand	6	3.36	-1.75	
	7	2.83	-1.5	Granule
	8	2.38	-1.25	
	10 (2.0 mm)	2.00	-1.0	
	12	1.68	-0.75	
	14	1.41	-0.5	Very Coarse Sand
	16	1.19	-0.25	
	18	1.00	0.0	
Medium Sand	20	0.84	0.25	
	25	0.71	0.5	Coarse Sand
	30	0.59	0.75	
	35	0.50	1.0	
	40 (0.425 mm)	0.420	1.25	
	45	0.354	1.5	Medium Sand
	50	0.297	1.75	
	60	0.250	2.0	
	70	0.210	2.25	
Fine Sand	80	0.177	2.5	Fine Sand
	100	0.149	2.75	
	120	0.125	3.0	
	140	0.105	3.25	
	170	0.088	3.5	Very Fine Sand
	200 (0.075 mm)	0.074	3.75	
	230	0.0625	4.0	
Fine-grained Soil:	270	0.0526	4.25	
	325	0.0442	4.5	Coarse Silt
Clay if PI ≥ 4 and plot of PI vs. LL is on or above "A" line and the presence of organic matter does not influence LL.	400	0.0372	4.75	
		0.0312	5.0	
		0.0156	6.0	Medium Silt
		0.0078	7.0	Fine Silt
		0.0039	8.0	Very Fine Silt
Silt if PI < 4 and plot of PI vs. LL is below "A" line and the presence of organic matter does not influence LL.		0.00195	9.0	Coarse Clay
		0.00098	10.0	Medium Clay
		0.00049	11.0	Fine Clay
(PI = plasticity limit; LL = liquid limit)		0.00024	12.0	
		0.00012	13.0	Colloids
		0.000061	14.0	

[1] ASTM Standard D 2487-92. This is the ASTM version of the Unified Soil Classification System. Both systems are similar (from ASTM (1994)).
[2] Note that British Standard, French, and German DIN mesh sizes and classifications are different.
[3] Wentworth sizes (in mm) cited in Krumbein and Sloss (1963).

2.4.2 Grain size units

The standard units of measurement for grain sizes are millimetres (mm) or microns (μm), where 1 mm = 1 x 10^3 μm. An alternative scale that is used by coastal engineers is the *phi* unit, denoted by the Greek letter phi (Φ). The conversion between phi and mm is as follows:

(phi size) = $-\log_2$(size in mm)
And:
(size in mm) = $2^{-(\text{phi size})}$

The phi system normalises the grain size distribution and allows calculation of other size statistics based on the characteristics of normal distributions (Larson *et al*, 1997). The advantages and disadvantages (according to CEM, p. III-1-9) of the phi system are :

Advantages:

- It has whole numbers at class intervals in the Wentworth classification system;
- Because it is dimensionless it allows comparison of different size distributions.

Disadvantages:

- Phi units become larger as grain size decreases, which is counter-intuitive and ambiguous;
- It is difficult to interpret phi sizes in the field;
- It cannot be substituted as a unit of length in physical expressions such as Reynolds numbers.

Only limited use is made of phi units in this study. In general, the millimetre unit is used to describe grain sizes.

2.4.3 Distributions

Particle size distributions are generally defined by the percentage of the sample which is finer, by mass, than the given sieve size. Examples of size distributions are shown in Figure 2.3 for two samples from Table Bay. The samples are plotted on a log-probability scale, with the median size indicated.

The first important parameter is the *median* size. It is that size for which half the sample is finer by mass. It therefore differs from the *average* size. The latter is difficult to determine from standard sieve analyses. Percentiles are also commonly used to characterise a sample,

the most frequently used being the 5th, 16th, 50th, 84th, and 95th percentile. These are referred to as "D" sizes, so D_5 is the fifth percentile, or the size for which 5 percent of the sample is finer by mass. The median size is therefore the D_{50}. In the examples shown in Figure 2.3, the median sizes are 0.34 mm and 0.78 mm.

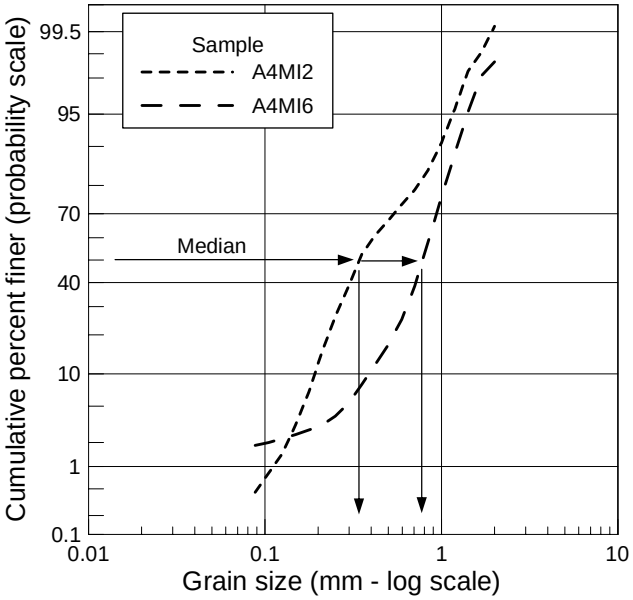

Figure 2.3: Two example sediment size distributions from Table Bay samples plotted on log-probability scale

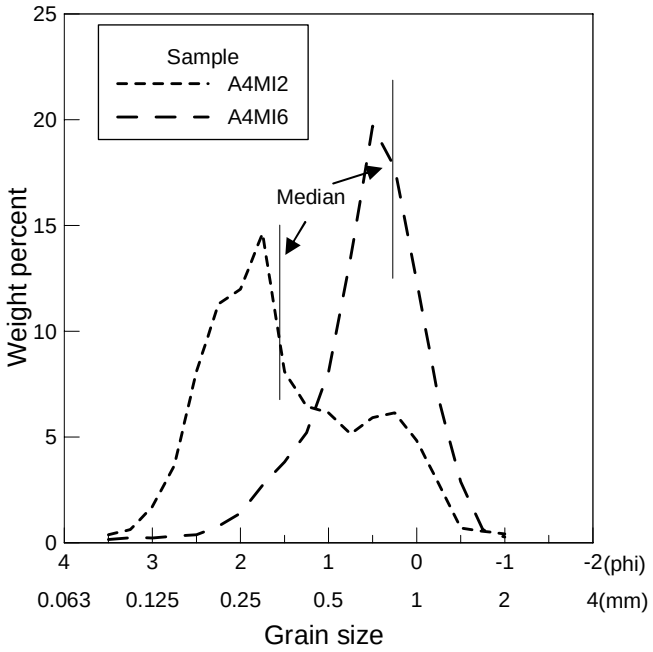

Figure 2.4: Example size distributions showing bimodal and unimodal distribution shapes

With experience, distribution plots such as Figure 2.3 can be easily interpreted in order to characterise the sediment sample. Characteristics such as a bimodal distribution, which is not

clear if only the size percentiles are available, are then visible. The distribution is more easily visualised when plotted as the weight percent occurring in distinct size bands. The two log-probability distributions shown in Figure 2.3 are re-plotted in this way in Figure 2.4. The phi scale is used on the horizontal axis to take advantage of the normal distribution characteristic of this scale. The corresponding sediment sizes in millimetres are also shown.

It is immediately clear that sample A4MI2 has a bimodal (two-peaked) distribution, with a dominant peak near 2 phi (0.25 mm) and a secondary peak between 1 and 0 phi (1 mm). The median size lies between the two peaks and closer to the larger. The distribution is wide at its base.

Sample A4MI6 has a steeply peaked uni-modal distribution. The peak lies between 0 and 1 phi. The distribution tapers gradually towards the higher phi values (finer sizes) but is much steeper on the lower phi (coarser size) side. In Figure 2.3 the distribution has an unremarkable shape, although a tail in the fine size range can be recognised.

Characteristics of grain size distributions, such as those above, can be more concisely described using three standard parameters. These are the standard deviation, or sorting; the skewness; and the kurtosis. All three make use of the phi system and the fact that the phi scale has a normal distribution.

The *phi standard deviation* (σ_Φ), or sorting, indicates the spread of sizes around the mean. A small standard deviation indicates a well-sorted sand. This sand is confined to a small range of sizes, with all particles having sizes that are close to the typical size. If the particle sizes are distributed evenly over a wide range of sizes, then the sample is said to be well-graded. A well-graded sample is poorly sorted; a well-sorted sample is poorly graded (CEM, 2002, p III-1-10).

Table 2.3: Qualitative description of grain size sorting

	Range	**Description**
$\sigma_\phi = \frac{(\phi_{16} - \phi_{84})}{4} + \frac{(\phi_5 - \phi_{95})}{6}$	<0.35	Very well sorted
	0.35-0.5	Well sorted
	0.5-0.71	Moderately well sorted
	0.71-1.0	Moderately sorted
	1.0-2.0	Poorly sorted
	2.0-4.0	Very poorly sorted
	>4.0	Extremely poorly sorted

With reference to the samples shown in Figure 2.4, sample A4MI2 has a standard deviation coefficient of 0.95, while that of sample A4MI6 is 0.68. The narrow distribution of A4MI6 is thus reflected in better sorting than A4MI2, which has a broader base to its distribution.

The *phi coefficient of skewness (α_Φ)* is a measure of the symmetry of the grain size distribution around the mean value (D_{50}). A perfectly symmetrical distribution would have a skewness value of zero. Positively skewnesses indicates the distribution has a tail of fine material, while negative skewnesses are indicative of coarse outliers.

Table 2.4: Qualitative description of grain size distribution skewness

$\alpha_\phi = \frac{\phi_{84} + \phi_{16} - 2(\phi_{50})}{2(\phi_{16} - \phi_{84})} + \frac{\phi_{95} + \phi_5 - 2(\phi_{50})}{2(\phi_5 - \phi_{95})}$	**Range**	**Description**
	<-0.3	Very coarse-skewed
	-0.3 to -0.1	Coarse-skewed
	-0.1 to +0.1	Near-symmetrical
	+0.1 to +0.3	Fine-skewed
	>+0.3	Very fine-skewed

Sample A4MI2 has a skewness coefficient of -1.66. It is extremely coarse skewed. This is a result of the second, smaller, peak in this bimodal distribution lying well on the coarse side (right-hand side in Figure 2.4) of the distribution. Sample A4MI6 has a skewness coefficient of +0.74 and therefore is very fine skewed. This is reflected in the tail of the distribution in Figure 2.4 extending into the fine size domain.

The *phi coefficient of kurtosis (β_Φ)* is a measure of the peakedness of the distribution, i.e. whether it has a sharp peak or is broader and flat. It thus provides an indication of whether the material is grouped around the mean, or is distributed towards the tails.

Table 2.5: Qualitative description of grain size distribution kurtosis

$\beta_\phi = \frac{\phi_5 - \phi_{95}}{2.44(\phi_{25} - \phi_{75})}$	**Range**	**Description**
	<0.65	Very platykurtic
	0.65-0.9	Platykurtic (low, wide peak around mean and thin tails)
	0.9-1.11	Mesokurtic (normal peakedness
	1.11-1.5	Leptokurtic (acute peak around mean and thick tails)
	1.5-3.0	Very leptokurtic
	>3.0	Extremely leptokurtic

Sample A4MI6 is leptokurtic (kurtosis value of 1.26). Its distribution is clearly more peaked than that of sample A4MI2 (platykurtic, kurtosis value of 0.85).

Chapter 3: Review of Literature on Cross-Shore Grain Size

3.1 Background

The distribution of grain sizes from the beach to beyond the wave breaking point is known to vary temporally and spatially. Temporal variation is driven by variations in wave conditions over time, both on short time scales (days to weeks, storms to calm periods) and seasonally (due to seasonal shifts in wave conditions, for example from summer to winter).

Spatial variation may be due to hydrodynamic features, such as rip currents, alongshore changes in wave conditions due to offshore bathymetric variations, the degree to which a beach is exposed or sheltered by a headland or breakwater, and changes in beach and offshore slope. Further, sources or sinks of sediment may be present along a beach, such as rivers or eroding headlands or dunes, or submarine canyons. These can result in sediment characteristics varying from one point to another.

3.2 Cross-shore size changes

The general patterns of grain size distributions on a beach have been established by researchers for some time (e.g. Komar, 1976) as being the following: sand sizes become finer from the beach towards the offshore. Landwards of the beach, toward the dune zone, the grain sizes are generally constant, unless other factors such as aeolian transport contribute by winnowing out (selectively removing) particular size classes. Aeolian transport contributes to removal of finer particles from the beach.

Anders *et al.* (1987) describe the results of an extensive sampling exercise (398 samples along 13 km of beach) conducted along the barrier coastline at Ocean City, Maryland, USA, in preparation for a beach nourishment. They found a clear decrease in size with increasing water depth, with the coarsest material occurred in the swashzone.

The change in grain size across the beach and nearshore profile appears to correspond to the wave energy dissipation and local turbulence. According to Bascom (1951), the grain size at a point on the profile is proportional to the amount of turbulence experienced at that point. The coarsest sizes are generally recorded near the wave plunge zones, with grain size decreasing both seaward and shoreward (p.347, Komar, 1976). Such plunge zones or peaks in energy

dissipation generally occur in the swash zone, where reformed waves collapse onto the shore, and near the longshore bar, where waves first break. Two peaks in grain size can therefore occur in the cross-shore direction (e.g. Stauble and Cialone, 1996). The coarsest sizes, however, are almost invariably found at the beach step, see Figure 2.1, where the inter-tidal and sub-tidal beach slopes meet (Bascom, 1951). Local plunging of waves and continuous turbulence of up and downward rushing water occurs here and acts as a good sorting mechanism. Fine particles are easily carried away by currents. A second peak in coarseness on the beach may be found at the crest of the beach berm (Figure 2.1), where the upward rushing water in the swash zone deposits coarse material.

On beaches where the surf zone is relatively narrow (~100 m) and wave energy is low, the swash zone and trough behind the nearshore bar may be difficult to distinguish and only a single peak in the grain size may occur at this merged zone. This was found by, for example, Medina *et al.* (1994), who performed repetitive measurements at El Puntal spit, Santander, Spain. They found that the trough/swash area consistently had the coarsest median grain size with the grain sizes here also exhibiting the greatest variability.

Measurements conducted along the Baltic Sea coast at Lubiatowo (Pruszak, 1993), under milder, dissipative wave conditions, indicated that sediment sizes become finer below water, but to only a limited extent. The data presented does indicate that peaks in median size tended to occur in the trough areas of this multi-barred profile. This beach has a wide surf zone (possibly over 300 m) and gentle seabed slope (water depth of only 4 m at a distance of 500 m from the shoreline). The average beach grain size is given as 0.22 mm, with storm wave conditions having wave heights of 2 to 2.5 m with periods of 5 to 7 s.

Using surface sediment samples from 52 profiles taken along Long Island, New York, between July and August (northern hemisphere summer), Liu and Zarillo (1989) investigate the relative abundance of four size fractions across the nearshore zone. They found that, for this coastline, beyond a depth of 16 m the sediment size was related to the inner shelf (i.e. offshore) seabed and beyond the influence of waves and nearshore currents. They found a distinct dominance of fine sediment seaward of the longshore bar, although this reduced as water depth increased, reflecting the increasing presence of shelf sediments. Occurrence of coarse grain sizes was highest in the surf zone. The general trend was for coarser sediments to occur further landwards.

Pruszak (1993) also presents cross-shore grain size data from the Bulgarian coastline in the Black Sea. This indicates a strong peak in size in the swash zone, with median sizes up to

three times those found on the beach. The beach sizes also appear to be highly variable, most likely due to the variability in wave conditions experienced here, as alluded to by the author. The lack of tidal variation would also lead to a constant focus of the swash energy in the same position on the profile. The beach is described as having a narrow surf zone, and, indeed, the longshore bar appears to be located only some 30 m from shore. The median sizes appear to be slightly finer in the trough area than along the remainder of the profile.

Repetitive measurements of cross-shore grain size at the Hazaki Oceanographic Research Station were analysed by Katoh and Yanagishima (1995) to examine changes during a storm. Fifteen sampling events were carried out over a 7 month period. The authors present only limited data on the cross-shore variation in median size. However, this does indicate that the coarsest sizes occur in the swash zone, with a secondary peak in coarseness occurring in the trough area, which also had the greatest variability in size. Seaward of the longshore bar, median grain sizes appear to become steadily finer. The site is exposed to the Pacific Ocean and a storm with significant wave height of over 5 m was recorded during the measurement period.

The Katoh and Yanagishima (1995) examined the changes that occurred during this storm and found that after the storm the beach retained its fine sand characteristic, but the beach step and trough area, both areas of high turbulence, became coarser. Material was generally fine on the longshore bar. After the storm the trough material was unimodal coarse but slowly reverted back to unimodal fine via a number of varying bimodal steps. Two possible explanations for the storm behaviour of the trough area were suggested:

- The trough area of the profile usually contains a mix of fine and coarse sand, with the fine fraction removed by the storm, leaving the coarse fraction as a lag deposit. (After the storm the fine material returns);
- An upper layer of fine sand is removed by the storm, leaving the underlying layer of coarser material behind. (Afterwards the fine layer returns).

The Katoh and Yanagishima (1995) do not conclude which is the most likely scenario.

Stuable (1992) describes an analysis of simultaneous bathymetric and cross-shore sediment sampling surveys conducted at Duck, North Carolina, USA, between March 1984 and September 1985. The data is analysed in Chapter 5. Sampling was conducted on an approximately monthly basis, with additional samples taken after storms.

The measurements described by Stuable (1992) indicate a clear offshore fining trend. The greatest temporal variation occurred in the samples from the beach and inter-tidal area. These samples were primarily bimodal. The bar/trough area showed less variability than the authors had expected and exhibited a mostly unimodal distribution. Coarse material was found after storms or when a sample was taken at the highly turbulent beach step. The least variability in sediment size was observed at the transition from nearshore to offshore, with only a slight coarsening observed after storms. This zone also showed the least profile change, as it is beyond the area of strong wave-driven transports.

It was found that after storms the sediments on the profile tended to be coarser, particularly in the beach and bar/trough zones (to a lesser extent in the offshore zone). After extended periods of low waves, the sediments became finer and better sorted.

Sediment sizes may also vary in the alongshore direction on a coastline. This can be because of proximity to a sediment source, such as a river, where the sediments have not yet been sorted by repeated wave action, or due to differential exposure to wave energy along the beach. Near a fluvial source, beach sediments may still retain the positive skewness typical of river sands as opposed to the negative skewness typical of beach, as shown by Friedman (1961). Self (1977) found that lighter, finer material was transported further away from the fluvial source than heavier, coarser grains.

3.3 Grain size and beach slope

Bascom (1951) took more than 600 samples from 40 beaches along the whole Pacific Coast of the United States in an effort to examine the link between beach slope and grain size. He concluded that the slope of the beach face is related to the median sand diameter and amount of wave energy reaching that point. Steeper (more exposed) beaches had coarser grain sizes. He introduced a standard "reference point" on the beach profile which was used to compare samples and beach slopes from different sites. This point was defined as the mid-tide level and recommended as the best location for obtaining a representative sample.

Recently, further efforts have looked at the relationship between grain size and beach slope. Noshi *et al.* (2006) provide the simple relation $\tan\beta = 0.16d$ between grain size, d, at a particular point and the beach slope, $\tan\beta$, at that point on the profile. Using samples from five Japanese beaches, they show that good results are obtained when the grain size having the highest occurrence at a particular location, is used in place of the median size.

3.4 Sampling methodologies

The methods used to obtain sediment samples vary depending on the application, environmental conditions, and availability of equipment. For obtaining samples in the sea, authors in the literature reviewed have used methods ranging from surface grabs (e.g. Medina *et al.,* 1994) to short coring (Anders *et al.,* 1987). The latter would be particularly useful when information on sediment bedding or layering is required, as is provided by an undisturbed core. The samples obtained from a grab, on the other hand, can be regarded as disturbed. For samples taken on the beach, a hand scoop is usually sufficiently sophisticated (Stauble and Cialone, 1996).

No method is recommended as being superior if an analysis of the grain sizes is the goal of the sampling. It would seem that any method that captures a sufficiently large and representative sample (no loss of fine material) would be adequate. Sample masses encountered in the literature ranged from 300 g (Losada *et al.,* 1994) to 3 kg (Katoh and Yanagishima, 1995). Samples of large volume usually require splitting in the laboratory in order to yield quantities suitable for analysis methods.

During repeated sampling of a line, Stuable (1992) recommends that care be taken to ensure the same profile zones are repeatedly sampled and compared. This is particularly the case for active beaches where nearshore bars can move on- or offshore rapidly and what was the trough area during one sampling campaign is the bar crest during the next. Sample spacing was usually such that there was sufficient distinction between morphological zones, with at least one sample in each zone. Along a cross-shore line, spacing between samples ranges from approximately equal horizontal distances (Katoh and Yanagishima describe sampling at 10 m horizontal intervals at the HORS pier, resulting in 50 individual samples per cross-shore line), to equal depth/elevation intervals (e.g. Anders *et al.,* 1987), to seemingly arbitrary intervals.

The temporal frequency of sampling is determined by the purpose of the measurements. Medina *et al.* (1994) describe sampling of the entire beach and nearshore profile at monthly intervals for a 20 month period, their aim being to establish seasonal trends in size evolution. At the opposite end of the spectrum, Stauble and Cialione (1996) describe daily sampling of the beach for a period of 18 days, with bi-daily sampling of the nearshore, during the DUCK94 experiments. The aim of this sampling exercise was to look at changes caused by storm waves and calm periods in the order of a few days. They found that the inter-tidal ("foreshore") sediments became coarser during and after the storm. The sediments in the bar

and trough area also became slightly coarser. Sediments in the nearshore area beyond 4 m depth, remained unchanged. The latter is probably due to this point being close to the closure depth at this site. Stauble and Cialione (1996) do not conclude on the sources of the coarser material, nor the fate of the previously finer sediments, but do suggest that the coarsening may be due to removal of previously overlying fine material.

In engineering work, it is often desirable to determine the definitive or representative grain size of a beach, an example of this being for the calculation of longshore transport. However, from the studies referred to in the previous paragraph it is clear that size variation is almost continuous. Obtaining a definitive size therefore becomes a difficult task. Anders *et al.* (1987) investigated the number of samples required in order to define the representative grain size of a particular beach. In the cross-shore direction, the different energy zones that occur (e.g. inter-tidal, swash zone, surf zone) imply greater size variability and therefore a high number of samples are required to accurately estimate the representative size. In the case of Ocean City, USA, where Anders *et al.* (1987) undertook their sampling, up to 76 samples per line were required for 0.25 phi accuracy and 95 percent confidence.

In the alongshore direction, energy conditions are generally more uniform, leading to less variation in size. Anders *et al.* (1987) outline the number of alongshore samples required to describe the average sediment size for the various cross-shore environments (upper beach, berm crest, etc) for various confidence levels. For example, only two samples would have been required to characterise the berm of this particular 13 km stretch of coastline (Ocean City, Maryland), while 43 samples would have been needed for the swash zone (to 0.25 phi accuracy and 95 percent confidence). These figures would differ for other beaches, particularly as Ocean City beach is long, straight and uniform. Anders *et al.* also found that in areas where grain sizes are coarser, more samples are required in order to establish the typical grain size. This is clear from the 43 samples required to define the swashzone size.

At times it may be desirable to characterise an entire beach and nearshore region with only one value, instead of separate size values for dune, beach, nearshore, etc. In this case a composite sample can be used. Composite samples can be useful to describe a zone of a profile, the whole profile, or the entire beach. They can be obtained from a larger set of individual samples of each zone by either combining the constituent samples physically prior to sieving, or mathematically after sieving by combining the individual sample weights (CEM, 1998). Of course, a lot of information on say, the cross-shore grain size variation is lost in this gross averaging process.

3.5 Predictive approaches

This thesis investigates the cross-shore changes in grain sizes with the specific aim of obtaining a better understanding of the characteristic grain size in the longshore transport zone. Some work has been done in literature to predict what the grain sizes will be in this zone.

Horn (1992) used offshore wave conditions (height, period), nearshore seabed slope and a wave friction energy dissipation coefficient as input to a numerical model to predict the changes in grain size from offshore towards the shoreline. The model is based on the principle that the grain size distribution is in equilibrium with the wave-generated hydraulic regime. Horn summarises (p. 163) two hypotheses that have been used in literature to explain shore normal changes (or sorting) of grain size on the profile:

- An *asymmetric threshold hypothesis*, based on the asymmetrical nature of the wave orbital motions in shallow water. The onshore motion has a high velocity but short duration, while the offshore motion has a lower velocity but longer duration. As larger size grains would have higher transport threshold velocities, the larger particles would be driven onshore over time by the high onshore velocity component. Finer particles would be moved offshore. Because asymmetry becomes more pronounced with decreasing depth, progressively greater sizes would occur in shallower water.
- The *null point hypothesis* includes the effect of bed slope on flow asymmetry, suggesting that each grain has a null point at which the onshore flow force is balanced by an offshore gravity force component as a result of the sloping seabed.

Horn (1992) describes a modification of the null point hypothesis based on the wave power at each point on the profile. This was used as the basis for her numerical model. Comparison of the predicted results to measurements indicated that the model did show landward coarsening of sizes, but the magnitudes of the predicted sizes were not accurate. Further, the cross-shore variability found in measurements was not represented, with the model indicating a smooth and steady shoreward increase in size that did not reflect the measured trends. The changes due to bars, troughs and the swash-zone step were not represented.

Uda *et al.* (2004) present a model of cross-shore profile changes using grain sizes and grain-size dependent beach slopes. Their approach is based on the null point hypothesis and uses an equilibrium slope for each grain size in order to arrive at the cross-shore profile and distribution of grain sizes. They present results showing good agreement between measured and calculated data for both the beach profile and grain sizes. Kumada *et al.* (2006) extended

this model to the longshore direction and the prediction of shoreline changes. Longshore transport calculations made use of the CERC formula (SPM, 1984), where the K term was used to introduce the grain size into the calculations.

While the articles mentioned in this paragraph do provide some predictive elements, it should be noted that they rely strongly on the grain sizes being known.

3.5.1 Conclusions

It has emerged from the literature survey that although changes in grain size in the cross-shore direction have frequently been measured, little, if any, effort has been expended on examining the relation between the size in the longshore transport zone and that of the beach sands. This is the primary aim of this thesis.

It also became clear that data on cross-shore changes in grain size would be required in order to investigate such a relationship. While some of the literature discussed in this chapter yielded grain size datasets that could be used towards the aim of this study, it was decided by the author to undertake additional field sampling. Together with the useable data from literature, this would form a broader database for this thesis. The additional field sampling is the subject of the following chapter.

Chapter 4: Sampling to Obtain a Cross-shore Grain Size Dataset

4.1 Introduction

It was decided to obtain data from a variety of beaches, as this would allow the investigation of the effects of different wave energy regimes, beach and nearshore slopes, and sediment characteristics. Publicly available data was obtained from the US Army Corps of Engineers Field Research Facility at Duck, North Carolina, with a second data set obtained from measurements conducted by Namdeb Diamond Corporation (Pty) Ltd at Bogenfels in Namibia.

Data from these two sources was supplemented with field sampling undertaken by the author in Table Bay, Cape Town, specifically for this thesis. The location, general bathymetry and layout of the sampling lines in Table Bay are shown in Figures 4.1 and 4.2 respectively. The field sampling and sediment size analysis that were conducted in Table Bay are described in the following sections.

Figure 4.1: Location of Table Bay in Cape Town, South Africa

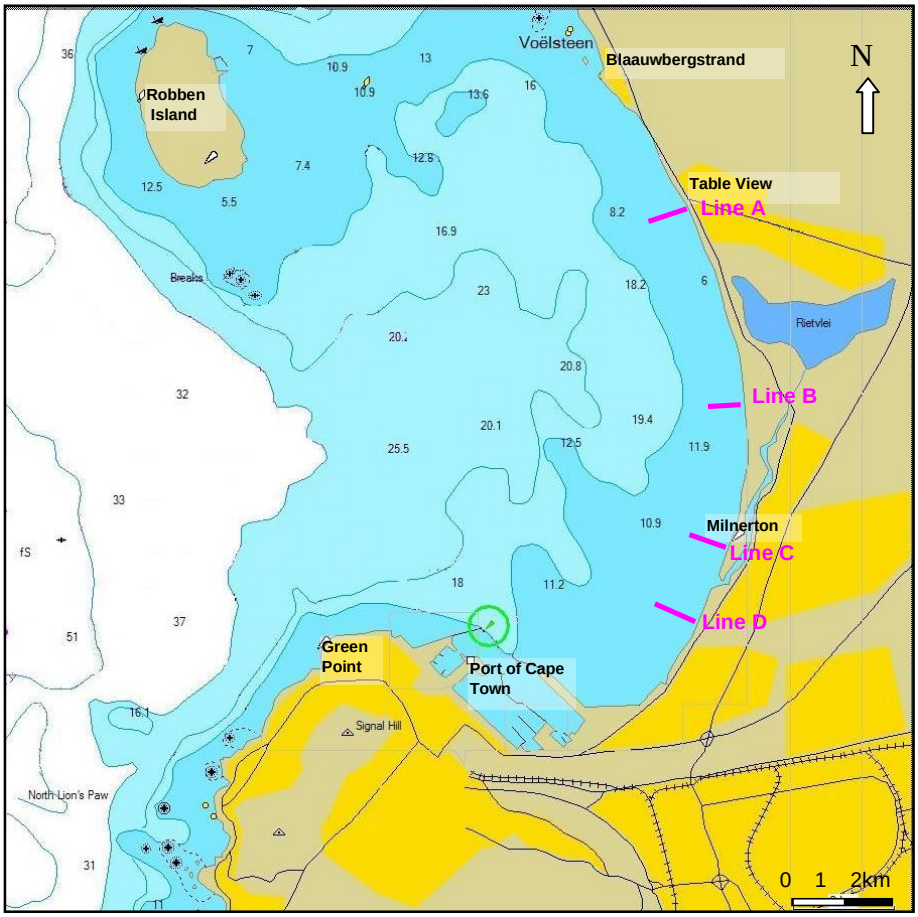

Figure 4.2: Bathymetry chart of Table Bay with location of the four sampling lines (Lines A, B, C and D) indicated

4.2 Field sampling

The fieldwork – location of sampling lines, position of samples on the cross shore profile, and sampling method – are described in this section. The grain size data are given in Appendix 3.

4.2.1 Location of sampling lines

Four sampling lines were selected in Table Bay. The locations are indicated in Figure 4.2 and were as follows:

A. Line A is located on the southern part of Table View Beach, near the junction of Blaauwberg Rd and Otto Du Plessis Drive;
B. Line B, opposite the Sunset Beach residential development north of the Milnerton golf course;
C. Line C, opposite the Zonnekus House on Woodbridge Island in Milnerton;
D. Line D, adjacent to the storm water outfall near the Spinnakers residential development south of the Diep River mouth.

The sample sites were chosen to take advantage of the varying degrees of wave exposure in Table Bay. For example, the southern part of the bay, where lines C and D are located, is sheltered from dominant south-westerly waves by the headland at Green Point (Figure 4.2). This wave sheltering and its effect on grain size is dealt with in detail in Chapter 5. Figure 4.3 shows a typical cross-shore seabed profile at each sampling line.

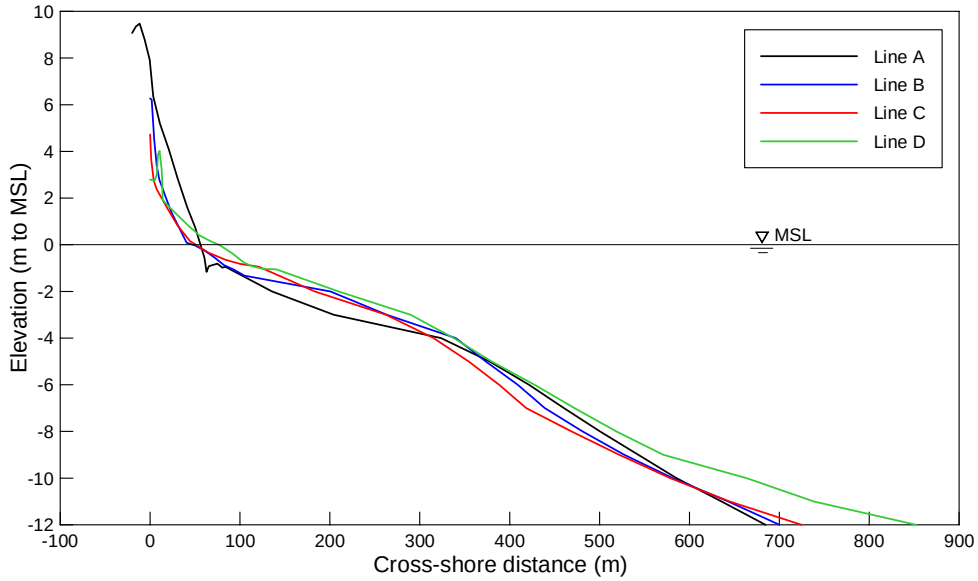

Figure 4.3: Typical cross-shore profile at Sampling Lines A, B, C and D in Table Bay

4.2.2 Position of samples on the cross-shore profile

It was decided to obtain sediment samples of the seabed from seaward of wave breaking, through the surf zone and up to the primary dune. Samples would be thereby obtained from the main morphological zones in a similar approach to that followed by a number of the authors encountered in the literature survey and that recommended by Stauble (1992). The following zones were sampled, with typical sample locations indicated in Figure 4.4:

- Offshore – samples at 10, 8, 6 and 5 m depth. The 10 m depth samples were usually only taken at Lines A and B;
- Breaker zone – samples at 4 and 3 m depth;
- Surf zone – between three and four samples, from the breaker zone to just seaward of the swash zone;
- Swash zone, at the beach step;
- Beach – samples at the mid-tide beach face, berm crest, upper beach and base of primary dune. The upper beach sample was frequently neglected, due to the beaches being very narrow.

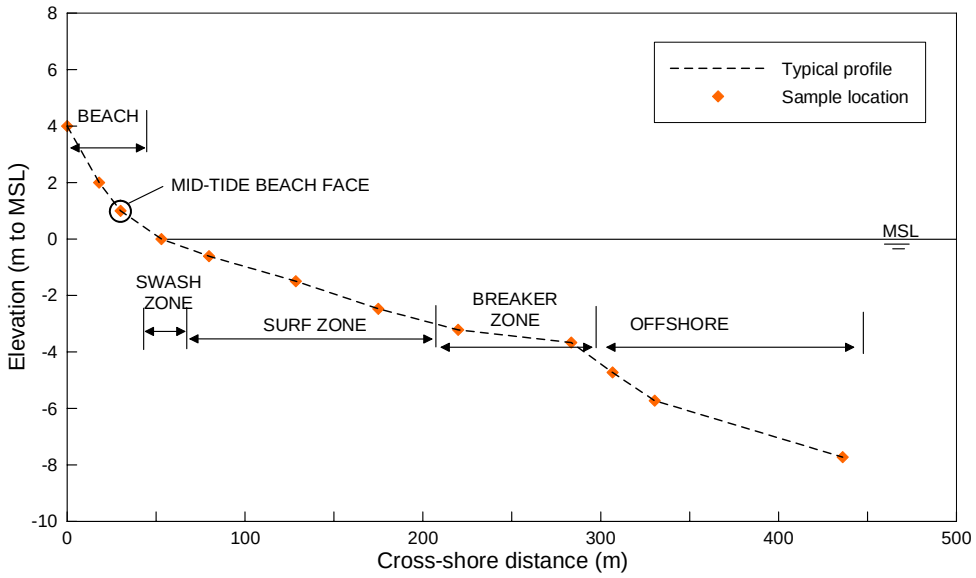

Figure 4.4: Indication of typical sampling locations on the cross-shore profile

4.2.3 Sampling methods

Three methods were used to obtain the samples:

1. Offshore and outer breaker zone samples, i.e. those from 10 m to 4 m depth, were obtained with a Van Veen grab (Figure 4.5) deployed from a semi-rigid inflatable boat. A sample volume of 500 ml was typically obtained with the grab. The depth of penetration was estimated to be generally less than 5 cm, gauged by examining the captured sediment after carefully opening the jaws of the grab. The deeper water samples in 10 to 5 m depth could be easily obtained. However, on occasion it was not possible to take grab samples shallower than this due to large waves breaking at the outer edge of the surf zone. The advantage of the boat-and-grab sampling was that the positions and water depths could be accurately obtained from the onboard GPS and depthsounder;
2. Surf zone and swash zone samples were taken by swimming out with snorkeling gear and using small PVC tubes to obtain a sample from the seabed surface. The tubes are illustrated in Figure 4.6 and have dimensions of 200 mm (length) x 50 mm (diameter), giving a sample volume of approximately 300 ml. Samples were taken from morphological zones that could be distinguished on the day, usually being: just seaward of the swash zone, landward of the breaking point, at the breaking point, and seaward of the breaking point. This sampling could only be done on days when wave conditions were small – breaking wave heights were less then 0.5 m on most occasions. Therefore the "breaking point" sample would lie landward of the point

where waves would break under higher wave conditions, such as the longshore bar. The "seaward of breaking point" sample is considered to be closer to this higher-wave breaking point. Thus there was a times overlap with the offshore and breaker zone sampling;

3. Samples from the beach zone were scooped from the upper 5 – 10 cm by hand.

All samples were sealed in zip-lock bags that had been pre-labelled with the line ID (A, B, C or D) and the location on the line (nomenclature was standardized to a three character descriptor). In the laboratory each sample was placed in a batch according to the sampling date and accorded a unique Sample ID.

Figure 4.5: Offshore sample recovery with the Van Veen grab off Woodbridge Island, Line C, on a calm day.

Figure 4.6: The small PVC core tubes used to collect samples from the surf zone

The frequency of sampling at each line is summarized in Table 4.1. A timeline of the sampling is shown in Figure 4.7.

Table 4.1: Summary of the number of samples collected at each line over the entire Table Bay field campaign

Location ID	Description	No. of samples per line				Total
		A	B	C	D	
1DU	Beach - toe of primary dune	5	3	5	2	15
2BB	Beach - Upper beach	0	0	2	1	3
3BE	Beach - Berm crest	5	3	6	2	16
4MI	Beach - Mid-tide beach face	5	3	6	2	16
5SZ	Swash zone - Beach step	5	3	6	2	16
6S1	Surf zone 1	5	3	6	2	16
7S2	Surf zone 2	5	3	6	2	16
8S3	Surf zone 3	5	3	6	2	16
9S4	Surf zone 4	3	2	3	0	8
03m	Breaker zone - 3m depth	2	1	2	1	6
04m	Breaker zone - 4m depth	3	2	3	2	10
05m	Offshore - 5m depth	4	3	4	3	14
06m	Offshore - 6m depth	4	3	4	3	14
08m	Offshore - 8m depth	4	3	4	3	14
10m	Offshore - 10m depth	4	3	1	1	9
	Total	59	38	64	28	189

A total of 189 samples were collected during six campaigns between 16 September 2005 and 27 September 2006. Lines A and C were sampled most comprehensively, with 59 and 64 samples respectively. The least samples were obtained from Line D – only 28 samples. Not all locations or each line was sampled in each campaign. For example, samples from the Upper Beach location were only obtained at Lines C and D, and then only for a total of three occasions. The beaches were frequently too narrow and/or this region was indistinct from the Dune or Berm Crest.

At times adverse sea conditions prevented sampling of the surf zone, while sampling of the offshore and breaker zones was dependent on both boat availability and favourable weather conditions. Towards the end of the field sampling campaign the boat was unavailable and thus

no offshore samples could be taken. Only beach and surf zone samples were taken on these occasions (25 July and 27 September 2006).

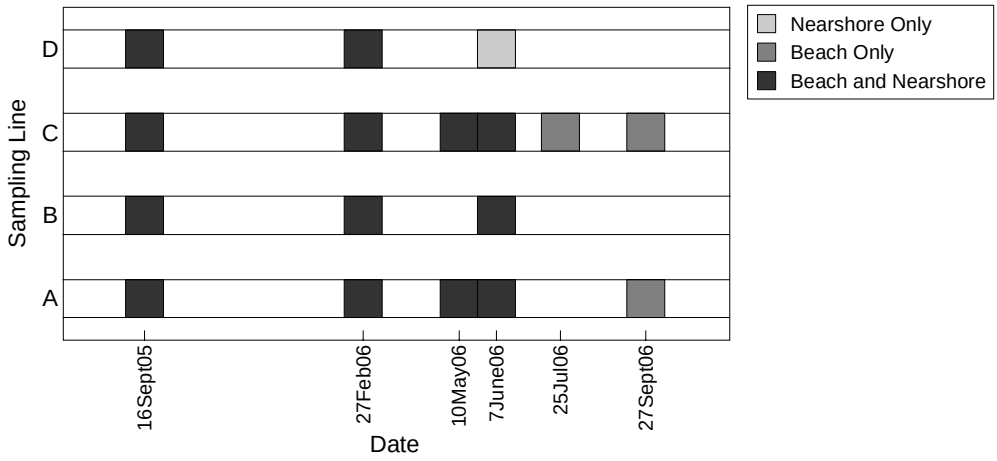

Figure 4.7: Timeline of sampling at each line

4.3 Sample processing

The particle size distribution was analysed using a settling tube at the CSIR's Marine Analytical Laboratory in Stellenbosch. The procedure followed in processing the samples through the settling tube is described in the following section.

4.3.1 Sample Preparation

In the preparation of the samples for grain size analysis, the material in each field sample was re-mixed (some separation of fine and coarse material would occur in the sample bags during transport from site) and split to obtain a sub-sample of approximately 25 ml. The remainder of the field sample was stored in re-sealable plastic bags and refrigerated. The sub-samples were spooned into pre-labelled aluminium foil pans and dried in a laboratory oven at temperatures between 50° C and 80° C for at least four hours. The dried material was then gently disaggregated with a mortar and pestle before being transferred to small re-sealable plastic bags. The disaggregation was required to break up clumps of material that had cemented together during the drying process. Salts were not removed from the samples. The samples were then ready to be analysed for particle size in the settling tube.

4.3.2 Description of settling tube

A settling tube, also sometimes called a fall tube, is an instrument used to determine the natural velocity with which a particle settles through the water column. This velocity is of interest to scientists and engineers because it determines for how long the particle remains

suspended in the water and is thus available to be transported by ambient currents (such as longshore currents in the surf zone).

The settling velocity is determined as follows:

Settling velocity (in m/s) = distance particle falls (in m) / time taken (in s)

The settling tube used in this study is illustrated in Figures 4.8 and 4.9. It is 1.7 m long, in terms of sediment falling distance, with an inner diameter of 150 mm and consists of the following main components:

1. A clear acrylic plate for inserting the sample;
2. A rotating cradle used to hold and lower the insertion plate at the top of the tube;
3. A dip switch that activates the timer;
4. A weighing pan at the bottom of the tube, 1.7m below the water surface;
5. The weighing pan is suspended by three thin, plastic coated wires from a strain gauge that is securely mounted to the wall;
6. A strain gauge amplifier, for amplifying the strain gauge signal;
7. An analogue to digital converter card that accepts the amplifier and dip switch signals and is housed in a PC;
8. Software to process the digitised strain signals.

The method of operation is briefly as follows: A sample, typically 2 – 3 ml of sand, is spread evenly onto the insertion plate in a layer one grain thick. The plate and the sample are moistened with water to ensure adhesion of the particles to the plate. The insertion plate and sample are inverted and placed into the cradle/collar at the top of the tube. Through a rotating motion the cradle is lowered smoothly until the insertion plate and sample make contact with the water. The sample is instantaneously released from the plate (the adhesive forces are broken), the dip switch triggers the PC software timer, and the particles start to fall down through the tube. After falling 1.7 m, the particles land on the weighing pan and the strain gauge registers the increasing strain as more and more of the sample starts to accumulate on the pan.

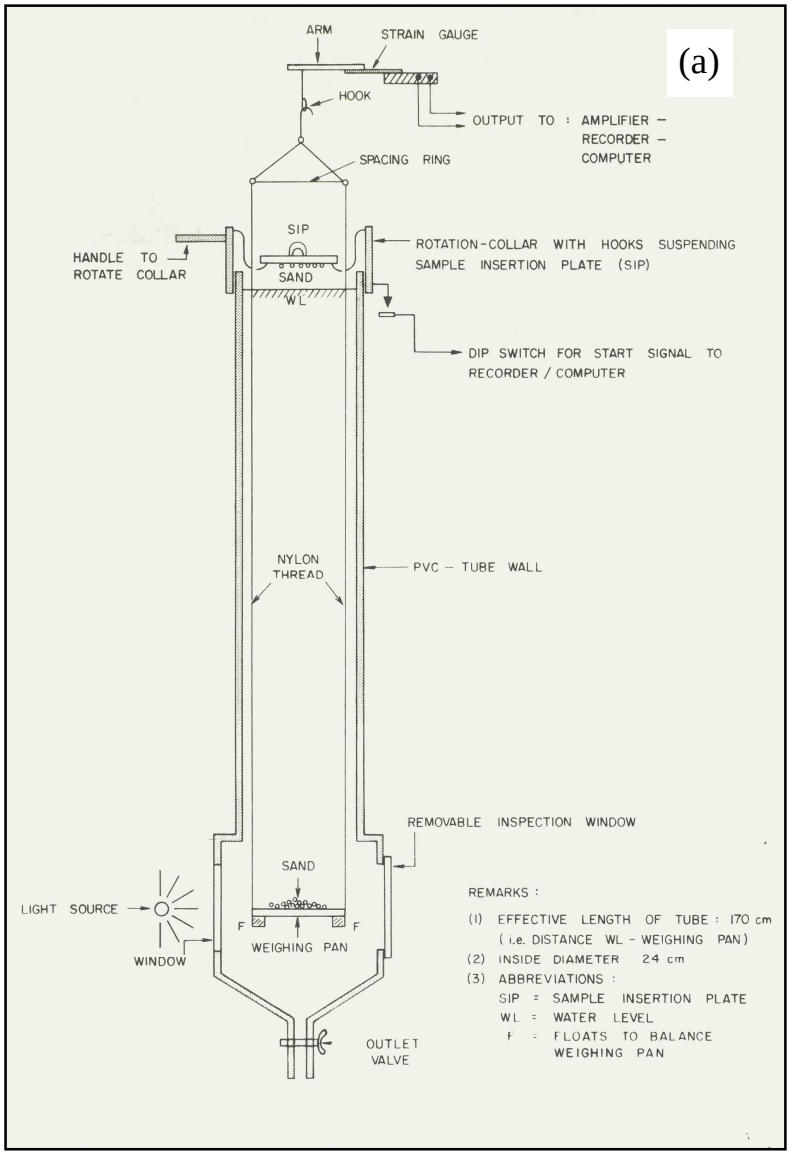

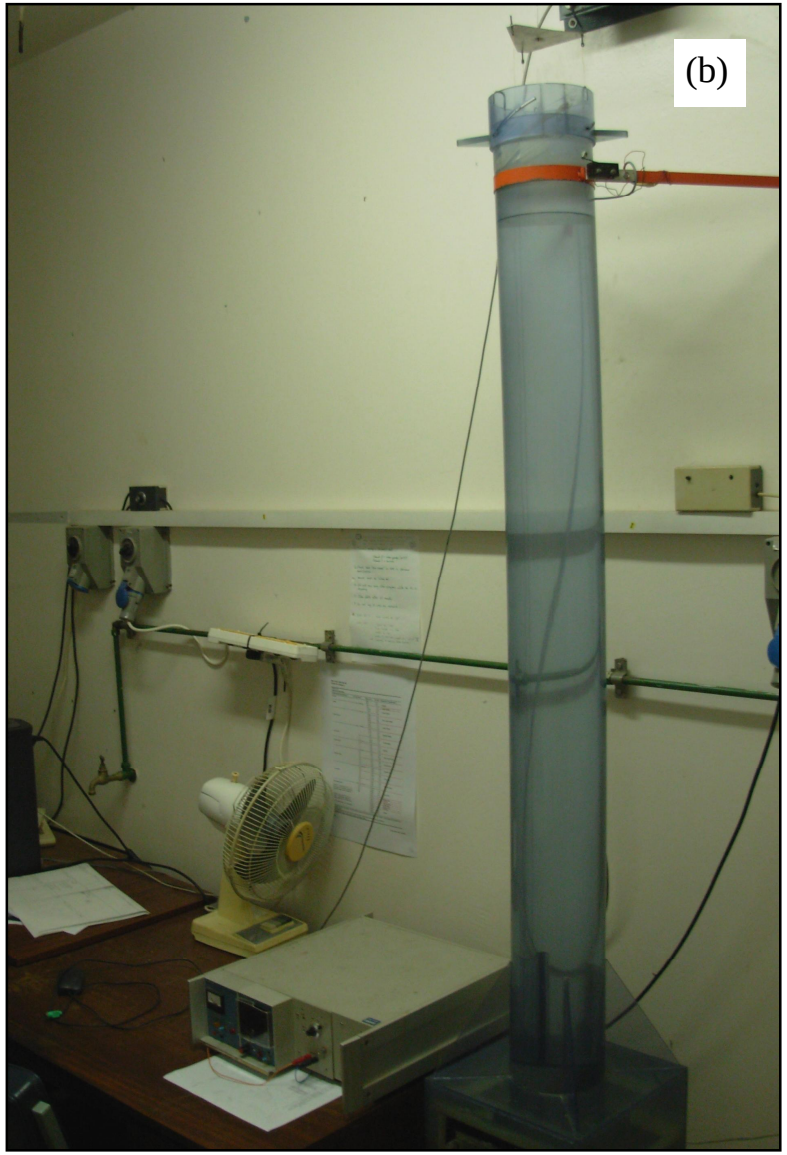

Figure 4.8: a) Schematic of a settling tube (from Fromme, 1977); b) Photo of the CSIR settling tube used in this study

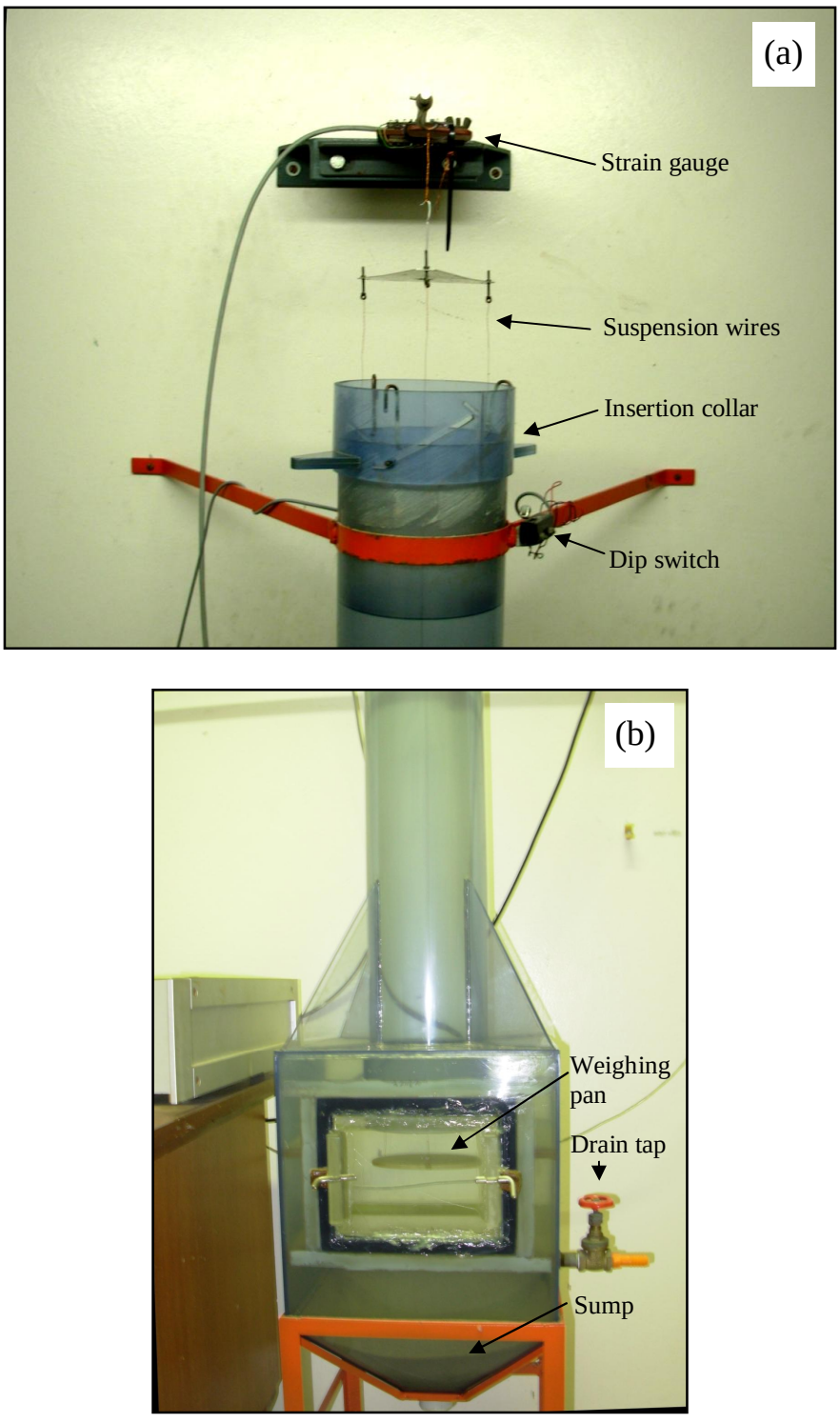

Figure 4.9: a) The upper part of the CSIR settling tube with strain gauge; and b) the lower part with weighing pan

The strain is captured in millivolts on the PC, which provides an instantaneous readout of the sample accumulation. An example result is shown in Figure 4.10 below, with the time after sample insertion shown on the horizontal axis and the increasing strain on the vertical axis.

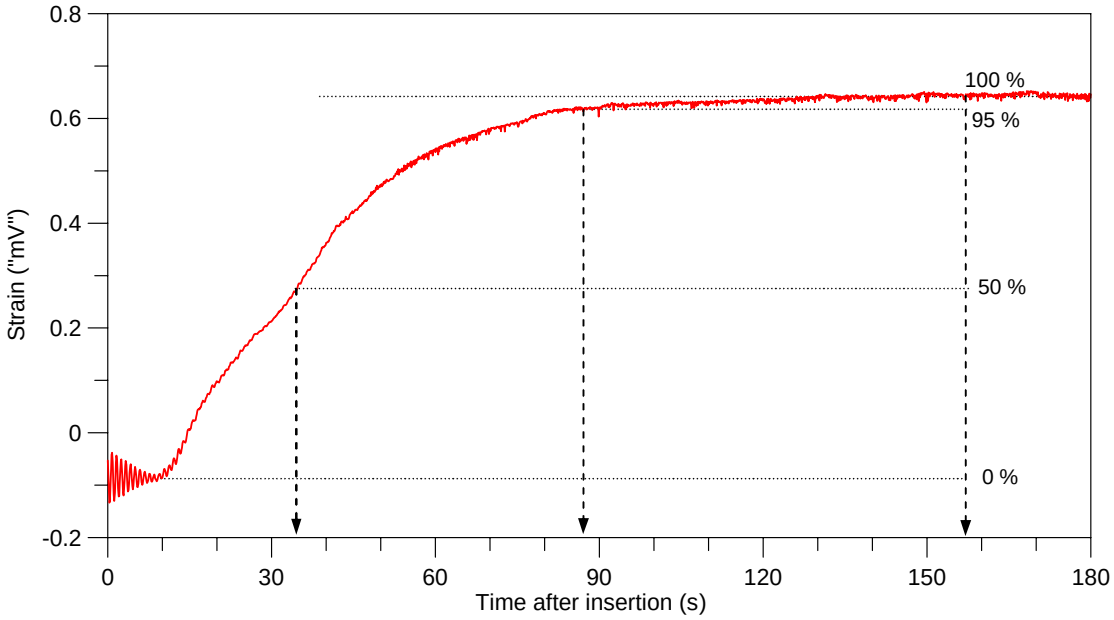

Figure 4.10: Raw output from the settling tube with approximate percentiles indicated

A completed sample shows an "S" shaped curve. In the example shown in Figure 4.10, the lower upward curve of the "S" indicates the first arrival of sand on the pan at approximately 10 seconds, i.e. the coarsest particles which have settled quickest. Material settles fairly rapidly thereafter, indicated by the steep slope. Flattening of the slope occurs after about 40 – 50 seconds as progressively finer material completes its settlement down the tube and accumulates on the pan. All of the particles have settled once the strain reading becomes constant, after approximately 157 seconds. In the example in Figure 4.10, fifty percent of the strain has occurred after approximately 34 seconds. Or, in other words, fifty percent of the material has settled after this time. The median settling velocity would therefore be 1.7 m/34 s = 0.05 m/s.

The instability seen in the strain record in Figure 4.10 during the first few seconds is due to slight disturbance of the strain gauge when the sediment is inserted. This is rapidly damped out.

Advantages of the settling method are given by Fromme (1977) as:

- The grain size characteristics obtained by settling are more representative of the actual hydraulic behaviour of the material than those obtained by sieving;

- The rapid nature of the method allows analysis time to be reduced to approximately a tenth of the time required for sieving. (This was an important consideration for this study);
- Sieving and weighing errors are excluded, while computerisation of the analysis further reduces human error.

The disadvantages of the method are given as:

- Settling results for grains with irregular shape or density will be poorly comparable to corresponding sieve results. For example, heavy minerals such as Ilmenite or Magnetite will appear to have a larger settling size than their corresponding sieve diameter. Flaky or shelly particles would settle slower due to their lower density and greater friction in water (compared to smooth quartz grains), resulting in an apparently finer grain size. On the other hand, in a sieve analysis such irregular shaped particles could be retained on a sieve much coarser than their true size;
- The accuracy of the settling analysis reduces for coarser grain sizes (Fromme indicates >0.5 mm as a reasonable upper limit for the *median* size). Large particles are too heavy to adhere to the insertion plate employed in this tube.
- The method relies on small sample sizes, as large sample sizes result in turbulence in the tube and begin to influence the falling behaviour. A too-small sample can result in a skewed result if it poorly represents the actual sizes present in the larger sample. Larger particles especially may not be represented proportionally.
- Settling velocities increase with increasing sample weight/volume.

For this study, the advantages of the settling method outweighed the disadvantages mainly because of the time advantages in processing the sample through the settling tube. Supporting the choice of the settling method was the fact that all the material would be coming from a similar environment (Table Bay), with sediments being from a similar geological origin. Nevertheless, verification of the settling tube analysis results was conducted.

4.3.3 Settling tube calibration

The settling velocities obtained from the settling analysis are of only limited use in typical engineering applications. The particle size is more frequently useful. The size and settling velocity are related through physical characteristics of the particle, the fluid through which it falls and its falling motion. The settling velocity for an ideal case – a spherical particle in an infinite, still fluid – is given by:

$$W_f = \left(\frac{4}{3} \frac{gD}{C_D} \left[\frac{\rho_s}{\rho} - 1 \right] \right)^{1/2} \quad (4.1)$$

(Equation 1-7, p III-1-21, CEM, 1998)

Where: W_f = fall velocity (m/s)

C_D = dimensionless drag coefficient

D = grain diameter (m)

ρ = density of water (kg/m^3)

ρ_s = density of the sediment (kg/m^3)

g = gravitational acceleration (m/s^2)

Equation 4.1 can be re-arranged to make D the subject and then grain diameters can be calculated from the fall velocity. However, this approach requires that the drag coefficient C_D be accurately known. The drag coefficient is a function of the Reynolds number, water temperature and viscosity and makes the equation difficult to solve in a practical application.

An alternative approach is to obtain a relation between the settling velocity measured with the settling tube and the grain size resulting from a standard sieve analysis of the sample.

This approach was taken by Fromme (1977) in the development of a "Standard Relation Curve" between grain size and settling velocity. Fromme compared a large number of sediment size distributions obtained from standard sieve analyses of typical quartz beach sands from the South African coastline to settling velocity distributions for the same sample. Fromme's relation was improved by Schoonees (pers comm.) using curve fitting to a large number of samples to yield the following relation:

$$D_x = 29730 w_x^2 + 4173 w_x + 67.38 \quad (4.2)$$

Where: D_x is the x^{th} percentile grain size (in microns).

w_x is the x^{th} percentile settling velocity (in m/s).

Equation 4.2 defines a parabolic relation between the settling velocity of a size fraction and its grain diameter. Applying the equation to the sample illustrated in Figure 4.10 (where the settling velocity was estimated to be 0.05 m/s) yields a median grain size of $29730*(0.05)^2 + 4173*0.05 + 67.38 = 350$ microns for that material.

A validation of Equation 4.2 was conducted for this study in order to test whether it was applicable to the material that was to be analysed. Samples from the Table Bay field campaign were sieved and then also run through the settling tube. The resulting sieved grain sizes and settling velocities of each sample are presented in Figure 4.11 with the graph of Equation 4.2 also plotted. Twenty-two actual samples were sieved. The grain size fractions shown are the D_5, D_{16}, D_{50}, D_{84} and D_{95}, i.e. those used most commonly in engineering applications.

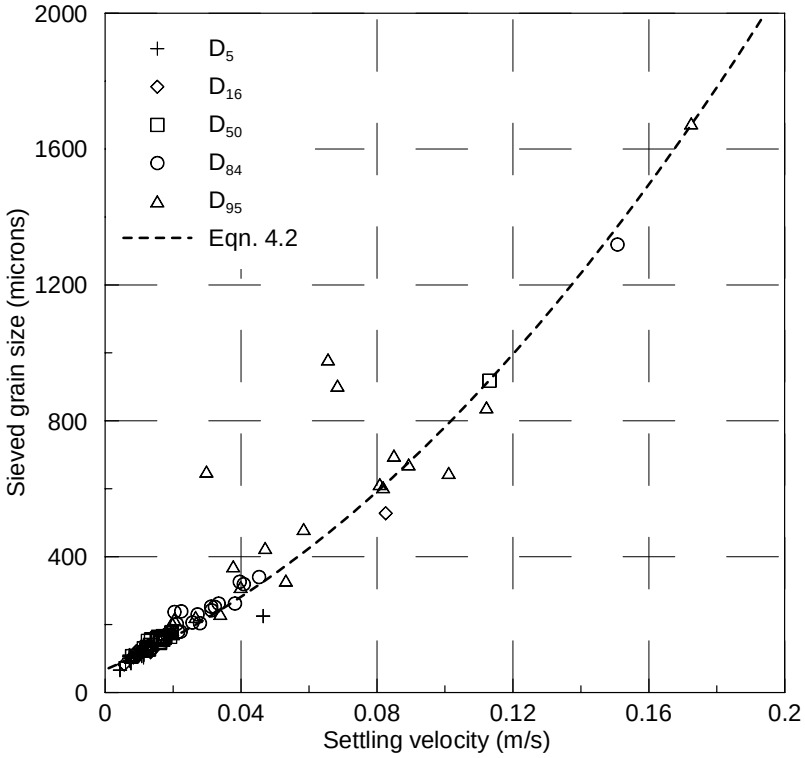

Figure 4.11: Validation of the settling tube with sieved grain size data

The results fit the parabolic relation well, apart from three points that indicate a coarser sieved size than what their settling velocity suggests. Closer examination of these sample points revealed that they are all from the D_{95} level, i.e. the coarse fraction. Visual inspection of the actual sample material indicated the presence of a small quantity of granular material (>2 mm). The remainder of the sample was in the fine sand range (0.125 to 0.250 mm). The coarse particles may not have been included in the small quantity of material used in the settling tube. The samples had skewness values less than -0.3, indicating them to be very

coarse skewed, i.e. a limited proportion of very coarse particles were present. This confirmed the visual observation of coarse grains in the sample.

One of these samples was re-processed in the tube, taking care to include some coarse grains. This led to higher settling velocity, particularly for the D_{95} fraction, meaning a better fit to Equation 4.2. However, considerable manipulation of the test sample was required and this was considered inappropriate. A second attempt to include granules resulted in them not adhering to the insertion plate and falling into the tube prematurely – the mass of the granules was too high.

These samples highlight two of the disadvantages of the settling tube, the first being that the very small sample used for the analysis may not correctly represent a very diverse sample, such as one with a few very large particles in it. Secondly, large particles overpower the sensitive physics/electronics of this tube.

This led to a reversion to sieve analyses for samples where granular content was visible. Five of the Table Bay samples required sieving.

4.3.4 A check on analysis repeatability

A second validation of the settling tube was to see whether repeated analysis of the same sample produced consistent results. This was therefore mainly a test of the effect of only using a very small sample in the tube – how representative would this be of the actual sample. The inter-tidal samples from lines A and C were used, with 18 analyses conducted of sample A4MI4 (Line A, inter-tidal beach position, fourth sampling series) and 25 of sample C4MI2 (Line C, inter-tidal beach position, second sampling series). The inter-tidal beach samples were used as they are of most interest in this study. The results are summarised in Tables 4.2 and 4.3.

Table 4.2: Results of repeatability tests on Sample A4MI4 (18 analyses)

	D_5	D_{16}	D_{50}	D_{84}	D_{95}
Average (microns)	177.4	230.1	304.2	766.1	1104.2
Standard deviation (microns)	8.3	8.3	13.8	47.7	65.0
Std dev as % of average	4.7	3.6	4.5	6.2	5.9

Table 4.3: Results of repeatability tests on Sample C4MI2 (25 analyses)

	D_5	D_{16}	D_{50}	D_{84}	D_{95}
Average (microns)	129.6	147.8	174.4	242.9	324.4
Standard deviation (microns)	3.4	2.7	3.7	7.2	16.2
Std dev as % of average	2.6	1.8	2.1	3.0	5.0

The average standard deviation taken as a percent of the average size was 3.9 percent, with a low of 1.8 (C4MI2, D_{16} fraction) and a high of 6.2 percent (A4MI4, D_{84} fraction). These provide an idea of the reliability of the results when a single sample is analysed. It takes into account deviations in the instrument and sampling procedure, but most importantly provides some quantification of the variation occurring due to using only a very small subset of the actual sample.

It is interesting to note that the variation is larger for samples composed of a larger range of sizes: For sample A4MI4 the D_5 to D_{95} range is 927 microns and the standard deviation as a percentage of the particle size ranges from 3.6 % to 6.2 %, while for sample C4MI2 the corresponding size range is only 195 microns and the standard deviation as a percentage of the particle size ranges from 1.8 % to 5 %. The variation is also larger for the larger size fractions, such as D_{95}, although this trend is not definitive in these limited tests. These observations concur with the finding of Anders *et al.* (1987), who concluded that, when taking samples of the beach, more samples are required in areas of coarse sand in order to reduce variation.

Fromme (1977) found a repeatability error of 1.6 percent in similar tests that he conducted. This is significantly better than that achieved here. However, it is understood that his assessment used samples which had been pre-sieved into a narrow size range and is therefore not directly comparable to the variation found here.

From the calibration and verification tests described above it is concluded that the settling tube method used in this thesis gives reliable grain size analysis results.

Chapter 5: Analysis of Cross-shore Grain Sizes from Three Data Sets

Three sets of cross-shore sediment size data are discussed and analysed in this chapter:

- An extensive dataset obtained from the US Army Corps of Engineers' Field Research Facility at Duck, NC;
- A smaller dataset obtained from Bogenfels beach in Namibia; and
- Thirdly, the samples from Table Bay, South Africa, that were collected and processed during the course of this study, as described in the previous chapter.

This chapter is composed of sections dealing with each set of measurements in succession. For each measurement set, sub-sections provide a brief background to the site, describe the measurement methodology, the analyses conducted for this thesis, and a synthesis of findings. Where relevant, the actual data or a condensed form thereof is provided in an appendix. A summary of the key findings is presented at the end of the chapter.

5.1 Duck

5.1.1 Background

The US Army Corps of Engineers' Field Research Facility (FRF) is located at Duck, North Carolina, on the east coast of the USA. The location is shown in Figure 5.1. The facility is extensively equipped for scientific measurements in the coastal zone, including: a 550 m long pier from which instrumentation can be deployed; permanent weather and wave measurement instruments; an Argus video monitoring station; and equipment for measuring and deploying instruments in the nearshore zone. Photos of the pier are shown in Figure 5.2. A number of large scale measurement campaigns have been conducted at the facility (e.g. Duck94, SandyDuck '97). Other measurements are ongoing.

This section deals with sediment data collected across the beach and nearshore zone at Profile 62 between March 1984 and September 1985. Profile 62 is located 489 m north of the FRF pier. The location and surrounding bathymetry, as measured in November 1984, are shown in Figure 5.3. Stauble (1992) provides a detailed description and analysis of this dataset. His work provides most of the general information used in this and subsequent sections. The raw data from Duck are also accessible from the FRF website (http://www.frf.usace.army.mil), from where grain size, bathymetry and wave data were obtained for this thesis work. The

Field Research Facility, Field Data Collections and Analysis Branch, US Army Corps of Engineers, Duck, North Carolina is acknowledged in this regard.

Stauble (1992) analysed and discussed the changes in sediment sizes over time. His particular interest was to correlate sediment changes to wave energy changes. Although cross-shore size variation is described, the relation between sizes from different morphological regions (e.g. beach vs. nearshore) is not explored.

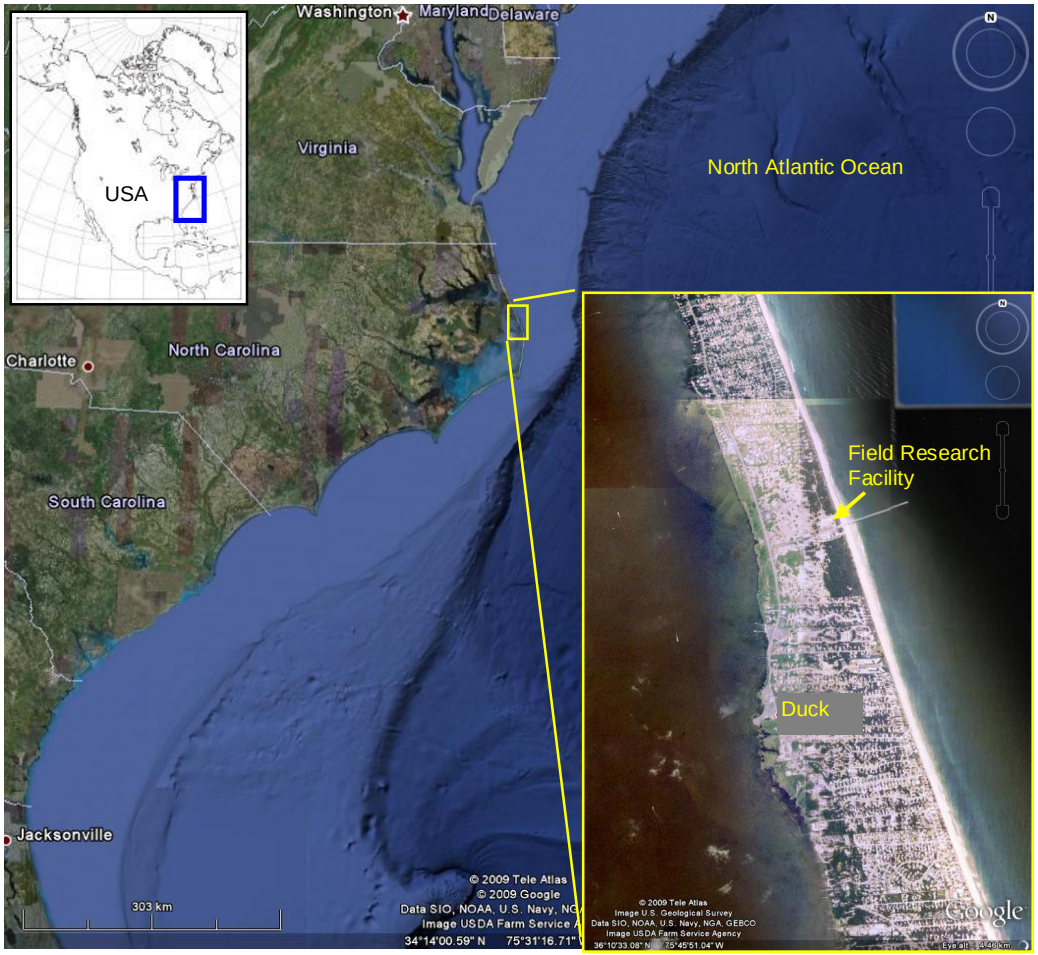

Figure 5.1: Location of the Field Research Facility at Duck, North Carolina

Figure 5.2: Looking southward toward the FRF pier at Duck. The Coastal Research Amphibious Buggy (CRAB) can be seen at sea in right hand photo (images: FRF website)

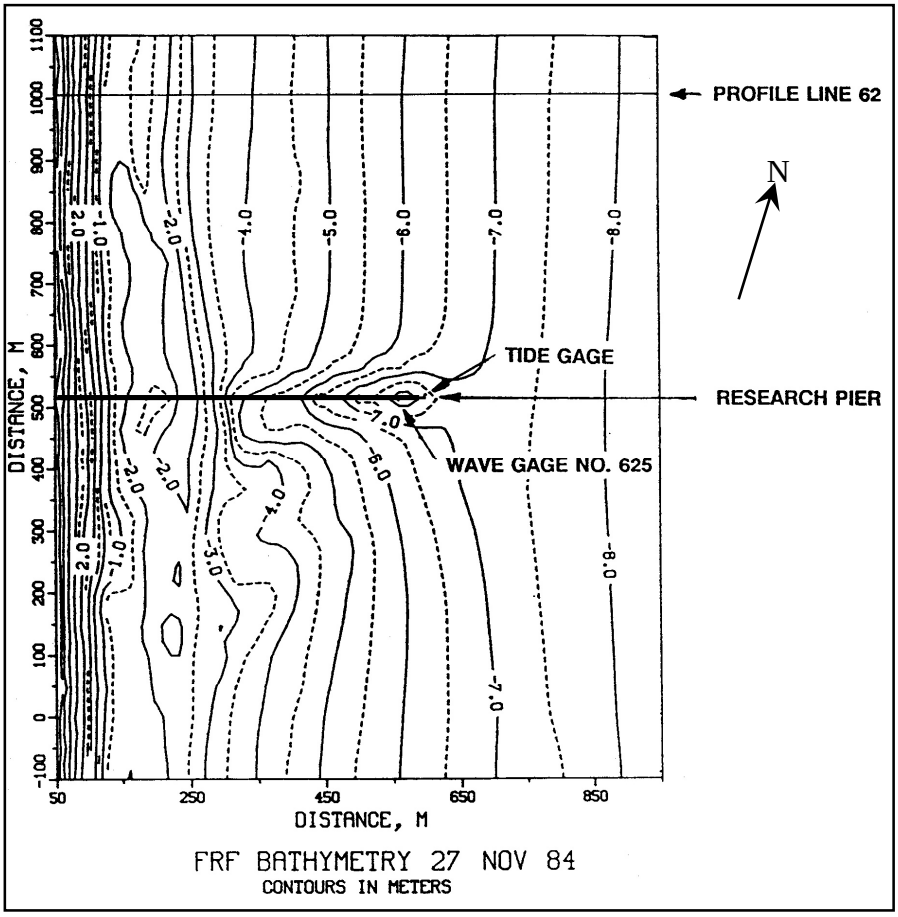

Figure 5.3: General bathymetry at Duck showing position of Profile Line 62 (from Stauble, 1992)

5.1.2 Environmental Conditions

The general environmental conditions are of relevance and are described in this section. The average annual wave height at Duck is approximately 1 m, according to records from the FRF's Waverider buoy. The instrument is located approximately 3 km offshore in a water

depth of 17.4 m. The average period is 8.7 seconds. The typical maximum annual storm wave height is 5 m. The typical tidal range is in the order of 0.8 m. Net longshore transport is from north to south.

Three typical beach and nearshore profiles measured at Profile 62 are shown in Figure 5.4. The inter-tidal beach face generally has a steep slope (1:7 is typical). The profile in the surf zone is very variable, and can evolve from a simple concave profile to one with up to three bars (Stauble, 1992). Different bar configurations are evident in Figure 5.4. Profile changes become less at a cross-shore distance of approximately 400 m. From this point deeper the profile has a gently sloping bottom, ranging from 1:90 at a water depth of 5 m to 1:300 at the end of the surveyed profile (8 m water depth). Birkemeier (1985) indicates the annual storm closure depth is approximately 6 m.

Using the average wave height at breaking and the inter-tidal beach slope, the surf similarity parameter ξ for the beach is determined as approximately 1.4.

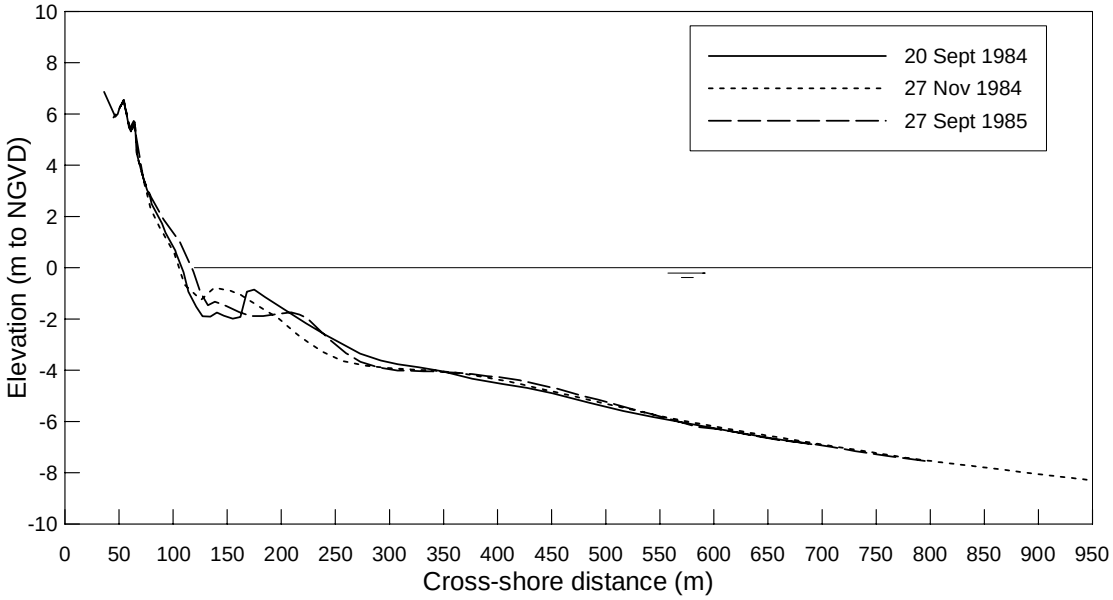

Figure 5.4: Typical beach and nearshore profiles at Profile 62, Duck

5.1.3 Measurement methodology

At Profile 62, 21 complete sets of grain size samples are available from the period March 1984 to September 1985. Each set consisting of samples taken from the dune seawards to approximately the 8 m depth contour, with all samples in a set usually collected on one day. Samples from above the low-water line were taken using a hand scoop. Samples from below the low-water line were collected with a grab deployed from the Coastal Research Amphibious Buggy (CRAB). This is a 10.7 m tall self-propelled tripod vehicle with a manned

operating platform at its apex, as shown in Figure 5.5. The CRAB can be used in wave heights of up to 2 m and water depths of up to 8 m. Bathymetric profiles were measured concurrent with the sediment sampling, using the CRAB as base for both. According to Stauble (1992), sediment samples were analysed using a sonic sifter instrument (i.e. sieving) at quarter phi intervals.

Figure 5.5: The CRAB amphibious buggy used to measure bathymetry and obtain grain size samples at Duck

In general, samples were taken at 17 cross-shore sampling stations along the profile line, as illustrated in Figure 5.6: two in the dune (Stations 1 and 2), four on the beach berm and inter-tidal area (Stations 3 to 6), four through the inner bar and trough area (Stations 7 to 10) and seven from the seaward edge of the inner bar to the limit of the profile (Stations 11 to 17). This provides a very detailed coverage of the profile, with stations spaced between 10 and 150 m apart, distances between offshore stations being greater than those between stations on the beach. The sampling attempted to locate each station at the same position during each sampling set, within the range bracket as shown in Figure 5.6. The location of the sampling stations did vary from one sampling set to another, but generally there was little or no overlap between adjacent stations.

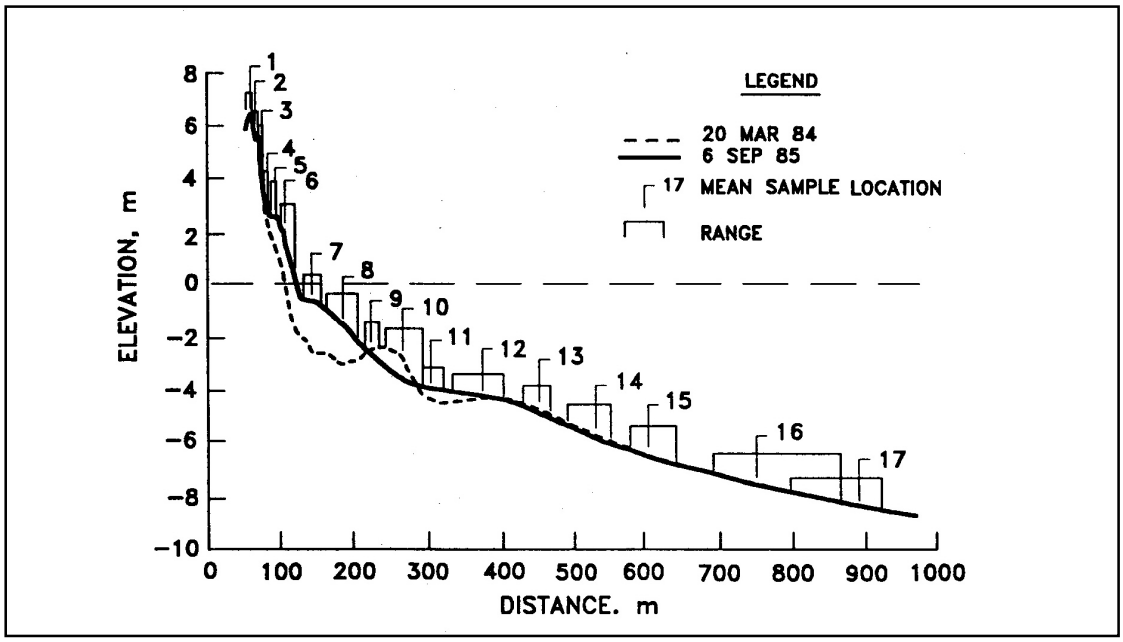

Figure 5.6: Location of cross-shore grain size sampling stations at Duck (from Stauble, 1992)

Sampling was conducted approximately monthly, although intervals were shorter or longer at times. The sampling period extended over 18 months and includes two summer and one winter period (northern hemisphere). The 21 sample sets consist of 319 individual sediment samples. Analysis and discussion of the grain size data follow.

5.1.4 Data Analysis

The sediment data from the FRF is provided in a sorted and classified format. All grain size fractions are available, together with the mean and median sizes. The following further processing was done for this study:

- Sorting to label each sample according to its location on the profile (numbered 1 to 17 in accordance with the designation of Stauble (1992), shown in Figure 5.6). This would allow the changes in grain size at the sample location to be evaluated temporally.
- Aggregation of samples in each set according to common beach or nearshore zones, as described further below.

This latter step was regarded as the most important part of the data processing. The samples were categorised into the following four zones:

1. Inter-tidal beach zone;
2. Surf zone;
3. Nearshore zone;
4. Longshore transport zone.

There is of course some overlap in these four categories – the surf zone is also part of the longshore transport zone – and this is intended, seeing as the aim is to look at the relation between and within zones. Stauble (1992) strictly investigated the dune, beach, bar/trough and nearshore zones. For this study the data were sorted so as to specifically examine the grain sizes in the longshore transport zone. Samples from the swash zone were not included in any of the four groupings. Due to strong cross-shore sorting processes, this narrow zone is usually dominated by very large particles.

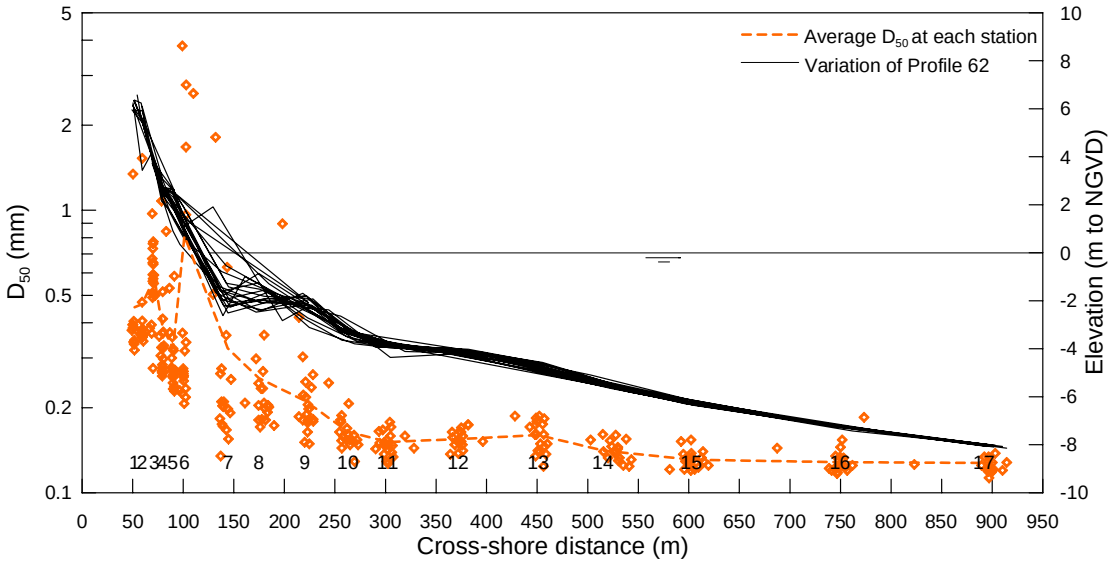

Figure 5.7: Median grain size at each cross-shore station for all 21 sampling sets, together with all Profile 62 profile measurements

The median size at each sampling station is plotted in Figure 5.7. The dots indicate the data from each sample set, while the dashed line indicates the average at each station. Grain sizes are plotted on a log scale (left side axis). The solid lines show the beach and nearshore profiles measured during the same period as the grain size sampling – March 1984 to September 1985.

It is observed that grain sizes become finer in the seaward direction. The beach sizes range between 0.2 and 4.0 mm, while nearshore sizes are typically finer than 0.2 mm. There is considerable variation at each sampling station – station numbers are indicated along the bottom of Figure 5.7. Most variation occurs from the dune (Station 1) to the inner surf zone (Station 9). The median sizes measured at what was defined by Stauble as the inter-tidal zone, Station 6, show the most variability, due to the occurrence on a number of occasions of very coarse material in this area – the smallest median size measured was 0.207 mm and the largest 3.82 mm. According to Stauble (1992), the beach material at Duck contains a layer of granular material (2 to 4 mm size range) that occasionally becomes exposed. Further, Stauble

(1992) indicates that samples at Station 6 were "collected somewhat randomly throughout the inter-tidal area and made it difficult to characterize this important zone." (p. 45). It is thus possible that at times the samples may have included material from the aforementioned granular layer or from the coarse swash zone.

It is likely that the samples from Station 6 do not provide a consistent indication of the samples to be found at the mid-tide line (which is, according to Bascom (1951), the suggested point to sample if the beach material is to be represented by a sample from a single location).

The median size for each of the samples from Station 6 is plotted against sorting in Figure 5.8. Most of the samples are grouped around an average of 0.265 mm (standard deviation 0.046 mm), with four clear outliers that are greater than 1.5 mm. Four of the 18 data points would need to be discarded if this station is to be used for comparisons. The number of samples which can be analysed and on which conclusions can be drawn would then be reduced. It would be useful if instead a different sampling station can be used to represent the inter-tidal beach zone.

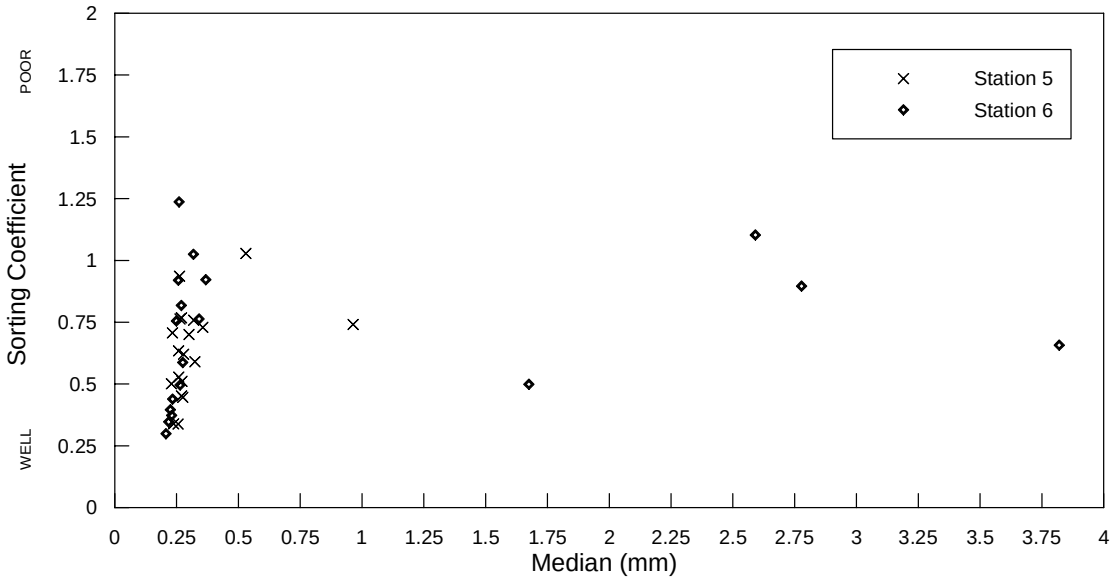

Figure 5.8: Median size (mm) vs. sorting at Stations 5 and 6

Also shown in Figure 5.8 are all the median sizes from Station 5. This station was usually located at the berm crest and therefore still within the active zone of the beach, albeit not as ideally as the mid-tide position. The average at Station 5 (0.274 mm, standard deviation 0.033 mm) is similar to Station 6 if the latter's outliers are ignored. Although there are two outliers in the Station 5 data, both of these are less than 1 mm. At the time that the outliers were found at Station 6, the samples at Station 5 did not show a similar swing to the coarse side.

There is thus fair agreement in grain sizes at Stations 6 and 5 for non-outlier samples. Station 5 will therefore be used in place of Station 6 to represent the inter-tidal beach at Duck in further analyses.

5.1.5 Longshore transport zone grain sizes

It was observed by Stauble (1992) that during the 18 months of his grain size measurements, the main changes of the beach and nearshore profile occurred only up to about the 4m depth contour. This is somewhat shallower than the approximately 6 m depth of closure measured and calculated by Birkemeier (se Section 5.1.2). The difference between the two may be due to Birkemeier applying a much smaller tolerance – several centimeters only – to defining the point beyond which no profile change occurs, while this level of precision was not the focus of Stauble's work. Whatever the case may have been, this difference in the depth of closure estimation points to it being at best only a rough estimate of the seaward limit of the longshore transport zone.

Further investigate was carried out by using "LongshoreTransport" module of the UnibestCL+ model (WL|Delft, 2005) to calculate the cross-shore distribution of longshore transport. The model gives a reasonable impression of the change in longshore current and transport across the profile (see Chapter 2). For this application at Duck, the three typical profiles shown in Figure 5.4 were used. A default grain size of 0.2 mm was used. The wave conditions used were those from 2008, as directional data were not recorded prior to 1996. One condition per 24 hour period was simulated, to ensure a variety of conditions. The average wave height was 0.94 m, with minimum and maximum of 0.27 and 2.8 m respectively.

The resulting transport distributions are shown in Figure 5.9. Three groups of transport distributions are shown, one for each of the three profiles illustrated in the figure. The same wave conditions discussed above were applied for each of the three profiles. In order to simplify the figure, only the positive distributions (i.e. those for southward longshore transport at Duck) are shown.

With reference to Figure 5.9, the larger waves result in transport occurring at greater depths and distances offshore, as seen in the peak in transport at a cross-shore distance of about 450 m. At this location the three nearshore profiles are very similar, with a subdued offshore

bar visible. All three distributions show a strong second peak prior to the inner bar. Transport rates reduce in the trough area, before a final, small, peak just seaward of the shoreline.

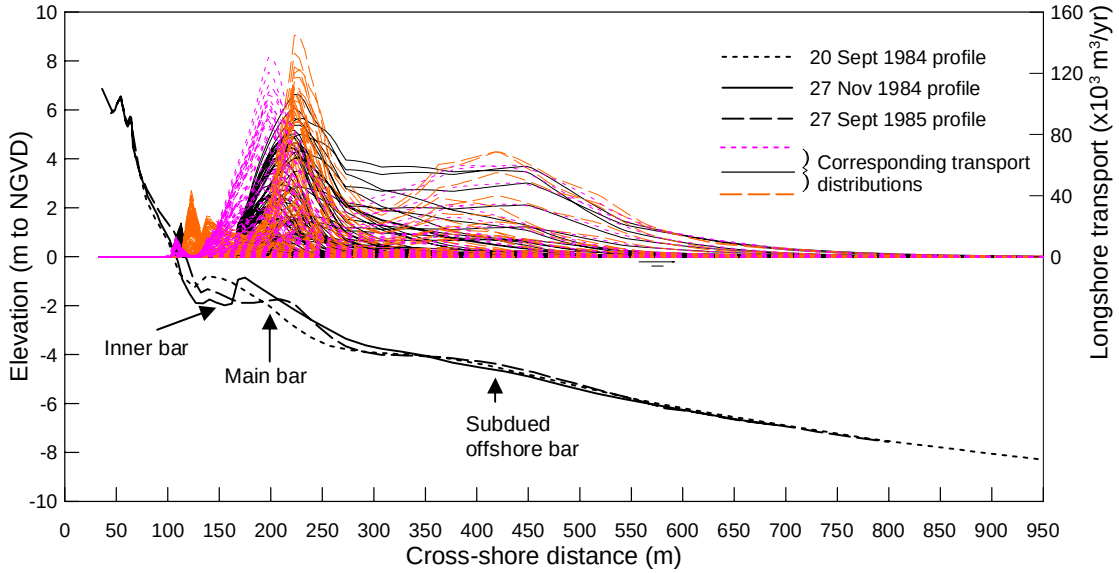

Figure 5.9: Cross-shore distributions of longshore transport simulated for three profiles at Duck

While great effort can be expended to discuss and analyse these transport distributions, it must be borne in mind that they are indicative only. The purpose here is to use them only to gain a better impression of where on the profile, and at what relative intensity, longshore transport occurs.

In general, therefore, it appears that most transport occurs from just seaward of the main bar, indicated in Figure 5.9, to the shoreline. This seaward point corresponds to a depth of approximately 3 m. Under large waves, though, transport occurs from seaward of the subdued offshore bar to the shoreline. The seaward point of transport then occurs at a depth of approximately 5 m. Both of these positions (3 m and 5 m depth) are shallower than the 6 m depth of closure indicated by Birkemeier. Stauble's observed depth of closure during the grain size measurements (4 m) lies between the two positions. Depending on the wave conditions, the seaward end of the longshore transport zone can be quite different. For this analysis, the 5m depth point will be used as it includes the effect of typical larger waves. Beyond this point, grain sizes become uniformly fine (see Figure 5.7).

The 5 m depth point lies approximately 450 m from the survey baseline at Profile 62 at Duck. This corresponds to about Station 13 in the Duck cross-shore sampling scheme – see Figure 5.7. As a first approximation, this point will be used as the seaward limit of the longshore transport zone. Stations 5, 7, 8, 9, 10, 11, 12 and 13 fall within this assumed longshore transport zone (Station 6 being excluded).

The median beach grain size (Station 5) is compared to the average of the median sizes from this longshore transport zone (Stations 5, 7, 8, 9, 10, 11, 12 and 13) in Figure 5.10 for each sampling set. For brevity, the term longshore transport zone will be abbreviated to LTZ. In Figure 5.10, the data are closely grouped, apart from one clear outlier (the 27 November 1984 sample set had a median beach size of 0.964 mm compared to the average of 0.274 mm), and indicate that the grain size in the LTZ is smaller than the inter-tidal beach size. The average beach size is 0.29 mm while the average LTZ size is 0.20 mm. The LTZ and inter-tidal beach size can be compared by considering the ratio between the two.

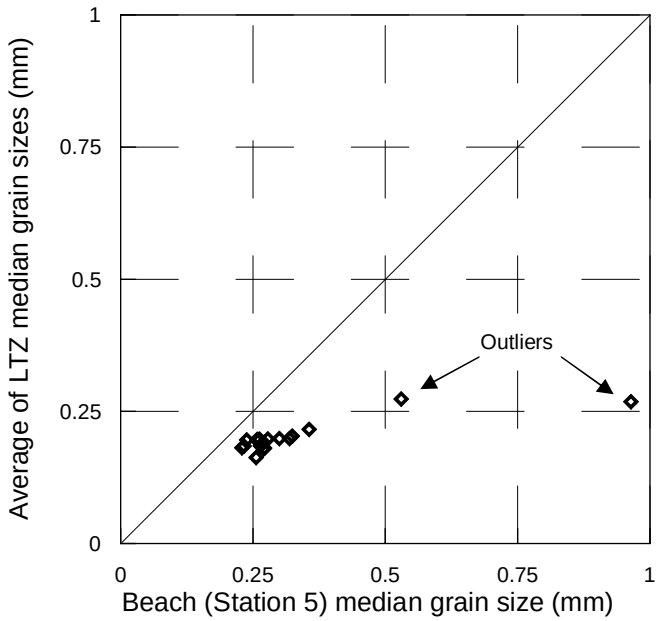

Figure 5.10: Longshore Transport Zone size compared to beach size for each sampling set

This ratio, of LTZ-to-beach median size, was calculated for each of the sample sets and is plotted in Figure 5.11. The LTZ-to-beach median size ratio lies between 0.6 and 0.8, except for two lower values (one being the earlier mentioned outlier) and one higher value. Disregarding the outlier, the average of the remaining 17 sets is 0.69 (standard deviation 0.08), indicating that the LTZ grain size is only 69 % that of the beach.

There is some variation of this ratio in time (Figure 5.11). It is possible that changing wave conditions, particularly storms, affect the distribution of particle sizes across the profile. A number of high wave events did occur during the sample period – the wave heights recorded in 17.4 m water depth offshore of the FRF pier at Duck are also shown in Figure 5.11. However, there is no clear response in the LTZ-to-beach median size ratio to wave height changes. The largest storm, with wave height exceeding 6 m, occurred after the sampling period. It could be that the moderate storm events that occurred during the sampling period

were of insufficient energy to change the grain size patterns. Alternatively, the LTZ-to-beach median size ratio is unaffected by storm events.

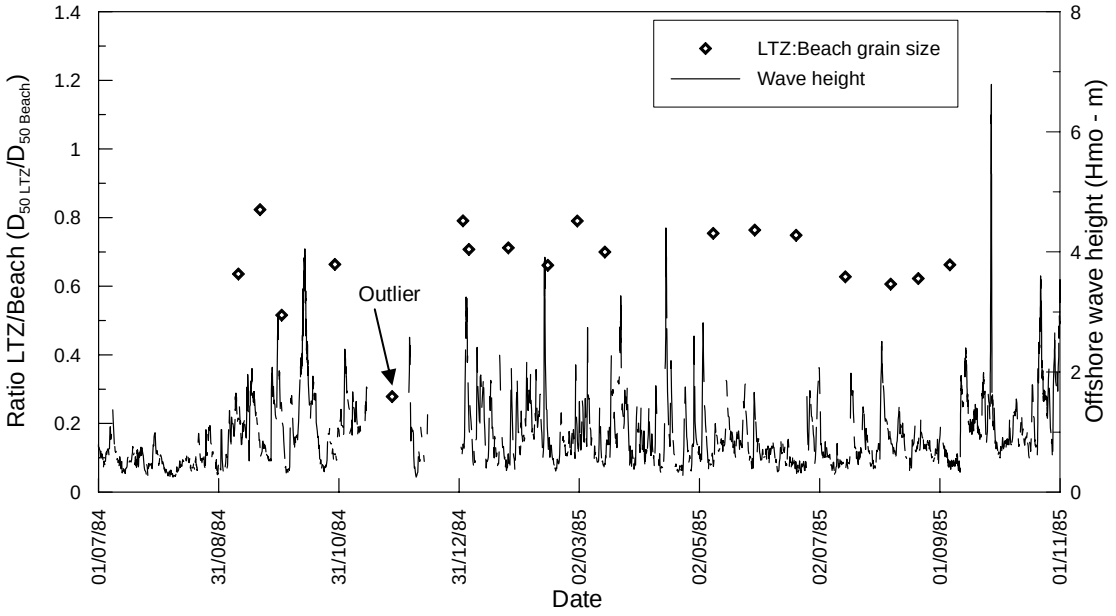

Figure 5.11: LTZ to beach grain size ratio in time compared to offshore wave heights at Duck

5.1.6 Synthesis

The comprehensive and detailed data from Duck show that the grain size on the inter-tidal beach is coarser than that in the longshore transport zone. It has been possible to substitute samples from the beach berm with those from the inter-tidal zone. Samples from the swash zone have been excluded due to the presence of large particles in this region of the profile at Duck. The extent of the longshore transport zone has been taken from the top of the beach berm to the seaward limit of typical longshore transport. The latter limit was evaluated using calculations of the cross-shore distribution of longshore transport.

A note of caution is here raised regarding the use of the depth of closure as representing the seaward limit of the longshore transport zone – it appears that this would overestimate the distance seaward to which longshore transport occurs. It is probable that the methods of Hallermeier and Birkemeier are too pedantic in defining the seaward limit of sediment movement for the purposes needed here.

The average ratio of the median LTZ-to-beach grain size for 17 cross-shore grain size sample sets at Duck has been determined to be 0.69. The ratio is reasonable consistent during an 18 months sampling period, the standard deviation being 0.08. There is no clear correlation to

changes in wave conditions during the year of grain size measurement. This average ratio has a very similar value to the inverse of the surf similarity parameter, i.e. $1/\xi = 1/1.4 = 0.7$.

5.2 Bogenfels

The second cross-shore grain size data set discussed here was obtained from Bogenfels beach.

5.2.1 Background

This isolated beach is located in southern Namibia (Figure 5.12), on a coastline exposed to severe wave conditions year round. Bogenfels beach is 3.5 km long and is one of a series of sandy beaches interspersed with rocky headlands. A photo looking downcoast (south-eastward) from a high ridge at the northern end of the beach is shown in Figure 5.13. A view of the beach is shown in Figure 5.14.

Bogenfels lies within a restricted mining area. During the course of investigations undertaken for the mining operation, it was possible to obtain (limited) bathymetric and cross-shore grain size data.

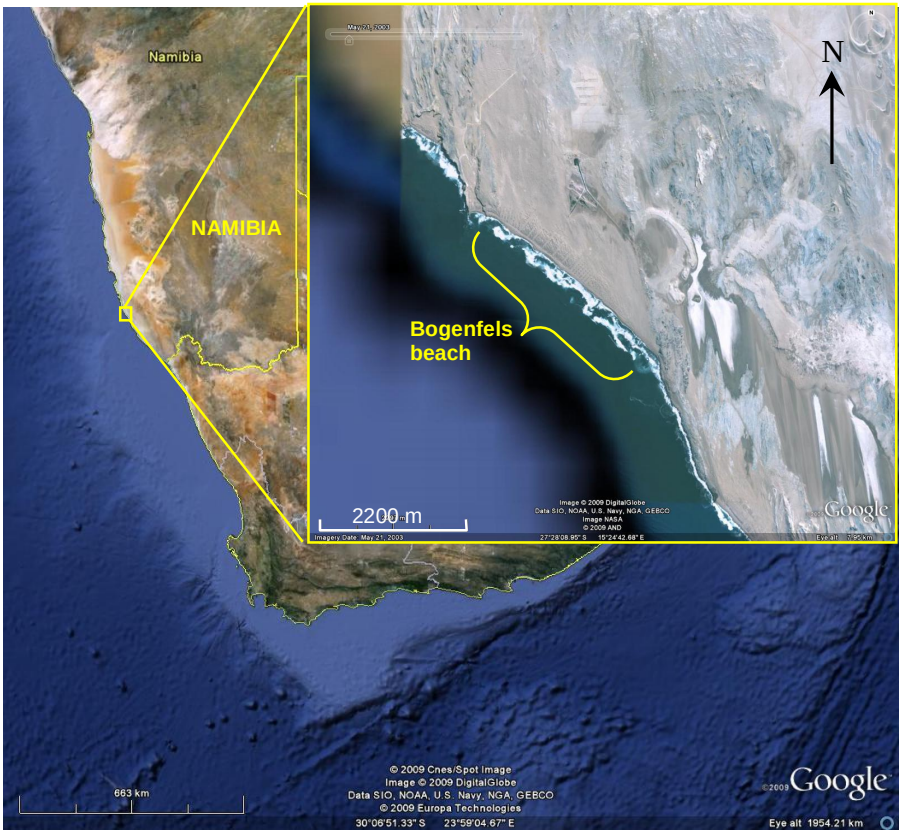

Figure 5.12: Location of Bogenfels beach

Figure 5.13: Oblique view looking south-east along Bogenfels Beach from the high ridge at its northern end

Figure 5.14: Photo of the inter-tidal beach at Bogenfels

5.2.2 Environmental conditions

The annual average offshore wave height is approximately 2 m, with an average period of 11 s. The annual highest offshore storm wave height is in the region of 6 m. The wave climate is thus considerably more energetic than at Duck, where the corresponding average wave height and period are only 1 m and 8.7 s respectively. The net longshore transport rate at Bogenfels is northwards.

The surf zone at Bogenfels, seen in Figure 5.13, is typically up to 300 m wide. Waves generally break on an offshore bar and may re-form and break again before finally plunging on the beach. This powerful final breaking point usually occurs as a plunging and surging breaker in the swash zone, as is visible in Figure 5.14.

The beach is typically steep, with an average slope in the order of 1 in 8. A beach and nearshore profile measured in May 2002 is shown in Figure 5.15. The offshore seabed also slopes steeply (slope 1 in 37), with the 30 m depth contour located only 1.3 km offshore. Seaward of this point the seabed profile starts to flatten somewhat.

Using the mid-tide beach slope and the average wave parameters seaward of breaking, the surf similarity parameter, ξ, has a value of 1.11.

A longshore bar is located some 275 m offshore, noting that profile data in the surf zone is lacking (the dotted line shown in Figure 5.15 indicates that this part is inferred). Observation of wave breaking patterns suggests the presence of a bar/trough system and that there can be multiple bars in the surf zone.

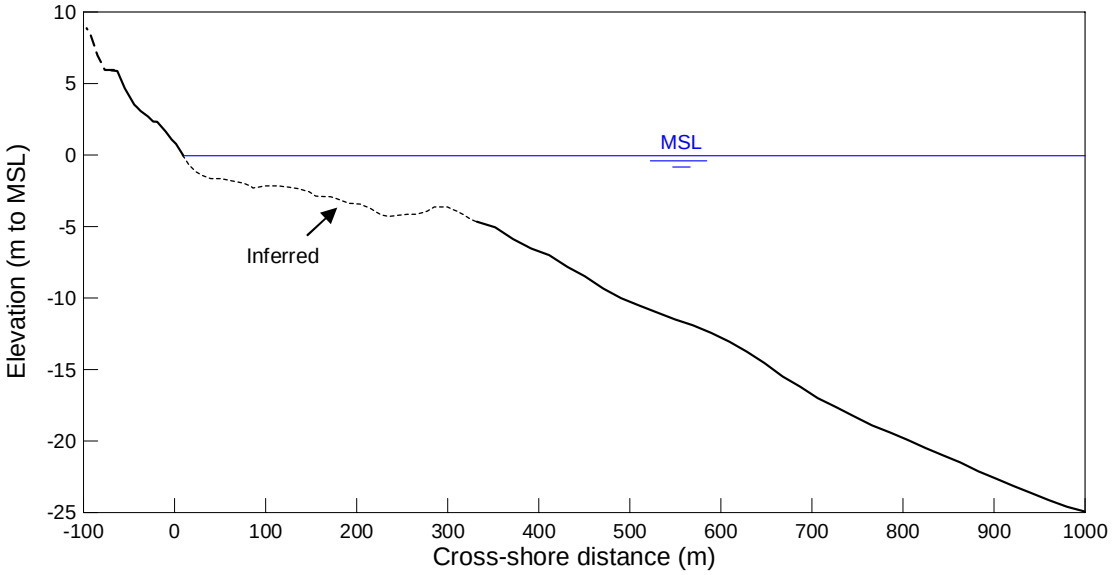

Figure 5.15: Typical beach and nearshore profile at Bogenfels

5.2.3 Measurement methodology

The grain size distribution data were obtained from two sampling lines, Line A and Line B, location shown in Figure 5.16. The lines were located approximately 750 m apart. Divers used 0.2 m long PVC core tubes to obtain between 300 and 1500 g of sand from the surface layers. Sample locations were planned to coincide with profile zones: upper beach, mid-tide

level, beach step, inner surf zone (two samples), trough, bar, seaward of bar (three samples). The location of the samples on the profile is shown in Figure 5.17.

Ten samples were obtained from Line A and nine from Line B. Sampling was conducted on a single occasion only (28 January 2005), yielding a limited dataset. The analysis of the data is therefore more simplistic: Outliers are not as easy to pinpoint and remove as this would reduce the size of the dataset too much; and natural variation cannot be accounted for, creating greater spread in the data.

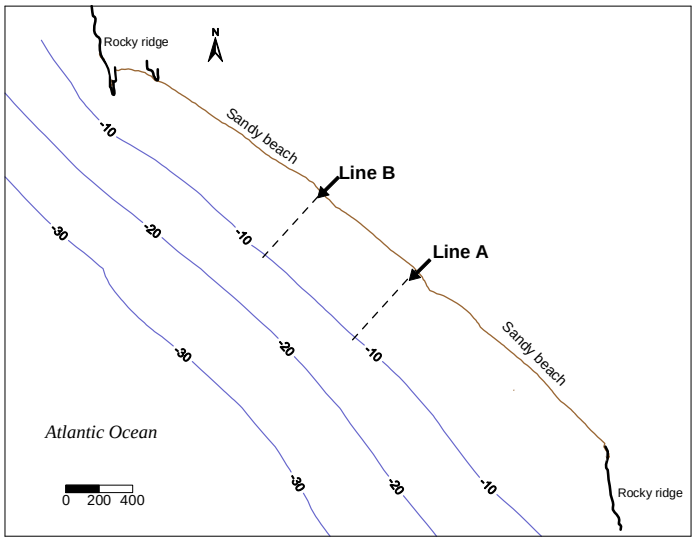

Figure 5.16: Location of the sediment sampling lines at Bogenfels

Sediment sizes were obtained by dry sieving. Only a limited range of sieves was available: 4.0, 2.8, 2.0, 1.4, 1.0, 0.71, 0.5, 0.25, 0.09 and 0.045 mm, much fewer than the recommended quarter phi intervals. The resulting grain size distributions were therefore somewhat unrefined and percentile calculations of lower precision than are considered ideal.

5.2.4 General grain size observations

The median grain sizes are shown superimposed on a typical beach and nearshore profile in Figure 5.17. It is immediately clear that the beach and the nearshore grain sizes are very different. The following are observed from the data shown in Figure 5.17:

- The median size decreases from the beach in the offshore direction;
- Sizes peak at the base of the beach profile, at the beach step (Station 3). There is a secondary peak in the area presumed as the bar (Station 7). (The position of the bar/trough during the sampling is not precisely known, as the nearshore profile shown in Figure 5.17 was not measured concurrent to the sediment sampling);
- Grain sizes seaward of the bar show a slight continuation of the fining trend;

- Both sampling lines show a similar pattern, although Line A had an additional coarse sample (Station 4 in Figure 5.17) in the inner surf zone.

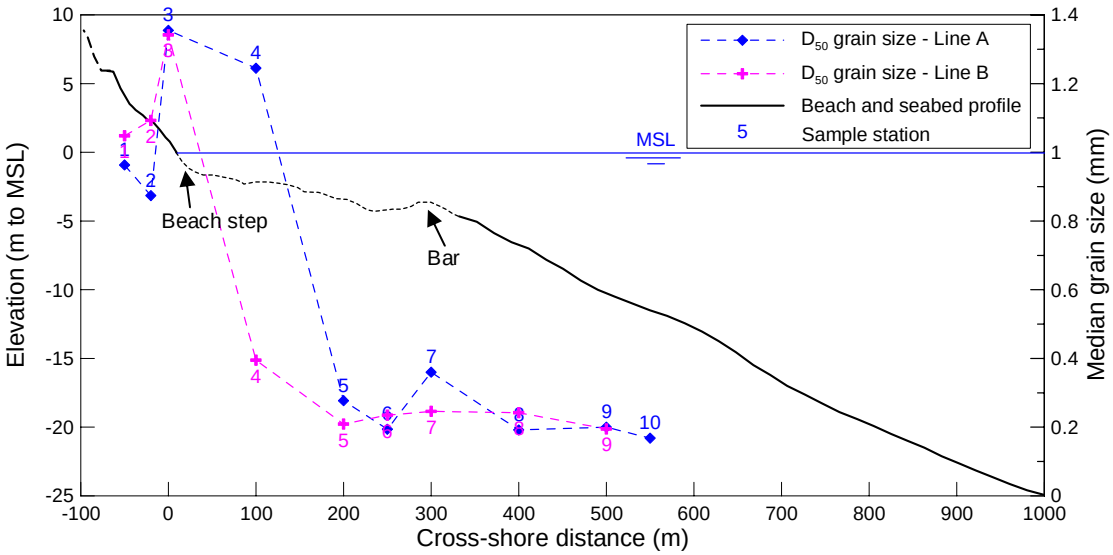

Figure 5.17: Cross-shore profile and median grain size at Bogenfels

5.2.5 Beach sizes

Stations 1, 2 and 3 (Figure 5.17) are from the beach. However, Station 1 was located at the base of the dune and thus unlikely to be frequently affected by wave transport mechanisms. Station 2 was located on the inter-tidal beach at the mid-tide level. This is the point that can be regarded as representative of the beach, Bascom's (1951) reference point. Station 3 was located at the beach step and thus, unsurprisingly, had the coarsest sizes, at well over 1 mm. Samples from this station will not be used in the size comparisons.

Therefore, sizes that will be used to represent the beach (Station 2) are 0.87 and 1.10 mm at Lines A and B respectively. The average of the two is 0.98 mm.

5.2.6 Longshore transport zone grain size

No repetitive bathymetric measurements are available at Bogenfels to delineate the zone of typical sediment movement, as was possible at Duck. Calculation of the cross-shore distribution of longshore transport was therefore used to delineate the longshore transport zone, as in Figure 2.2 (Chapter 2) and at Duck in the previous section. This was done with the Unibest model for 670 typical wave conditions that ranged in height from 5 m to 0.2 m at 12 m depth. The resulting individual distributions are shown together in Figure 5.18 for the Bogenfels typical cross-shore profile. (It should be noted that in Figure 5.18, the same

durations are assigned to each wave condition and the transports shown are therefore not representative of the net longshore transport at this beach).

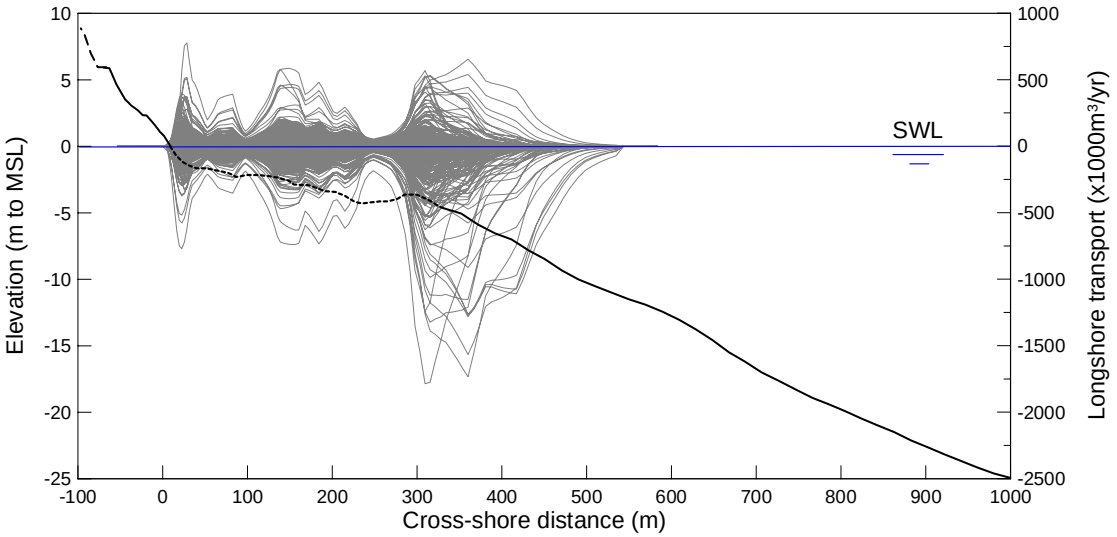

Figure 5.18: Calculated cross-shore distribution of longshore transport for typical wave conditions

Considerable variation is evident, as would be expected for the large number of wave conditions used and the irregular shape of the profile in the surf zone. The graphs in the figure reveal a large peak in transport at the seaward point of the longshore bar, with secondary peaks in the inner surf zone, which is generally less than 3 m deep in this case. A final peak occurs at the shoreline. These calculated distributions of longshore transport indicate the seaward limit of significant transport to occur seaward of the bar, or a depth of approximately 7 m in Figure 5.18. Only limited transport is calculated to occur seaward of this point and then only for extreme conditions. This point will therefore be termed the **likely** limit of longshore transport.

Applying Birkemeier's (1985) depth of closure method to the annual storm wave height (6 m offshore) yields a seaward limit of profile movement of 9.9 m to MSL (mean low water taken as -0.5 m MSL). With reference to Figure 5.18, longshore transport to this depth would clearly occur very infrequently, if at all. This can be termed the **extreme** limit of longshore transport.

Birkemeier's method is typically applied to determine the annual depth of closure, and therefore the annual, extreme, wave height is used. However, it is useful here to provide an indication of more typical closure depths by assuming the effective wave height to be the average wave height at Bogenfels (2 m). This yields a depth of closure of 3.5 m to MSL,

which corresponds approximately with the crest of the longshore bar in Figure 5.18. This point can be regarded as the **average** limit of the longshore transport zone.

The grain sizes from the likely, extreme and average longshore transport zone were compared as follows (sample positions as shown in Figure 5.17):

- Median sizes from each zone for Lines A and B were averaged;
- The mid-tide sample (Station 2) was used to represent the beach;
- Samples from position 2, 4, 5, 6, 7 and 8 were used to represent the **likely** longshore transport zone. Grain sizes from the beach, surf zone, trough, bar and seaward of bar were included;
- Samples from position 2, 4, 5, 6, 7, 8 and 9 were used to represent the **extreme** longshore transport zone. Grain sizes from the beach, surf zone, trough, bar, seaward of bar as well as depth of closure were included;
- Samples from position 2, 4, 5 and 6 were used to represent the **average** longshore transport zone. Only grain sizes from the beach, surf zone, trough and bar were included;
- In all three cases, samples from the beach step (Station 3) were excluded.

The resulting D_{50} grain sizes are summarised in Table 5.1 below.

Table 5.1: Longshore transport zone grain size at Bogenfels

Definition of longshore transport zone:	Beach (mid-tide) median size (mm)	LTZ median size (mm)	LTZ-to-Beach ratio
Likely (beach to seaward of bar)	0.98	0.45	0.46
Extreme (beach to annual depth of closure)	0.98	0.41	0.42
Average (beach to average depth of closure - bar)	0.98	0.51	0.52

The data indicate a longshore transport zone to beach size ratio of between 0.42 and 0.52, with a likely value of 0.46.

5.2.7 Synthesis

The samples from Bogenfels indicate fining of material in the offshore direction. Similarly to Duck, the material in the swash zone was coarse and granular and was excluded from the analysis. The small overall data set – only two sample sets – leads to uncertainty in the grain size analysis. It is therefore not possible to determine whether samples are representative of

the general beach conditions, or atypical. It is likely that natural variability was not well represented in the available samples.

Three approaches have been used to located the seaward limit of longshore transport zone. Two, using the annual and what has been termed the average depths of closure, provide an upper and lower estimate, 0.52 and 0.42 respectively, of the LTZ-beach size ratio. A third approach, using modelled cross-shore distributions of longshore transport to delineate this zone, yields a LTZ-beach size ratio, between these two, at 0.46. This is quite similar to the average and extreme values, suggesting that the ratio is not that sensitive to where the seaward limit of longshore transport is taken.

At Bogenfels, this typical LTZ-beach median grain size ratio, of 0.46, is somewhat dissimilar to the inverse of the surf similarity parameter $1/\xi = 1/1.11 = 0.9$.

5.3 Table Bay

5.3.1 Background

Between September 2005 and September 2006 a field sampling campaign was undertaken in Table Bay by the author. Four sample lines were established along the bay in order to obtain data from beaches with varying sediment and beach profile characteristics and different degrees of wave sheltering. Accessibility of the sampling line was also taken into account, as surf zone samples would be collected by swimming from the shore. The lines were therefore chosen to be within a short walk from a public carpark.

The measurement methodology and sample processing has been described in detail in Chapter 4. The location of the sampling lines and general bathymetry of Table Bay are shown in Figure 5.19.

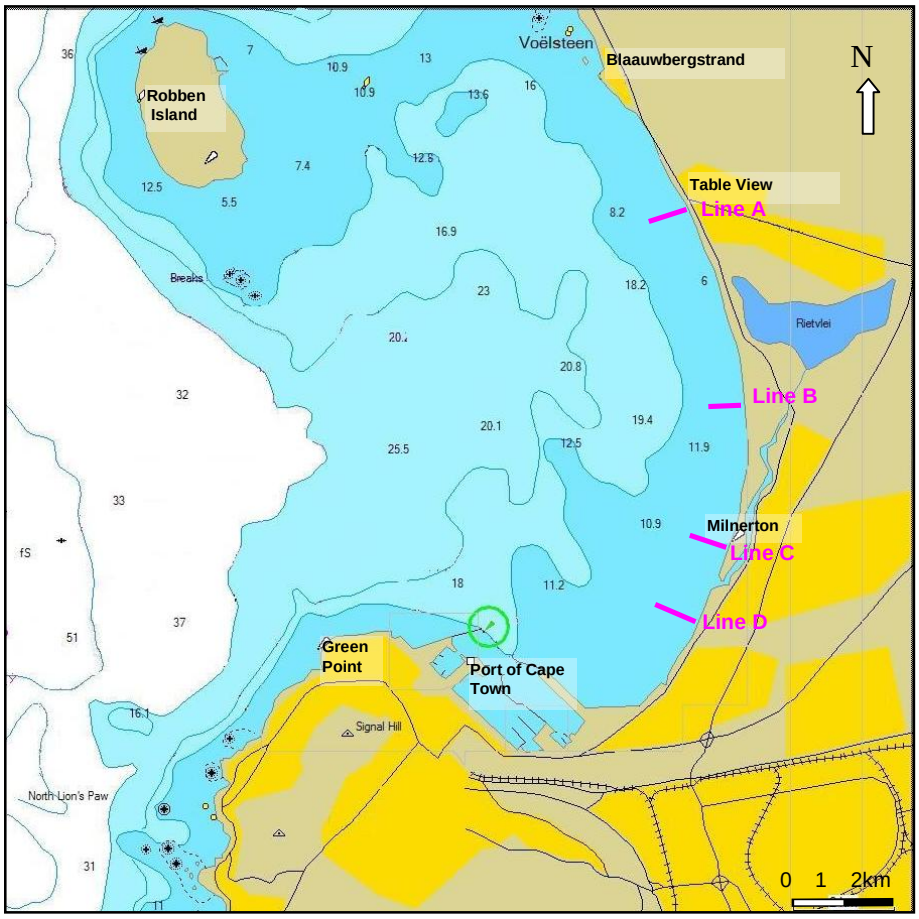

Figure 5.19: General bathymetry of Table Bay with position of sampling lines indicated

5.3.2 Environmental Conditions

Table Bay is a curved bay forming the northern boundary of the Cape Peninsula. The bay faces westward towards the Atlantic Ocean with the city of Cape Town nestled at its southern end. This southern corner of the bay is sheltered from the predominant south-westerly swells

by the promontory of Green Point and, to a degree, by the harbour breakwaters. This sheltering can be seen in Figure 5.20, which shows a wave refraction modeling result for a typical wave condition (offshore: Hs = 2.5 m, Tp = 13 s, direction = 225°).

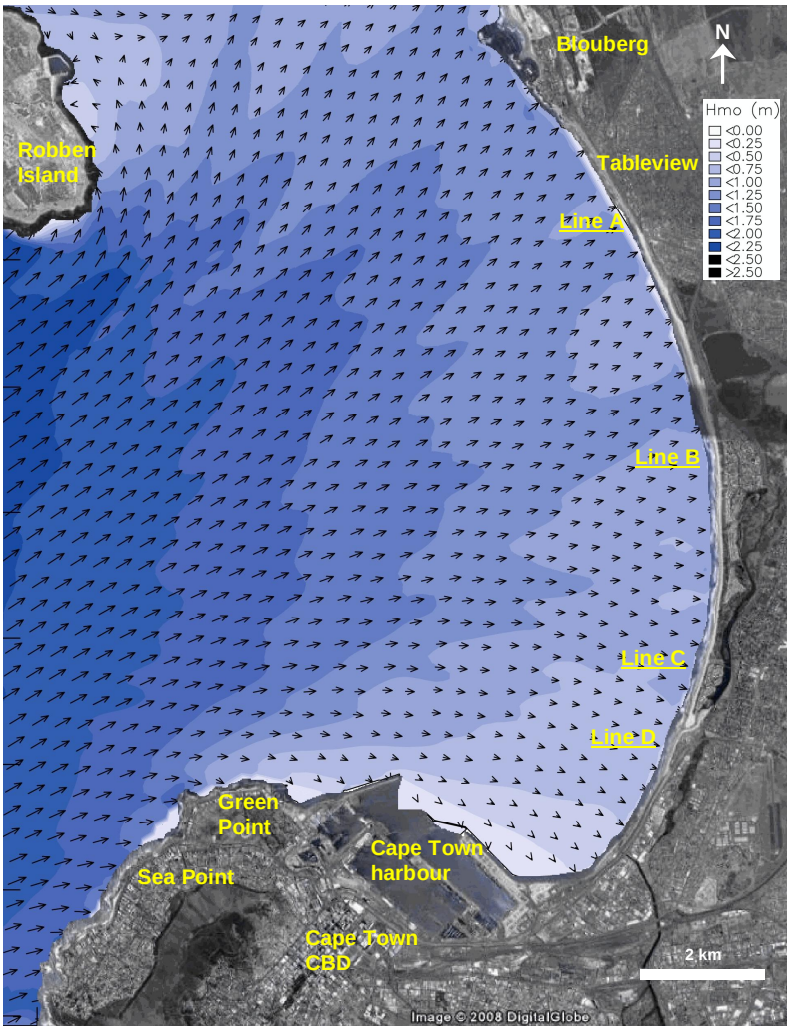

Figure 5.20: Typical gradation of wave heights in Table Bay

The bay opens to the north, with wave exposure gradually increasing. The most northern parts (north of Blouberg) begin to experience some wave sheltering under (infrequent) westerly to north-westerly wave conditions, due to the presence of Robben Island to the west. The coastline is heavily developed in places, with roads, residential areas and a golf course situated close to the shoreline. Net longshore transport rates are estimated to be low (Smith et al, 2000) and directed northerly.

The average annual offshore significant wave height is 2.2 m, with an annual storm significant wave height in the region of 8 m. Near beach wave conditions are considerably smaller than offshore though, due to the sheltering indicated above and seen in Figure 5.20.

While typical offshore wave heights are thus larger than at Bogenfels, the Table Bay beaches are not as exposed.

The predominant offshore wave direction is from the south-west. Wave period is typically between 10 and 14 s, indicating a swell dominated wave climate. Wave heights are generally larger in winter. Westerly to north westerly winds are typically associated with winter frontal systems, while south-westerly to south-easterly winds predominate in summer.

5.3.3 Description of beach characteristics

The beach profiles at Lines A, B, C and D are shown in Figure 5.21. Profiles were measured with a total station survey instrument from the dune to wading depth (approximately 1 meter below MSL). Representative beach slopes were determined from these surveyed profiles using the approach of Bascom (1951), whereby the slope at the mid-tide line is taken to be representative of the beach. The complete beach, nearshore and offshore profile for each line are shown in Figure 5.22.

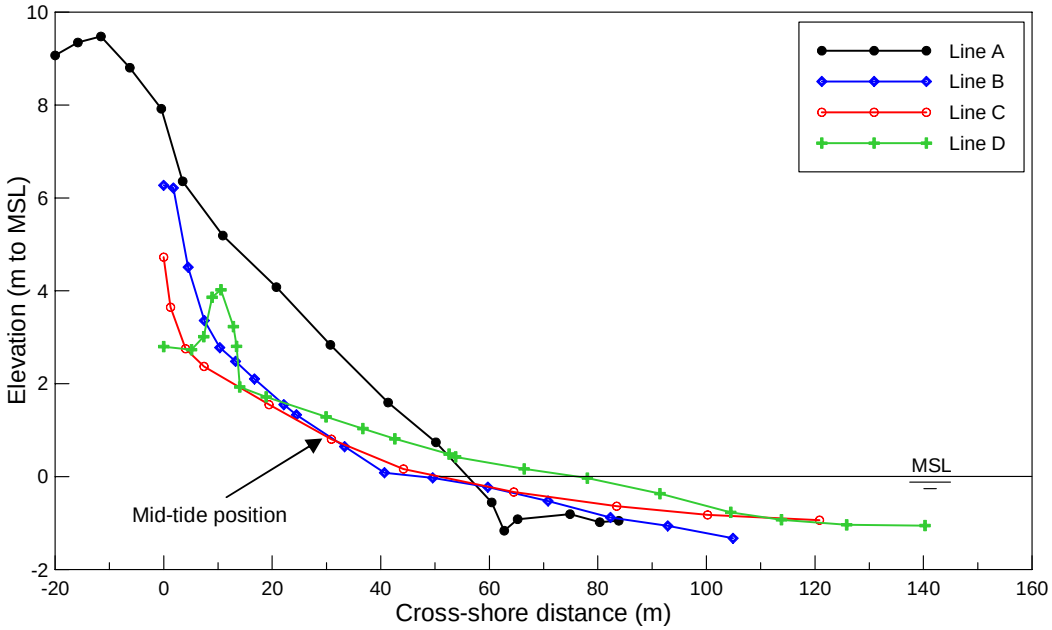

Figure 5.21: Typical beach profiles measured at Lines A, B, C and D in 2005.

Typical nearshore wave conditions were evaluated using wave refraction diagrams such as that given in Figure 5.20 and site observations.

The surf similarity parameter was applied to assist the beach type classification at the four sampling locations. The mid-tide beach slope and average wave height seaward of breaking were used to determine the surf similarity parameter (see Section 2.2). This is summarised in Table 5.2 for each of the sampling lines.

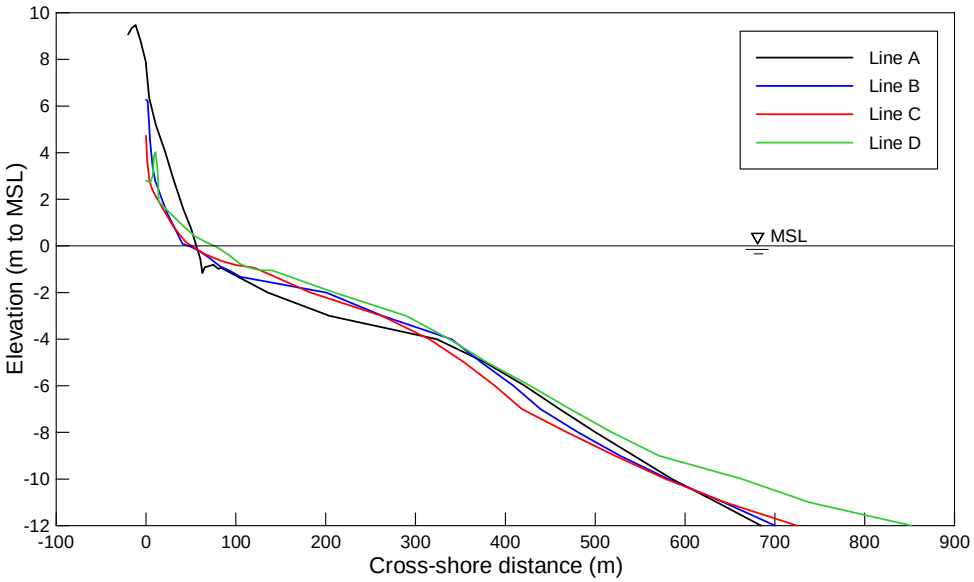

Figure 5.22: Beach and nearshore profiles at the four sampling lines in Table Bay

The depth of closure was evaluated using Birkemeier's (1985) formulation (Eqn 2.3). The effective wave height required for Birkemeier's formula was obtained from analysis of wave refraction results for a west-south-westerly storm wave with offshore height of 8 m. The refraction results were used to transform this wave condition to the location in Table Bay of each sampling line. A constant of 0.5 m was added to Birkemeier's depth of closure in order to convert the depths to relative to MSL (Birkemeier's formula gives the depth of closure relative to mean low water, which is approximately 0.5 m below MSL in Cape Town).

The beach characteristics are summarized in Table 5.2 below and discussed in the sub-sections that follow.

Table 5.2: Beach and nearshore characteristics at the four sampling lines

	Sampling Line			
Parameter	**A**	**B**	**C**	**D**
Beach slope	1:7	1:12	1:14	1:25
Wave exposure	Exposed	Partly exposed	Partly sheltered	Sheltered
Surf similarity parameter, ξ, for the beach	2.0	1.3	1.2	0.8
Beach type	Transitional (reflective beach face, dissipative nearshore)	Intermediate	Intermediate	Intermediate to Dissipative
Typical average annual wave height (m), nearshore	1.1	0.9	0.8	0.5
Annual 12-hour storm nearshore wave height (m)	3.7	3.1	2.8	2.2
Depth of closure (m to MSL)	6.3	5.4	4.9	4

Line A

Line A was located on the southern part of Table View beach, Figure 5.19. This is the most exposed part of the coastline, facing towards the dominant south-westerly swells. This high energy is reflected in the main recreational usage being watersports such as surfing and kiteboarding. Bathing conditions can be unpleasant due to powerful collapsing and surging breakers at the beach step, as illustrated in Figure 5.23, a photo looking seaward at Line A.

Figure 5.23: Photos looking northward and seaward at Line A, Table View

The step can be clearly seen as a sharp junction in the measured profile (Figure 5.21) at approximately the -1 m MSL level. Waves will, however, typically first break further seaward before re-forming closer inshore and plunging and rushing up the beach in an energetic swash zone. The beach slope is steep, while the nearshore zone is gently sloping (see below). At high tide waves are reflected from the steep beach face. The beach is thus a combination of a reflective beach and a dissipative nearshore and can be termed a transitional type beach (Woodroffe, 2002).

The beach has an almost linear slope of approximately 1:7 from the base of the dune, at 6 m elevation, to the beach step (Figure 5.21). The nearshore profile, illustrated in Figure 5.22, shows a steepening of the slope at the outer edge of the surf zone at approximately a cross-shore distance of 320 m, or 270 m from the shore. The nearshore bar/trough system is poorly defined, unlike the profiles at Duck and Bogenfels where a bar and trough were clearly evident. The offshore part of the profile has a constant slope of 1:40 to beyond 12 m depth.

The annual depth of closure is estimated to be at 6.3 m to MSL (Table 5.2).

Line B

Line B was located in the Sunset Beach residential development. This area faces due west and is moderately exposed, experiencing some sheltering due to its location further southward than Line A, towards the sheltered part of the bay. The beach profile has a concave shape, as opposed to the linear slope at Line A. The beach slope at Line B is also milder, at 1:12. See Table 5.2.

There is generally no distinct nearshore step, although beach cusps were noted on one of the sampling occasions and during other visits to this part of Table Bay. Another characteristic of this area is an accumulation of large pebble to cobble size material (16 mm to 256 mm) on the inter-tidal beach face. At times this can form a more than 0.2 m high berm at the runup limit. The pebbles can be seen in Figures 5.24 as the darker material in the middle foreground.

Figure 5.24: Photos looking northward and seaward at Line B, Sunset Beach

The beach can be classified as being of intermediate type (ξ = 1.3). Plunging or collapsing waves are typical of this beach. Annual depth of closure is estimated as 5.4 m to MSL.

Line C

Line C was located on Milnerton Beach, opposite Zonnekus House on Woodbridge Island. This beach is in the curved part of the bay and partly sheltered. Photographs of the beach are shown in Figure 5.25. The typical beach slope is 1:14 (Table 5.2). The upper beach is generally narrow, being less than 20 m wide at mid-tide.

Similarly to Line B, the beach can be classified as an intermediate type (ξ = 1.2), with plunging and collapsing breakers. Large mega-cusps, or embayments in the shoreline with rhythmic bar and rip channel features, were observed at times at this location. The annual depth of closure is estimated to be 4.9 m to MSL.

Figure 5.25: Photos looking northward and seaward at Line C, Milnerton

Line D

The most southerly line, Line D, was located south of the Diep River mouth, opposite the Spinnakers residential development. This area is in the most sheltered part of Table Bay, with typical wave heights only half those found further north at Lines A or B. Photographs of the beach are shown in Figure 5.26. While the surf similarity parameter classifies the beach type as intermediate (ξ = 0.8), observations indicate that wave breaking is dissipative at times.

Figure 5.26: Photos looking northward and seaward at Line D, south of the Diep River mouth

The beach slope is gentle (1:25) with the beach face having a constant slope, as opposed to the typical concave shape observed at Lines B and C. The upper beach has a low elevation (+2 m to MSL) and is backed by a low, narrow dune that is artificially stabilised in places. The typical annual depth of closure is estimated to be 4 m to MSL (Table 5.2).

The beaches at the four sampling sites are quite different. This is clear from the descriptions in the previous paragraphs and the summary of beach statistics in Table 5.2. Beach slopes and typical wave heights and breaker conditions change progressively from north (Line A) to

south (Line D). How these differences are reflected in the beach and nearshore grain sizes is discussed in the following section.

5.3.4 General grain size trends

Samples were generally collected at 12 cross-shore stations at each line. The stations were located from the base of the dune to 10 m depth (8 m in the case of Lines C and D). The location of the stations has been described in detail in Chapter 4. Figure 5.27 below provides a summary of the position of sampling stations.

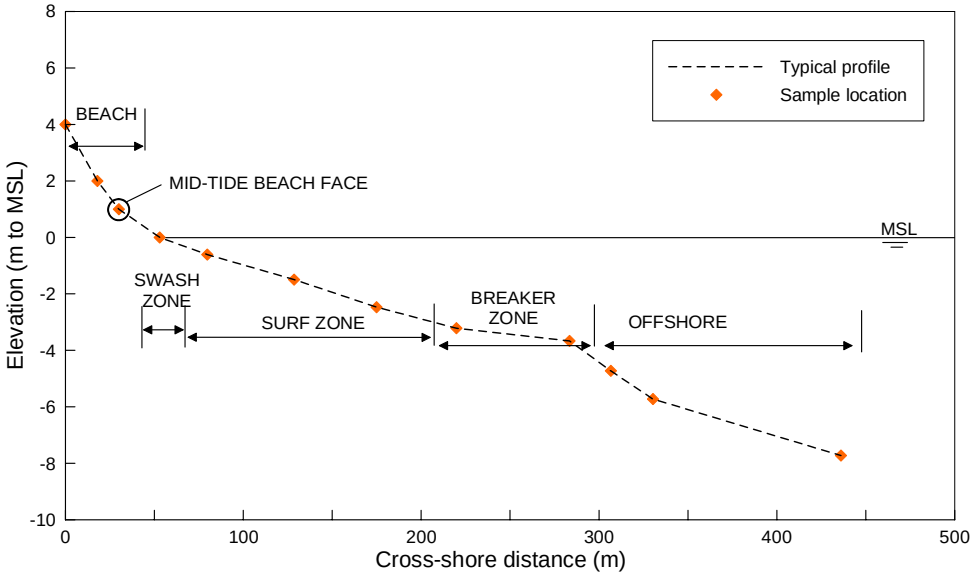

Figure 5.27: Typical sample locations on the cross-shore profile

Lines A and C were sampled most comprehensively (four data sets each), while Lines B and D were sampled less comprehensively (three and two complete data sets respectively). For some datasets only samples from the beach were available, with none from the nearshore, and vice versa (see Chapter 4). In this analysis, only the complete datasets are used, i.e. where both beach and nearshore samples were taken at approximately the same time. This is because one of the objectives of this study is to investigate the relation between grain sizes on the beach and those in the nearshore. Partial datasets would not be useful for such an investigation. (All datasets are given in Appendix 3).

Where shore based samples, such as those of the deeper part of the surf zone, coincided with the position of nearshore samples, these were combined according to the depth and distance offshore of the sample. There was most overlap for the 3 m depth samples.

The resulting median grain sizes at each station are shown super-imposed on the beach and nearshore profiles in Figure 5.28, noting that the grain sizes are plotted to a log scale. A number of general observations follow.

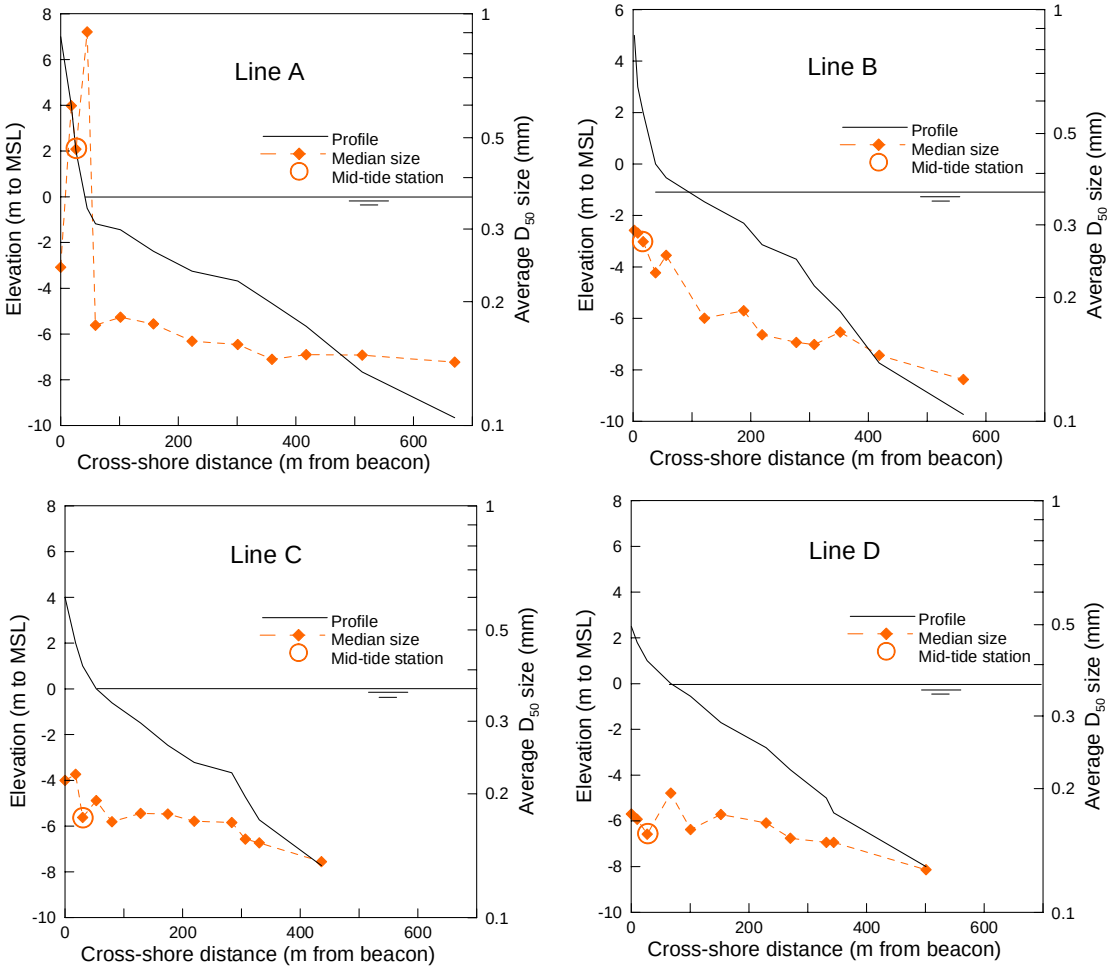

Figure 5.28: Cross-shore profile and average median grain size at each sampling station

At each line, grain sizes decrease from the beach seawards. This seaward fining is relatively gradual, except at Line A, where the beach sizes are much coarser than the surf zone and nearshore samples – the mid-tide beach size is 0.469 mm while the surf zone and nearshore grain sizes are all finer than 0.2 mm. At Line D the beach and nearshore grain sizes are virtually identical.

The average median grain sizes from each line are plotted together in Figure 5.29. Size is plotted logarithmically on the vertical, against, on the horizontal axes, cross-shore distance and depth in Figures 5.29a and 5.29b respectively. The following are observed:

- The beach grain sizes become progressively finer in a southward direction within Table Bay – median inter-tidal beach sizes decrease from 0.469 mm to 0.273 mm to 0.175 mm to 0.155 mm from Lines A through to D respectively;

- Grain sizes in the surf zone are remarkably similar at all the lines. Between 1 m and 5 m depth the grain sizes at each line show a similar fining trend, with sizes from one line to the next being virtually identical. For example, at 5 m depth the grain sizes vary by only 0.01 mm from a coarsest of 0.155 mm at Line C to a finest of 0.145 mm at Line A;
- Differences between lines are slightly more at greater depths, with the coarsest material found in the north at Line A and progressively finer material in the south towards Line D. This is likely a reflection of the very low wave energy in the southern area, with very fine material being deposited on the offshore seabed.

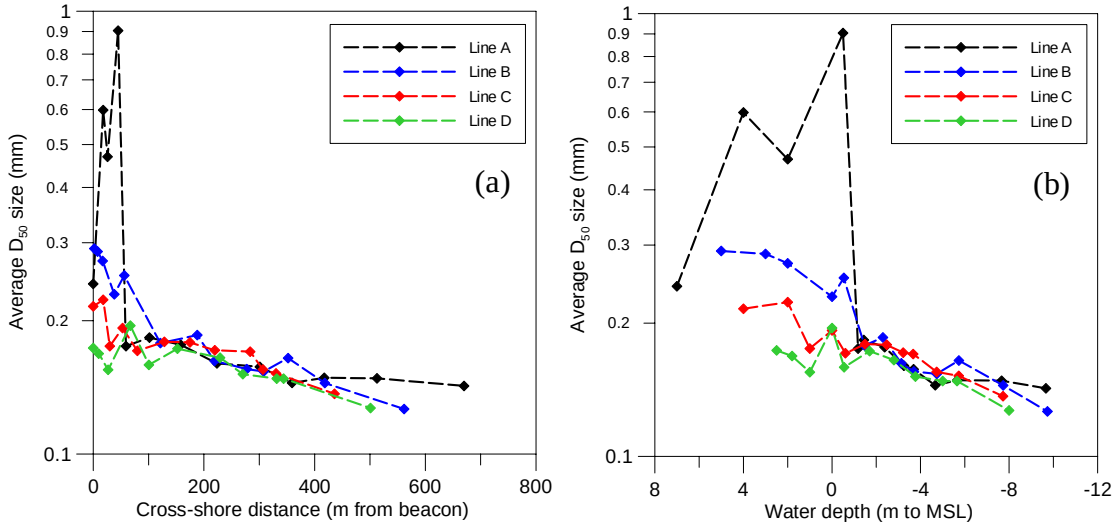

Figure 5.29: Grain sizes in Table Bay grouped by a) cross-shore distance and b) water depth

5.3.5 Longshore transport zone grain sizes

It was necessary to delineate the longshore transport zone in order to evaluate the grain sizes that occur in this zone of the cross-shore profile. A similar approach was followed as at Duck and Bogenfels: The Unibest model was used to calculate the cross-shore distribution of longshore transport for typical wave conditions at each sampling line. The surveyed beach and nearshore profiles (Figure 5.22) were applied in the model, together with a range of typical wave conditions. These included an annual return interval storm, with offshore significant wave height of 8 m. The resulting individual distributions are shown together for each of the four profiles (Lines A to D) on Figure 5.30, noting that identical durations were assigned to each wave condition. The transports shown are therefore comparative between wave conditions and not representative of the actual net longshore transport rates in Table Bay.

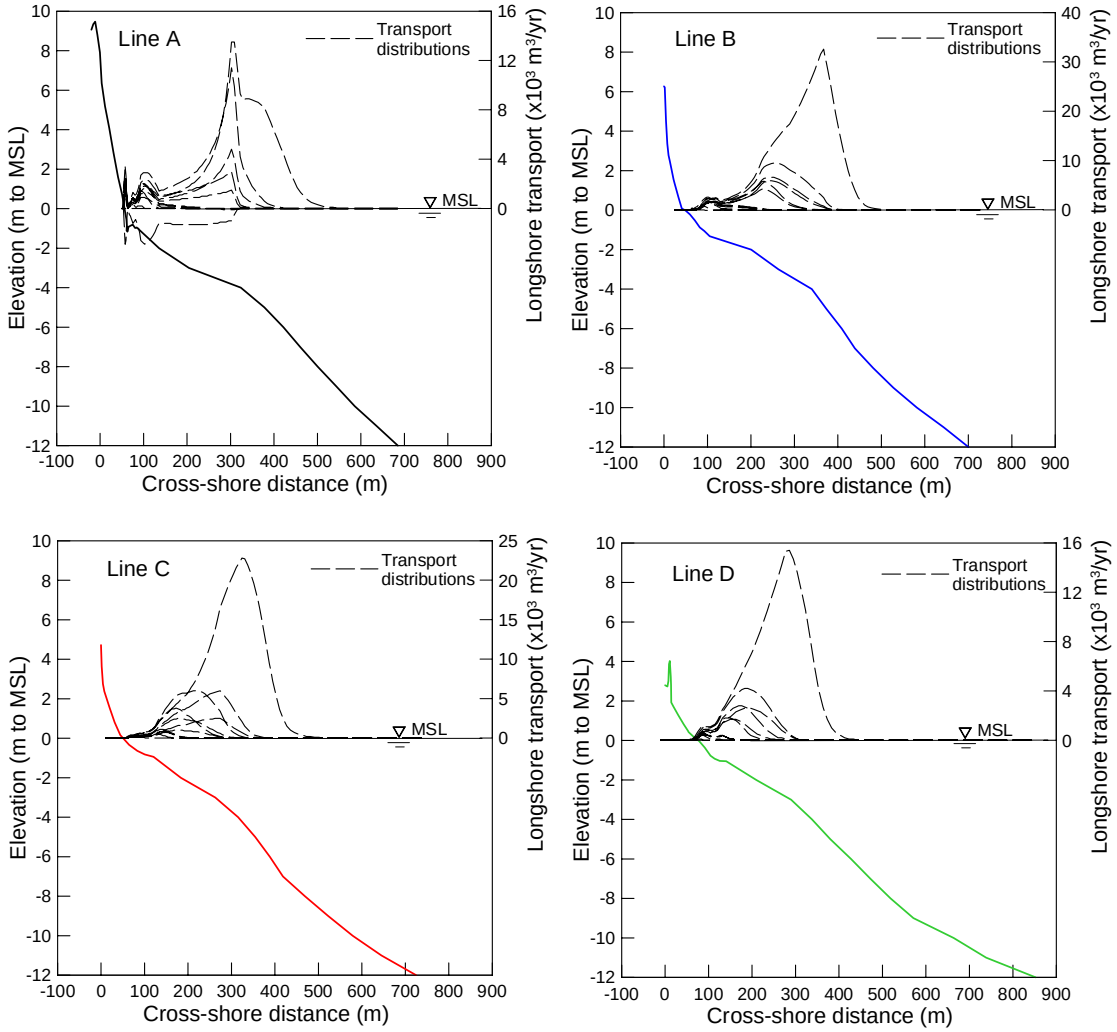

Figure 5.30: Indicative cross-shore distributions of longshore transport at Lines A to D in Table Bay

With reference to Figure 5.30, the following are observed:

- Considerable variation is evident at each line. This is the result of the different wave conditions whose transport is represented. The largest peak at each line is the result of the annual storm condition;
- The transport distributions at Lines B, C and D are very similar and unimodal, with the longshore transport at Line D occurring dominantly in shallower water due to the more sheltered conditions;
- The transport distributions at Line A are different to those at the other three lines and are frequently bimodal, with a high seaward peak and secondary peak closer to shore. An occasional third peak occurs in the swash zone. This well reflects the wave breaking patterns observed at Line A (see Section 5.3.3), with initial breaking, reforming and then final collapse in the swash zone.

The typical seaward limit of longshore transport at each line generally lies at or landward of the transport peak resulting from the annual storm condition. This peak provided a clear point at each sampling line, and, although longshore transport does occur seaward of this point, it does so under only extreme conditions, such as the annual storm condition. The resulting seaward longshore transport limits are summarised in Table 5.3. The depth of closure is given for comparative purposes. As can be seen, the likely limit lies landward (shallower) of the depth of closure. A similar situation was observed at Duck and Bogenfels.

Table 5.3: Seaward limit of longshore transport in Table Bay

Location	Likely seaward limit of longshore transport (depth on profile) (m)	Depth of closure (m)
Line A	5.0	6.3
Line B	4.0	5.4
Line C	3.8	4.9
Line D	3.0	4

This likely seaward limit is now used to examine the grain sizes in the longshore transport zone.

Again, an approach similar to that for Duck and Bogenfels is taken to define the landward end of the longshore transport zone: only beach samples from the inter-tidal location are included and the swash-zone step sample is excluded. The zones included in the longshore transport zone were the following:

- Beach – mid-tide beach face;
- Inner surf zone;
- Trough area – poorly defined in Table Bay, so samples from the seaward part of the surf zone, just prior to the breaker zone, were used;
- Bar – similarly to the trough area, this region is poorly defined on the Table Bay profiles, so samples from approximately the typical breaker zone were used – 4 m depth (Line A) and 3 m depth (Lines B and C). At Line D the total surf zone is very narrow (refer Figure 5.26) and therefore the inner surf zone and trough samples were considered adequate representation of the general surf/breaker zone area;
- Nearshore – sample closest to the likely limit of longshore transport as defined in Table 5.3.

The longshore transport zone grain size is then taken as the simple average of the median grain sizes of all these zones.

The values used are summarised in Table 5.4 below and are the averages of all the median grain sizes sampled at that location.

Table 5.4: Grain sizes in the longshore transport zone at Table Bay

	Line A	Line B	Line C	Line D
Mid-tide	0.469	0.273	0.175	0.155
Inner-surf	0.175	0.253	0.171	0.159
Trough	0.177	0.186	0.179	0.173
Bar	0.157	0.162	0.172	-
Nearshore	0.145	0.156	0.170	0.165
Average of Longshore Transport Zone	0.225	0.206	0.173	0.163
LTZ-beach ratio	0.48	0.75	0.99	1.05
Surf similarity (ξ)	2.0	1.3	1.2	0.8
1/ ξ	0.5	0.78	0.83	1.25

From the table it can be seen that the longshore transport zone grain size is largest at Line A (0.225 mm) and finest at Line D (0.163 mm). However, the grain sizes from the Inner surf zone to Nearshore areas are very similar for all four sample lines, as was observed in the previous section. Therefore the main cause of the change in LTZ grain size is the change in the Mid-tide grain size. This ranged from largest at Line A to finest at Line D. This is revealed in the LTZ-to-beach grain size ratio, which changes from 0.48 at Line A to 1.04 at Line D. This means that at Line A the LTZ grain size is about half the beach size, while at Line D the LTZ grain size is approximately the same as the beach grain size.

5.3.6 Synthesis

The grain sizes in Table Bay show a general cross-shore fining trend, with sizes decreasing from the beach seaward. Sizes sampled from the inter-tidal beach are coarsest in the north of the bay (Line A), becoming finer southward (furthest south – Line D). This reflects other changes that occur from north to south in the beach and nearshore environment – from north to south:

- The beach slope becomes flatter;
- Wave exposure decreases;

- The surf similarity parameter decreases;
- The beach type changes from intermediate/reflective to intermediate/dissipative;
- Wave heights decrease;
- Depth of closure decreases;
- Inter-tidal median beach grain size decreases.

In contrast to these changes, the grain size in the surf and nearshore zones remains remarkably constant from north to south. The result is that the ratio of the mid-tide beach median size to longshore transport zone median size increases from north to south; in the north the LTZ size is about half the beach size, while in the south the LTZ size is the about equal to the beach size, i.e. a ratio of 1:1.

Of the environmental parameters assessed, this change is most similar to the inverse of the surf-similarity parameter. The inverse of this parameter increases from 0.5 in the north to over one in the south.

5.4 Summary of Findings

5.4.1 General

How the longshore transport zone is defined determines the sediment samples that are included in this zone. Considerable difficulty was experienced in this thesis in delineating the longshore transport zone. This was partly because this zone continually changes as waves and tides change and even as the beach and nearshore profile evolves. There appear to be no rapid methods to determine its cross-shore extent. The depth of closure, as defined by Birkemeier, provides some approximation. Calculations of the cross-shore distribution of longshore transport were undertaken with the Unibest model. Bearing in mind the relative (in)accuracy of such models, this approach suggests that the seaward limit of longshore transport occurs landward of the depth of closure. Intuitively, this is to be expected.

Some interpretation of these modelled transport distributions has been required in resolving the seaward transport limits at each study site. A realistic, or likely, limit was found to be just seaward of the deepest longshore bar. This point corresponds approximately to the calculated transport peak for the annual storm wave condition at the beaches assessed in this study.

The landward point of longshore transport was taken as being the mid-tide beach. The mid-tide beach size is generally coarse, yet the beach only occupies a very small part of the longshore transport zone. Grain sizes from the beach step were excluded from the longshore transport zone. This beach step zone generally only occupies a fraction of the cross-shore profile and its uniquely coarse grain size appears to be related only to localised cross-shore sorting processes.

In this study, the grain sizes from all zones, except the beach step, have been averaged in a simple manner. An alternative approach could be to average them according to the relative weight of longshore transport in each zone.

5.4.2 Cross-shore grain size

The four sampling sites in Table Bay represent quite different beaches, with, for example, beach slopes ranging between 1 in 7 to 1 in 25 and wave exposure that ranges from an exposed to sheltered classification. The one location, Table Bay, has therefore effectively yielded cross-shore grain size information for four different beach types. Together with the datasets from Duck and Bogenfels, six datasets have therefore been compiled in this study. The following were generally observed at these six beaches:

- Grain sizes become finer from the beach seawards;
- Grain sizes at the beach step are usually coarser than those found elsewhere on the profile;
- Beaches with steeper inter-tidal beach slopes have coarser median grain sizes than more gently sloping beaches;

The mid-tide beach and longshore transport zone grain sizes for the six different beaches are summarised in Table 5.5, together with each beach's surf similarity parameter, ξ, and its inverse, $1/\xi$.

Table 5.5: Summary of longshore transport zone grain sizes at all study beaches

Beach	Beach (mid-tide) size (D_{50}, mm)	Longshore transport zone size (D_{50}, mm)	LTZ to beach grain size ratio	Surf similarity parameter, ξ	$1/\xi$
Duck	0.29	0.20	0.69	1.4	0.71
Bogenfels	0.98	0.51	0.52	1.1	0.9
Table Bay, Line A	0.469	0.225	0.48	2.0	0.5
Table Bay, Line B	0.273	0.206	0.75	1.3	0.78
Table Bay, Line C	0.175	0.170	0.97	1.2	0.83
Table Bay, Line D	0.155	0.161	1.04	0.8	1.25

With regard to the grain sizes in the longshore transport zone, the following were observed:

- On the energetic beaches, Sampling Line A in Table Bay and Bogenfels, longshore transport zone grain sizes are significantly finer than those on the mid-tide beach, by more than half;
- At the beaches that can be classified as only slightly exposed, such as Duck and Sampling Line B in Table Bay, the longshore transport zone grain sizes were also finer than the mid-tide beach grain sizes, although less so than for the exposed sites;
- At the beaches that approach a sheltered state, such as Sampling Lines C and D in Table Bay, the longshore transport zone grain sizes are virtually the same as those found on the mid-tide beach.

The ratio of longshore transport zone grain size to the mid-tide beach grain size varied between 0.48 and 1.04. Similar variation is observed in Table 5.5 for the inverse of the surf

similarity parameter. The ratio of longshore transport zone grain size to the mid-tide beach grain size corresponds reasonably well to the inverse of the surf similarity parameter at Duck and all four beaches in Table Bay. The correspondence is less clear at Bogenfels. Possibly this is because this beach had the poorest quality cross-shore grain size data.

Chapter 6: Conclusions and Recommendations

A review of literature on beach grain size, and cross-shore changes in grain size in particular, indicates that a general pattern is understood to exist: grain sizes become finer from the beach seawards. This general pattern was confirmed at the sites assessed here. Research has often looked at understanding the grain size patterns at a particular site, be they cross-shore or alongshore patterns. The literature indicates that limited effort has expended to develop a better general understanding of grain sizes in the longshore transport zone.

In this thesis, field work, entailing collection of cross-shore samples, and the subsequent sample processing for grain sizes, analysis and interpretation have been undertaken for four sites in Table Bay. A cross-shore grain size dataset has been compiled from these samples. In addition, two further datasets, from Duck in the USA and Bogenfels in Namibia, have been obtained and interpreted in order to gain better understanding of grain sizes in the longshore transport zone.

On five of the six beaches studied, the exception being Bogenfels where grain size data was poor, the ratio between longshore transport zone grain size and mid-tide beach grain size was found to be similar to the inverse of the surf similarity parameter. (The latter was defined using the average wave height seaward of breaking, and the mid-tide beach slope). This finding was consistent across the five beaches, which ranged from exposed to sheltered in character. This finding suggests that the longshore transport zone grain size can be estimated if the mid-tide beach grain size is measured and the typical wave height and beach slope are known. The latter two are required in order to estimate the surf similarity parameter.

The above should be regarded as a tentative conclusion. A considerable amount of interpretation was involved in this study in defining the limits of the longshore transport zone, as well as in determining a representative grain size from all the samples from this zone. It is recommended that future research consider using the relative distribution of longshore transport to assist in obtaining a single representative grain size for the longshore transport zone. In addition, further work should be undertaken to better understand the limits of the longshore transport zone. It is also recommended that the tentative relation developed here be tested at a wider variety of beaches.

Finally, it is concluded that the investigations described in this thesis have contributed to a better understanding of the grain sizes in the longshore transport zone and have provided

insights for coastal engineers as to the representative grain size to be used in sediment transport calculations.

References

Anders, F.J., Underwood, S.G. and Kimball, S.M., 1987. Beach and Nearshore Sediment Sampling on a Developed barrier, Fenwick Island, Maryland. Proceedings, Coastal Sediments 1987. ASCE, New York, pp. 1732 – 1744.

Bascom, W.N., 1951. The relationship between sand size and beach-face slope. Transactions, American Geophysical Union, 32, number 6.

Bijker, E.W., 1968. Litoral Drift as a Function of Waves and Currents. Proc. 11th ICCE. ASCE, pp. 415 – 435.

Birkemeier, W.A., 1985. Field Data on Seaward Limit of Profile Change. Jnl Waterways, Port, Coastal and Ocean Engineering, ASCE, 111, No. 3, pp 598-602.

CEM, 1998. Coastal Engineering Manual. U.S. Army Corps of Engineers, Washington, DC.

Friedman, G., 1961. Distinction between dune, beach and river sands from their textural characeristics. Jnl. Sedimentary Petrology, 31, pp. 514 – 529.

Fromme, G.A.W. 1977. Establishment of a standard relationship between settling velocity and grain size of coastal sand. CSIR Research Report 356, Stellenbosch, South Africa.

Hallermeier, R.J., 1978. Uses for a Calculated Limit Depth to Beach Erosion. Proc. 16th International Conference on Coastal Engineering, Hamburg, ASCE, pp 1493 – 1512.

Horn, D.P., 1992. A review and experimental assessment of the equilibrium grain size and the ideal wave-graded profile. Marine Geology, 108, pp. 161 – 174.

Kamphuis, J.W., 1991. Alongshore Sediment Transport Rate. J. Waterways, Port, Coastal and Ocean Eng., ASCE, Vol. 117(6), pp. 624 – 640.

Katoh, K. and Yanagishima, S., 1985. Changes in Sand Grain Distribution in the Surf Zone. Proceedings Coastal Dynamics '95. ASCE, New York, pp. 639 – 650.

King, D. P., 2006. Dependence of the CERC Formula K-coefficient on Grain Size. Proceedings 30th International Conference on Coastal Engineering, ASCE, pp 3381 – 3389.

Komar, P. D., 1976. Beach Processes and Sedimentation. Prentice-Hall, Englewood Cliffs, New Jersey, USA.

Kumada, T., Uda, T., Serizawa, M and Noshi, Y., 2006. Model for predicting changes in grain size distribution of bed materials. Proceedings 30th International Conference on Coastal Engineering, ASCE, pp 3043 – 3054.

Larson, R., Morang, A. and Gorman, L., 1997. Monitoring the coastal environment: Part II: Sediment sampling and geotechnical methods. Journal of Coastal Research, 13 (2), pp 308 – 330.

Liu, J.T., Zarillo, G.A., 1989. Distribution of grain sizes across a transgressive shoreface. Marine Geology, 87, pp 121-136.

Medina, R., Losada, M. A., Losada, I.J., Vidal, C. 1994. Temporal and Spatial Relationship between Sediment Grain Size and Beach Profile. Marine Geology, 118, pp195-206.

Noshi, Y., Kobayashi, A., Uda, T., Kumada, T. and Serizawa, M., 2006. Relationship between local seabed slope and grain size composition of bed material. Proceedings 30th International Conference on Coastal Engineering, ASCE, pp 3030 – 3042.

Pruszak, Z., 1993. The Analysis of Beach Profile Changes Using Dean's Method and Empirical Orthogonal Functions. Jnl Coastal Engineering, 19, pp 245-261.

Shore Protection Manual, 1984. CERC, Waterways Experiment Station, Vicksburg, USA.

Self, R.P., 1977. Longshore variation in beach sands, Nautla area, Veracruz, Mexico. Jnl. Sedimentary Petrology, 47, pp. 1437 – 1443.

Smith, G.G., Dunkley, E. and Soltau, C., 2000. Shoreline response to harbour developments in Table Bay. In Proc: 27th International Conference on Coastal Engineering, Sydney, Australia. American Society of Civil Engineers. pp 2822-2835.

Soltau, C., 2005. Towards Predicting Nearshore Grain Size. Proc. Fifth Int. Conference on Coastal Dynamics. Barcelona, Spain.

Stauble, D.K., 1992. Long-term profile and sediment morphodynamics: Field Research Facility case history. Technical Report CERC-92-7. USACE.

Uda, T., Kumada, T. and Serizawa, M., 2004. Predictive model of change in longitudinal profile in beach nourishment using sand of mixed grain size. Proc. 29th Int. Conference on Coastal Engineering, ASCE, pp 3378-3390.

Van Rijn, L.C., 1993. Principles of Sediment Transport in Rivers, Estuaries and Coastal Seas. Aqua Publications, Amsterdam.

Van Rijn, L.C., 2002. Longshore Sand Transport. Proc. 28th Int. Conference on Coastal Engineering, ASCE, pp 2439 – 2451.

Van Rijn, L.C. and Boer, S., 2006. The effects of grain size and bottom slope on sand transport in the coastal zone. Proceedings 30th International Conference on Coastal Engineering, ASCE, pp 3066 – 3078.

WL|Delft, 2005. Unibest CL+ 6.0. User and Theoretical Manual. WL Delft Hydraulics.

Woodroffe, C.D., 2002. Coasts: Form, process and evolution. Cambridge University Press.

APPENDIX 1: Soltau, C., 2005. Towards Predicting Nearshore Grain Size. Proceedings of Fifth International Conference on Coastal Dynamics, Barcelona, Spain. ASCE. 2005.

TOWARDS PREDICTING NEARSHORE GRAIN SIZE

Christoph Soltau

Environmentek, CSIR, PO Box 320, Stellenbosch, 7599, South Africa.
csoltau@csir.co.za.

Abstract: Grain size is an important input parameter for longshore transport calculations. However, measurements and sampling in the longshore transport zone can be difficult and costly. This paper presents initial investigations aimed at predicting the median grain size in the longshore transport zone, based on measuring only the beach grain size. The data analysed to date suggests that the longshore transport zone grain size is close to half that found on the beach. Factors that could influence this relation are mentioned. The work is ongoing.

INTRODUCTION

Grain size is an important input parameter for the calculation of longshore sediment transport. For waves to suspend and transport coarse material requires a greater amount of energy than for an equivalent amount of fine material. In calculating wave driven longshore transport, the grain size being used as the input parameter to our equations and models should be representative of the material that is being transported. This is where difficulties arise in prototype applications:

We often rely on an estimate of the representative grain size as it is difficult to obtaining rapid and easy measurement of the grain size across the surfzone, which is precisely the region where most longshore transport occurs. (Without knowledge of this grain size, an additional degree of uncertainty is introduced into our model calibration procedure).

This is particularly the case along the Southern African coastline, where the surfzone is frequently inaccessible for measurement because of persistent high wave energy. Expensive and/or sophisticated measurement techniques are infrequently available to the coastal engineer.

In contrast to the surfzone, it is generally easy to measure the grain sizes of the intertidal and upper beach. This zone of the active beach profile is accessible for sampling under all but the most extreme wave and tide conditions. On most beaches, cross-shore transport processes dynamically link the sediments on the upper beach to those below water. The question that can be posed is thus:

> Is it not possible to predict the grain size occurring in the area of longshore transport by only sampling the upper beach and incorporating other knowledge of the important environmental parameters that influence the beach?

This is the question that the investigations described in this paper aim to explore. The aim is not to predict the precise changes in grain size from deep water to the dune, as researchers such as Horn (1992) have attempted. Rather, it is to develop a (fairly) simple relation between the median grain size in the longshore transport zone and that of the intertidal beach, which can be readily applied for coastal engineering studies at most beaches without the need for extensive measurements.

As a first step, the importance of using the appropriate grain size in longshore transport calculations will be established. Existing understanding of the distribution of grain sizes in the cross-shore will be reviewed, followed by an initial attempt at developing a relation between beach and surfzone grain sizes based on limited measurements. Finally, a start is made at defining the influencing factors that would make such a relation more widely applicable and accurate. Conclusions are provided.

BACKGROUND

Assumptions

These investigations are not meant to trivialize a complex, dynamic system. The type and size of material found on a beach may be influenced by a number of factors, amongst them:

- Local geology;
- Sediment sources (rivers, artificial nourishments, eroding cliffs);
- Marine life (shells, coral);
- Cross-shore changes in seabed (rock outcrops, marine vegetation);
- Heavy minerals.

If they were all to be incorporated into a predictive relation, they would present a maze of intricacies that are not relevant to the aims of this paper. For the purposes of this initial investigation, the interest is in open, sandy coastlines that are dominated by wave driven transport processes.

Grain Size Effects on Transport

The importance of using the correct grain size in longshore transport calculations is illustrated in Figure 1, which compares the longshore transport rates calculated for varying median grain sizes. Calculation results for the Van Rijn and Bijker equations (as set out in the Unibest model (WL|Delft Hydaulics 1999) and the Kamphuis equation are shown for the same wave and beach profile condition. The comparison is purely to show

the greater and lesser extents to which the median grain size controls the transport in a calculation. An error in grain size of 0.05 mm could easily lead to a 30% miscalculation in longshore transport, which could have serious effects on, for example, a beach nourishment project.

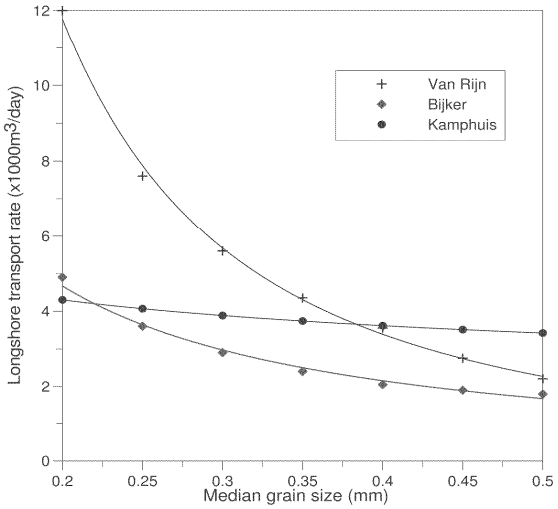

Figure 1: Example calculations showing longshore transport rate dependence on grain size

LITERATURE SURVEY

A review of literature on cross-shore changes in grain size revealed that the general patterns of grain size becoming finer from the beach to beyond the surfzone have been established for some time (e.g. Komar 1976; Bascom 1951). Landwards of the beach, toward the dune zone, the grain sizes are generally constant, unless other factors such as aeolian transport contribute by winnowing out particular size classes. Similar patterns exist at beaches throughout the world.

Bascom (1951) suggested that the grain size at a point on the profile is proportional to the amount of turbulence experienced at that point. The highest wave energy dissipation and turbulence are generally recorded near the wave plunge zones. Such plunge zones or peaks in energy dissipation generally occur in the swash zone, where reformed waves collapse onto the shore, and near the offshore bar where waves first break. Two peaks in grain size can therefore occur in the cross-shore direction, as noted by e.g. Stauble and Cialone (1996). The coarsest sizes, however, are almost invariably found in the swash zone (Bascom 1951) due to the continuous turbulence of up and downward rushing water acting as a good sorting mechanism. Considering the part of the profile above mean water, another peak in coarseness may be found at the crest of the summer berm, where uprush deposits coarse material

On beaches where the surfzone is relatively narrow (~100 m) and wave energy is low,

the swash zone and trough behind the nearshore bar may be difficult to distinguish and only a single peak in the grain size may occur at this merged zone. This was found by, for example, Medina *et al.* (1994), who performed repetitive measurements at El Puntal spit, Santander, Spain. They found that the trough/swash area consistently had the coarsest median grain size with the grain sizes here also exhibiting the greatest variability.

Liu and Zarillo (1989) investigated the relative abundance of four size fractions across the nearshore zone at Long Island, New York. The general trend was for coarser sediments landwards, with highest occurrence of coarse grain sizes in the surfzone. The found a distinct dominance of fine sediment seaward of the nearshore bar, although this reduced as water depth increased, reflecting the increasing presence of shelf sediments.

Pruszak (1993) presents cross-shore grain size data from the Bulgarian coastline in the Black Sea, where tides are virtually absent. The data indicated a strong peak in size in the swash zone, with median sizes up to three times those found on the beach.

Katoh and Yanagishima (1995) describe repetitive measurements over a 7 month period at the Hazaki Oceanographic Research Pier in Japan. These indicated the coarsest sizes to occur in the swash zone, with a secondary peak in coarseness occurring in the trough area. Beyond the bar, median grain sizes appeared to become steadily finer.

While it is implicit in their measurements, none of the authors mentioned above quantified the relationship between the size of the sand occurring on the beach and that in the zone of longshore transport. As this is the focus of the investigations in this paper, data was sought out where this relation could be investigated, bearing in mind the criteria stated in the assumptions.

MEASUREMENTS

Thus far it has been possible to obtain two data sets: the first was measured at Bogenfels, Namibia (location, Figure 2) specifically for an application where it was critical that the longshore transport rates were accurately calculated. The second data set is from the US Army Corps of Engineers Field Research Facility at Duck, North Carolina. The background to each dataset and its analysis are discussed below.

Bogenfels

Limited data was available at this site for the calibration of a longshore transport model. In order to reduce the uncertainty in the longshore transport calculations, a concerted effort was made to obtain grain size samples that spanned the surfzone, which is typically 300 to 400 m wide at this site, to a water depth of 10 m. Samples were taken along two lines (indicated in Figure 2) spaced 750 m apart. Divers used 0.2m long PVC tubes to obtain between 300 and 1500 g of sand from the surface layers. The median

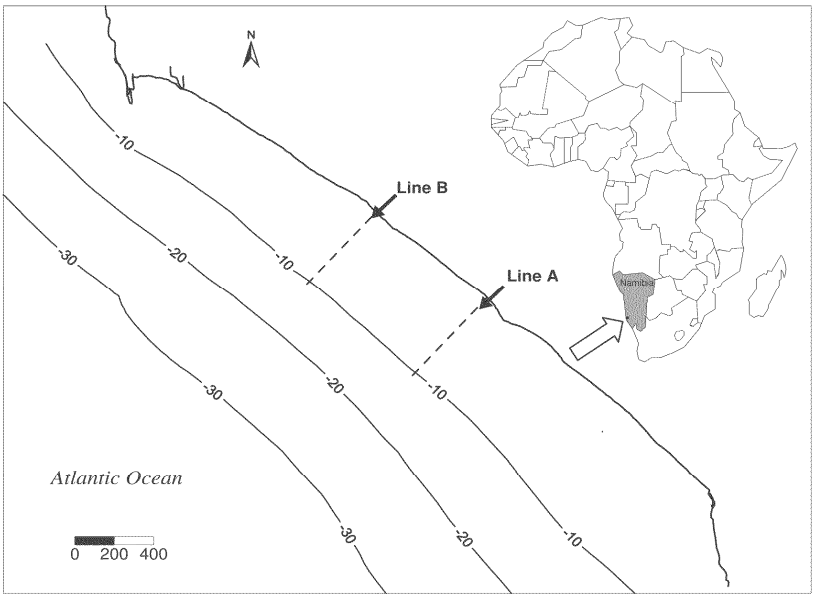

Figure 2: Location of Bogenfels beach indicating sampling lines A and B

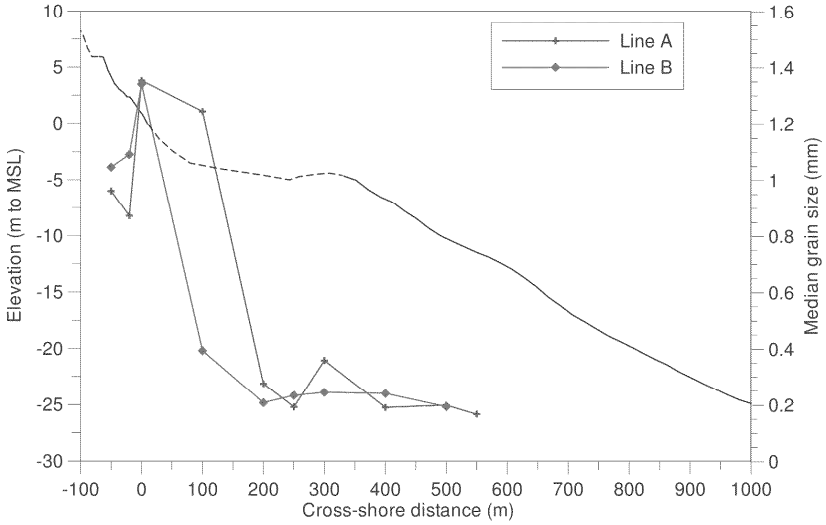

Figure 3: Median grain size measured across the profile at Bogenfels

grain sizes, superimposed on a typical beach and nearshore profile in Figure 3, confirmed the expected cross-shore trend:

The median size decreases from the beach in the offshore direction; sizes peaked in the swash-zone with a secondary peak in the area of the bar (The position of the bar/trough during the sampling is not precisely known, as the nearshore profile shown in Figure 3

was not measured concurrent to the sediment sampling); grain sizes change little beyond the bar. Both sampling lines show a similar pattern.

What was unexpected though was the large difference between the beach and the nearshore grain sizes: the average nearshore size (0.24 mm) is less than a quarter of the average beach size (1.11 mm).

Duck

Between March 1984 and September 1985, 21 complete sets of grain size samples were collected across the beach and nearshore at Profile 62, Duck. Bathymetric profiles were measured concurrent to the sediment sampling, both being conducted from the CRAB. Stauble (1992) provides a detailed description of this dataset, which is also accessible from the FRF website. Up to 17 stations were sampled each time: two in the dune, four on the beach berm and inter-tidal area, four through the inner bar and trough area and seven from the seaward edge of the inner bar to the limit of the profile. Figure 4 shows a typical bathymetric profile together with the median grain sizes sampled at the same time.

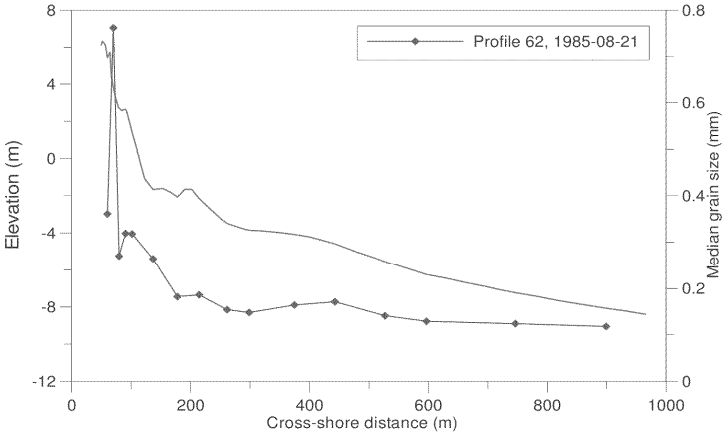

Figure 4: Median grain size measured across the profile at Duck

The expected offshore fining trend can be observed. Anomalously, the coarsest material is found at the base of the dune, which appears to be a characteristic feature at this site (Stauble, 1992). The coarse material in the swash zone is not represented, as samples were not consistently taking from this area. Muted coarsening occurs in the nearshore zone, showing some correspondence with the location of nearshore bars.

Of interest is to compare the beach grain sizes (beach berm and inter-tidal sampling stations) to the below-water samples (inner bar and trough to limit of profile stations), in order to compare this to the similar relation from the Bogenfels samples. Taking the average of the respective stations over all the sampling instances, it is found that the average median grain size on the below-water part of the profile (0.18 mm) is just less than half of the average found on the beach (0.49 mm). This is much greater than the

one-quarter relation determined for the Bogenfels samples, though these did include coarse swash-zone samples with the beach average. If a similar below-water to beach relation had been found for these two beaches, it would have been quite surprising. The main similarity between the two beaches is that they are composed of sand (and some shell) which is moved around by wave action; the differences between the two are numerous. Yet, with a little thought and knowledge of the sites, these differences can be quantified. If these quantifications can then be factored into the relation, should it not be possible to frame the relation such that it is applicable to both sites?

TOWARDS A RELATIONSHIP

The first additional factor that needs to be incorporated, or corrected for, in the above comparisons is the factor that goes back to the aim of this investigation, namely that the relation should allow prediction of the grain size in the *longshore transport zone*, and not the general below-water or nearshore area. After all, the measurements at both Bogenfels and Duck were only limited in their seaward extend by the sampling methods employed. The area on the profile to which the relation is applicable must be meaningfully constrained to prevent it being skewed by unnecessary information. The cross-shore boundaries of the longshore transport zone are a logical constraint.

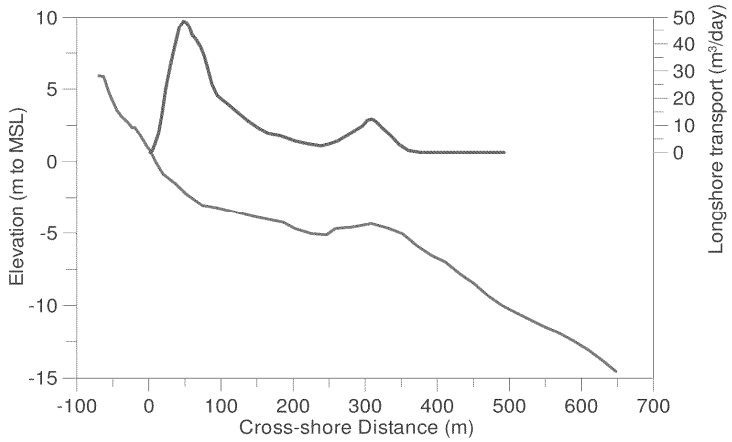

Figure 5: Example of calculated cross-shore distribution of longshore transport

This does, however, introduce further uncertainty: the longshore transport zone is ill-defined, it varies with wave conditions and nearshore/surfzone bathymetry. Both of the latter would require extensive measurement in order to define them precisely. There is, however, some guidance. Measurements such as those of Kraus *et al* (1988) indicate that most transport occurs landward of the wave breaking point. The UNIBEST CL+ shoreline model (WL|Delft Hydraulics 1999) also provides a calculated determination of the cross-shore distribution of longshore transport, thereby delineating the longshore transport zone for a particular wave condition. An example of a distribution calculated with the model is shown in Figure 5, assuming an average wave condition for the Bogenfels area (Hs = 2 m, Tp = 12 s) breaking on the profile shown in Figure 3.

This calculated result suggests that transport begins just beyond the wave breaking point and, for this wave and profile condition, has a bimodal shape with most of the transport occurring close to the shoreline. Under different wave conditions or profiles a different distribution would result. However, assuming that this average transport distribution was applicable to the period that the grain size samples were taken, the extents of the distribution can be used to decide which samples are relevant for determining the longshore transport zone average grain size. The beach sizes have also been included in the longshore transport zone average, as this material is also transported alongshore. The corresponding median size (0.55 mm) is shown in the table below.

The Duck samples span a 17 month period, during which the longshore transport zone is likely to have varied greatly. In selecting which samples to use, the depth of closure was selected as the seaward limit. Stauble (1992) indicates the depth of limiting change to be approximately -7 m. Samples from the beach to this depth were therefore used to determine the longshore transport zone average shown in Table 1. The relation of longshore transport zone to beach is given in the last column.

Table 1: Comparison of median longshore transport zone and beach grain sizes

	Longshore transport zone (mm)	Beach (mm)	Relation (longshore trans. zone/beach)
Bogenfels	0.55	1.11	0.50
Duck	0.27	0.49	0.55

If it was necessary to determine the appropriate grain size to use in a longshore transport calculation at Bogenfels, then a factor or relationship of 0.5 could be applied to the measured median beach size. Likewise, a relation of 0.55 could be appropriate for Duck. Considering that these beaches are located on different continents thousands of kilometers apart, the relations are in fair agreement. They relations represent an initial estimate that, in the absence of better site data, could be useful.

POTENTIAL INFLUENCING FACTORS

These relations derived for the two beaches correspond more closely than the initial beach to below-water comparison. The correction that brought about this improvement was the limitation of the grain size assessment (to some degree) to the on and offshore extents of the longshore transport zone at each beach. This simplistic assessment has not yet accounted for other differences between the two beaches. Differences that come to mind, and could be evaluated without having the luxury of extensive site data, are:

1. Breaker type – plunging or spilling. This can be easily judged from site observations or descriptions;
2. The beach state – e.g. reflective or dissipative. This can also be judged from site observations;
3. Inter tidal beach slope. This can be estimated or easily measured;
4. Offshore seabed slope. Hydrographic charts usually have sufficient detail to determine whether the slope is steep or mild.

Most of these influencing factors (it should not be read as being a complete list) can be qualitatively determined or also quantified. A method of a quantification is the surf similarity parameter, which gives a dimensionless value that takes into account most of factors 1 and 4. Through further work it is intended to develop a predictive relationship of the form:

$$D_{50LTZ} = (F_1F_2F_3)D_{50} \qquad (1)$$

where D_{50LTZ} is the appropriate median grain diameter for the longshore transport zone, D_{50} is the measured median beach grain size and F_1, F_2 and F_3 are beach specific modifying factors.

CONCLUSIONS

An initial investigation of the relation between grain sizes in the longshore transport zone and those on the beach has been conducted for the beach at Duck, USA, and Bogenfels, Namibia. The investigation suggests that the median grain size in the longshore transport zone is approximately half that found on the beach. However, significant further investigations are required before a predictive relationship can be presented with any degree of certainty. Further work should focus on at least the following: collecting beach and nearshore grain size data from more beaches; quantifying the influencing factors; testing the temporal and spatial applicability of the relation at a particular beach and comparison of the predicted longshore transport zone grain size to that actually used in calibrated longshore transport calculations.

ACKNOWLEDGEMENTS

I wish to thank Don Stauble for sending me a copy of Technical Report CERC-92-7, which proved invaluable in understanding the Duck measurements. Data from Bogenfels beach is used with the permission of Namdeb Diamond Corporation.

REFERENCES

Anders, F.J., Underwood, S.G. and Kimball, S.M. (1987). "Beach and Nearshore Sediment Sampling on a Developed barrier, Fenwick Island, Maryland", *Proceedings Coastal Sediments 1987*. ASCE, New York, pp. 1732 – 1744.

Bascom, W.N. (1951) "The relationship between sand size and beach-face slope", Transactions, American Geophysical Union, 32, number 6.

Horn, D.P. (1992) "A review and experimental assessment of the equilibrium grain size and the ideal wave-graded profile", *Marine Geology*, 108, pp. 161 – 174.

Katoh, K. and Yanagishima, S. (1985) "Changes in Sand Grain Distribution in the Surf Zone", *Proceedings Coastal Dynamics '95*. ASCE, New York, pp. 639 – 650.

Komar, P. D. (1976) "Beach Processes and Sedimentation", Prentice-Hall, Englewood Cliffs, New Jersey, USA.

Kraus, N. C., Gingerich, K. J. and Rosati, J. D. (1988). "Toward an improved empirical formula for longshore sand transport", *Proceedings of the 21st International Conference on Coastal Engineering*, ASCE, 1182-1196.

Liu, J.T. and Zarillo, G.A. (1989) "Distribution of grain sizes across a transgressive shoreface", *Marine Geology*, 87, pp 121-136.

Medina, R., Losada, M. A., Losada, I.J. and Vidal, C. (1994) "Temporal and Spatial Relationship between Sediment Grain Size and Beach Profile", *Marine Geology*, 118, pp195-206.

Pruszak, Z. (1993), "The Analysis of Beach Profile Changes Using Dean's Method and Empirical Orthogonal Functions", *Jnl Coastal Engineering*, 19, pp 245-261.

Stauble, D.K. (1992) "Long-term profile and sediment morphodynamics: Field Research Facility case history". Technical Report CERC-92-7, U.S. Army Engineer Waterways Experiment Station, Coastal Engineering. Research Center, Vicksburg, MS.

WL|Delft Hydraulics (1999) "UNIBEST-CL+ User manual" WL|Delft Hydraulics, Rotterdamseweg 185, The Netherlands.

APPENDIX 2: Grain Size Data from Bogenfels Beach

ALL GRAIN SIZE SAMPLES FROM BOGENFELS:

(Sampling by Namdeb divers (Dewald Duvenhage), sample processing by Namdeb laboratory “Mooimeisies”)

	Cumulative percentage passing sieve (mm size)										
Sample	**4**	**2.8**	**2**	**1.4**	**1**	**0.71**	**0.5**	**0.25**	**0.09**	**0.045**	**Diver's description**
A1	100	99.9	98.5	84.5	53.3	24.8	8.7	1	0	0	On dry beach before base of the dune
A2	100	100	99.8	94.2	63.4	29.8	13.5	1.4	0	0	inter-tidal beach face
A3	100	99.7	96	55.9	8	1.4	0.4	0	0	0	Low-water mark
A4	100	100	100	99.9	99.6	99.1	97.1	77.9	0.2	0	250m from shore approx. depth 3m
A5	100	100	100	99.5	95.2	87.9	74.7	22.9	0	0	300m from shore where waves break on an average day. Depth 4m
A6	100	100	100	99.9	99.4	98.7	97.4	78.7	0.3	0.1	400m from shoreline beyond furthest are of wave breaking. Depth approx. 6m
A7	100	100	100	99.8	99.4	98.7	97.3	73.5	0.3	0	Approx. 500m from shore Approx. depth 10m
A8	100	100	100	99.9	99.6	99.1	98.1	89.3	1.9	0	approximately 550m from shore. Approx depth 10m
A3A	100	99.5	95.4	64.3	24.4	7.9	2.8	0.4	0	0	100m from shore. Depth approx. 2.5m
A3B	100	100	100	100	99.7	98.2	94.8	39.4	0	0	200m from shore. Depth approx. 1.5m (sand bar)
B1	100	99.9	98.4	83.4	43.8	17.3	7.1	0.5	0	0	On dry beach before base of the dune
B2	100	100	99.5	87.6	34.2	9.7	2.6	0.4	0	0	inter-tidal beach face
B3	100	99.4	93.4	55.9	14.8	4.8	2.8	0.5	0	0	Low-water mark
B4	100	100	100	99.8	99.4	98.1	95.8	56.6	0	0	250m from shore approx. depth 3m
B5	100	100	99.9	99.6	98.8	97.6	95	51.5	0	0	300m from shore where waves break on an average day. Depth 4m
B6	100	100	100	99.9	99.8	91.2	89.9	53.3	0	0	400m from shoreline beyond furthest are of wave breaking. Depth approx. 6m
B7	100	100	100	99.8	99.4	98.5	97	76.7	0.3	0	Approx. 500m from shore Approx. depth 10m
B3A	100	100	99.9	99.2	95.1	85.7	69	16.6	0	0	100m from shore. Depth approx. 2.5m
B3B	100	100	100	99.9	99.4	98.5	97.1	70.6	0	0	200m from shore. Depth approx. 1.5m (sand bar)

APPENDIX 3: Grain Size Data Collected in Table Bay

AVERAGE D_{50} SIZE (MM) OF ALL COMPLETE (BEACH AND NEARSHORE) GRAIN SIZE SETS IN TABLE BAY:

	Line A	Line B	Line C	Line D
Dune	0.242	0.291	0.216	0.174
Berm	0.598	0.287	0.223	0.169
Mid-tide	0.469	0.273	0.175	0.155
Swash-zone	0.904	0.23	0.193	0.195
Inner-surf 1	0.175	0.253	0.171	0.159
Inner-surf 2	0.183	0.178	0.179	0.173
Inner-surf 3	0.177	0.186	0.179	
3 m depth	0.160	0.162	0.172	0.165
4 m depth	0.157	0.156	0.17	0.152
5 m depth	0.145	0.154	0.155	0.148
6 m depth	0.149	0.165	0.152	0.148
8 m depth	0.148	0.145	0.137	0.127
10 m depth	0.143	0.126	No samples	No samples

ALL TABLE BAY GRAIN SIZE SAMPLE DATA:

Key to Sample ID:

First letter = line (A, B, C or D)

Middle three characters = position on line, as follows:

1DU	Base of primary DUne
2BB	upper beach
3BE	Crest of beach BErm
4MI	MId-tide beach face
5SZ	Swash Zone step
6S1	Surf zone, shore based sample
7S2	Surf zone, shore based sample
8S3	Surf zone, shore based sample
9S4	Surf zone, shore based sample
03M	3m depth, boat based sample
04M	4m depth, boat based sample
05M	5m depth, boat based sample
06M	6m depth, boat based sample
08M	8m depth, boat based sample
10M	10m depth, boat based sample

Last character = Sample set (1 = 16 September 2005; 2 = 27 February 2006; 3 = 10 May 2006; 4 = 7 June 2006; 5 = 25 July 2006; 6 = 27 September 2006)

Sampling date	Sample ID	Depth (m to MSL)	Offset from beacon (m)	Grain size (mm)									Sorting	Skew-ness
				D5	D10	D16	D25	D50	D75	D84	D90	D95		
160905	A1DU1	+7	0	0.111	0.121	0.133	0.145	0.175	0.202	0.217	0.235	0.27	0.39	0.05
160905	A2BB1													
160905	A3BE1	+4	18	0.197	0.253	0.298	0.382	0.679	1.032	1.289	1.521	1.857	1.07	0.82
160905	A4MI1	+2	26	0.384	0.479	0.577	0.696	0.924	1.197	1.338	1.445	1.61	0.65	0.57
160905	A5SZ1													
160905	A6s11	-1.3	65	0.108	0.116	0.123	0.136	0.172	0.255	0.338	0.455	0.934	0.88	-3.11
160905	A7s21	-1.8	123	0.095	0.099	0.103	0.111	0.134	0.19	0.319	1.092	3.543	1.28	-11.75
160905	A8s31	-2.8	185	0.101	0.108	0.115	0.131	0.221	0.46	0.72	1.129	1.629	1.33	-4.52
160905	A9S41													
160905	A03M1	-2.65	218	0.099	0.104	0.109	0.116	0.143	0.187	0.27	0.455	0.91	0.86	-3.77
160905	A04M1	-3.65	285	0.1	0.107	0.114	0.124	0.151	0.191	0.227	0.321	0.637	0.69	-2.07
160905	A05M1	-4.65	368	0.11	0.116	0.122	0.13	0.146	0.163	0.178	0.204	0.582	0.54	-1.91
160905	A06M1	-5.65	435											
160905	A08M1	-7.65	523	0.104	0.109	0.114	0.119	0.133	0.148	0.153	0.156	0.164	0.22	0.02
160905	A10M1	-9.65	662	0.098	0.104	0.11	0.115	0.129	0.143	0.15	0.155	0.161	0.23	0.03
270206	A1DU2	+7.0	0	0.147	0.161	0.178	0.198	0.248	0.373	0.566	0.783	0.948	0.87	-2.18
270206	A2BB2													
270206	A3BE2	+4.0	18	0.2	0.261	0.323	0.427	0.742	0.979	1.103	1.212	1.355	0.90	1.97
270206	A4MI2	+2.0	26	0.169	0.189	0.213	0.247	0.34	0.625	0.827	0.982	1.165	0.95	-1.66
270206	A5SZ2	-0.5	45	0.192	0.235	0.271	0.316	0.904	1.647	1.949	2.358	3.203	1.39	1.73

Sampling date	Sample ID	Depth (m to MSL)	Offset from beacon (m)	Grain size (mm)									Sorting	Skew-ness
				D5	D10	D16	D25	D50	D75	D84	D90	D95		
270206	A6S12	-1.1	65	0.122	0.13	0.137	0.149	0.19	0.271	0.564	0.911	1.256	1.07	-4.63
270206	A7S22	-1.6	105	0.111	0.12	0.126	0.133	0.147	0.166	0.172	0.182	0.208	0.26	-0.04
270206	A8S32	-2.1	145	0.115	0.122	0.129	0.136	0.155	0.175	0.19	0.257	0.755	0.59	-2.52
270206	A9S42	-3.6	225	0.104	0.11	0.117	0.125	0.146	0.161	0.168	0.195	0.326	0.41	-0.52
270206	A03M2													
270206	A04M2	-3.7	320	0.115	0.122	0.133	0.144	0.167	0.194	0.321	0.754	1.618	0.95	-5.61
270206	A05M2	-4.7	368	0.103	0.108	0.115	0.123	0.14	0.155	0.161	0.17	0.187	0.26	0.03
270206	A06M2	-5.7	435	0.104	0.11	0.117	0.124	0.146	0.17	0.19	0.299	2.947	0.98	-9.30
270206	A08M2	-7.7	523	0.1	0.107	0.114	0.123	0.142	0.158	0.166	0.174	0.195	0.30	0.05
270206	A10M2	-9.7	662	0.11	0.119	0.123	0.131	0.145	0.158	0.162	0.166	0.173	0.21	0.06
100506	A1DU3	+7	0	0.168	0.194	0.214	0.239	0.289	0.542	0.68	0.759	0.845	0.81	-1.56
100506	A2BB3													
100506	A3BE3	+4	18	0.19	0.235	0.277	0.334	0.474	0.704	0.847	1.007	1.214	0.85	-0.10
100506	A4MI3	+2	26	0.156	0.172	0.193	0.213	0.272	0.363	0.443	0.568	0.756	0.68	-0.89
100506	A5SZ3													
100506	A6S13	-1.2	55	0.119	0.128	0.138	0.147	0.173	0.2	0.235	0.436	1.018	0.71	-3.17
100506	A7S23	-1.2	100	0.136	0.152	0.168	0.19	0.262	0.479	0.662	0.832	1.068	0.99	-2.30
100506	A8S33	-1.7	140	0.118	0.125	0.133	0.142	0.167	0.187	0.195	0.207	0.32	0.38	-0.29
100506	A9S43													
100506	A03M3	-2.7	264	0.123	0.132	0.139	0.148	0.171	0.191	0.198	0.204	0.218	0.27	0.07
100506	A04M3	-3.7	298	0.11	0.119	0.127	0.136	0.154	0.17	0.177	0.182	0.188	0.25	0.09
100506	A05M3	-4.7	358	0.111	0.118	0.123	0.129	0.148	0.164	0.169	0.173	0.178	0.23	0.07
100506	A06M3	-5.7	398	0.108	0.115	0.121	0.128	0.145	0.162	0.168	0.172	0.176	0.24	0.06
100506	A08M3	-7.7	512	0.114	0.123	0.129	0.138	0.163	0.184	0.191	0.197	0.209	0.29	0.10
100506	A10M3	-9.7	697	0.108	0.115	0.122	0.129	0.149	0.168	0.174	0.178	0.183	0.25	0.08
070606	A1DU4	+7	0	0.141	0.165	0.183	0.206	0.257	0.325	0.374	0.449	0.54	0.58	-0.23
070606	A2BB4													
070606	A3BE4	+4	18	0.18	0.233	0.263	0.325	0.497	0.649	0.708	0.768	0.838	0.73	1.08
070606	A4MI4	+2	26	0.174	0.202	0.227	0.247	0.34	0.702	0.809	0.957	1.115	0.91	-1.61
070606	A5SZ4													
070606	A6S14	-0.4	55	0.12	0.128	0.134	0.143	0.166	0.196	0.208	0.225	0.281	0.36	-0.18
070606	A7S24	-0.9	100	0.125	0.135	0.142	0.153	0.19	0.25	0.421	0.733	1.14	0.92	-3.73
070606	A8S34	-2.4	180	0.118	0.127	0.133	0.142	0.163	0.195	0.205	0.217	0.352	0.42	-0.52
070606	A9S44	-3.4	220	0.118	0.128	0.14	0.152	0.181	0.208	0.218	0.233	0.378	0.44	-0.34
070606	A03M4													
070606	A04M4													
070606	A05M4	-4.6	343	0.111	0.116	0.122	0.129	0.145	0.163	0.171	0.175	0.183	0.24	0.02
070606	A06M4	-5.6	401	0.111	0.119	0.126	0.135	0.155	0.175	0.182	0.191	0.206	0.28	0.05
070606	A08M4	-7.6	492	0.113	0.121	0.127	0.135	0.155	0.175	0.183	0.188	0.196	0.26	0.06
070606	A10M4	-9.6	658	0.107	0.114	0.121	0.13	0.147	0.162	0.167	0.171	0.176	0.24	0.09
270906	A1DU6	+7	0	0.162	0.181	0.203	0.229	0.292	0.363	0.455	0.595	0.733	0.65	-0.59
270906	A2BB6													

Appendix 3: Grain Size Data Collected in Table Bay

Sampling date	Sample ID	Depth (m to MSL)	Offset from beacon (m)	Grain size (mm)									Sorting	Skew-ness
				D5	D10	D16	D25	D50	D75	D84	D90	D95		
270906	A3BE6	+4	18	0.215	0.268	0.311	0.368	0.519	0.764	0.901	1.016	1.15	0.79	0.11
270906	A4MI6	+2	26	0.292	0.397	0.483	0.592	0.778	0.987	1.108	1.228	1.402	0.68	0.74
270906	A5SZ6													
270906	A6S16	-1.9	55	0.178	0.230	0.290	0.381	0.630	1.050	1.323	1.707	2.743	1.21	-0.54
270906	A7S26	-1.7	80	0.132	0.141	0.148	0.157	0.178	0.203	0.217	0.244	0.308	0.34	-0.23
270906	A8S36	-2.9	140	0.132	0.142	0.151	0.163	0.19	0.221	0.238	0.261	0.377	0.42	-0.35
270906	A9S46	-3.9	190	0.117	0.126	0.135	0.144	0.163	0.181	0.188	0.193	0.21	0.26	0.06
160905	B1DU1	+5	2	0.110	0.129	0.144	0.170	0.239	0.296	0.337	0.396	0.571	0.70	-0.02
160905	B2BB1													
160905	B3BE1	+3	8	0.187	0.216	0.237	0.265	0.309	0.354	0.382	0.416	0.487	0.40	0.07
160905	B4MI1	+2	17	0.215	0.242	0.264	0.294	0.352	0.449	0.539	0.626	0.770	0.56	-0.49
160905	B5SZ1	0	38											
160905	B6S11	-0.7	55	0.139	0.171	0.192	0.225	0.295	0.403	0.489	0.618	0.812	0.76	-0.55
160905	B7s21	-1.5	136	0.128	0.143	0.152	0.166	0.190	0.226	0.328	0.471	0.614	0.65	-1.53
160905	B8s31	-2.5	206	0.125	0.137	0.146	0.158	0.183	0.209	0.279	0.787	1.781	0.87	-5.37
160905	B9S41													
160905	B03M1	-2.5	230	0.111	0.121	0.130	0.143	0.174	0.233	0.317	0.465	0.794	0.79	-2.47
160905	B04M1	-3.5	279	0.108	0.116	0.123	0.134	0.158	0.191	0.240	0.385	0.677	0.68	-2.17
160905	B05M1	-4.5	324	0.112	0.118	0.128	0.137	0.158	0.192	0.233	0.322	0.607	0.62	-1.87
160905	B06M1	-5.5	382	0.110	0.119	0.128	0.140	0.174	0.228	0.279	0.354	0.492	0.64	-1.04
160905	B08M1	-7.5	414	0.105	0.112	0.117	0.124	0.148	0.179	0.195	0.225	0.281	0.42	-0.33
160905	B10M1	-9.5	561	0.094	0.097	0.102	0.108	0.126	0.152	0.165	0.258	0.469	0.56	-1.74
270206	B1DU2	+5	2	0.169	0.214	0.24	0.274	0.334	0.401	0.456	0.55	0.992	0.66	-0.74
270206	B2BB2													
270206	B3BE2	+3	8	0.153	0.174	0.206	0.25	0.341	0.457	0.54	0.639	0.79	0.74	-0.02
270206	B4MI2	+2	17	0.125	0.132	0.142	0.155	0.197	0.245	0.269	0.291	0.333	0.47	-0.06
270206	B5SZ2	0	38	0.114	0.125	0.135	0.15	0.202	0.285	0.325	0.36	0.418	0.63	-0.28
270206	B6S12	-0.9	68	0.119	0.128	0.138	0.153	0.2	0.297	0.425	0.588	0.961	0.91	-2.73
270206	B7S22	-1.4	138	0.118	0.127	0.133	0.141	0.161	0.183	0.195	0.211	0.264	0.33	-0.15
270206	B8S32	-1.9	188	0.114	0.125	0.134	0.152	0.217	0.421	0.591	0.755	0.948	1.04	-2.63
270206	B9S42	-3.4	218	0.106	0.112	0.119	0.13	0.158	0.19	0.23	0.326	0.549	0.63	-1.51
270206	B03M2													
270206	B04M2	-3.9	276	0.11	0.116	0.122	0.13	0.153	0.189	0.21	0.25	0.348	0.47	-0.64
270206	B05M2	-4.9	324	0.104	0.11	0.117	0.127	0.149	0.169	0.176	0.195	0.241	0.35	-0.07
270206	B06M2	-5.9	345	0.108	0.117	0.123	0.131	0.15	0.168	0.176	0.182	0.197	0.27	0.05
270206	B08M2	-7.9	414	0.098	0.106	0.111	0.119	0.136	0.154	0.161	0.17	0.203	0.31	-0.04
270206	B10M2	-9.9	561	0.088	0.093	0.097	0.103	0.12	0.136	0.143	0.147	0.158	0.28	0.04
070606	B1DU4	+5	2	0.174	0.202	0.224	0.249	0.3	0.348	0.366	0.383	0.439	0.40	0.21
070606	B2BB4													
070606	B3BE4	+3	8	0.144	0.156	0.166	0.179	0.21	0.246	0.26	0.266	0.283	0.32	0.07
070606	B4MI4	+2	17	0.172	0.187	0.2	0.218	0.27	0.331	0.352	0.371	0.392	0.40	0.09
070606	B5SZ4	0	38	0.15	0.167	0.183	0.203	0.257	0.299	0.316	0.338	0.38	0.42	0.22

Sampling date	Sample ID	Depth (m to MSL)	Offset from beacon (m)	Grain size (mm)									Sorting	Skew-ness
				D5	D10	D16	D25	D50	D75	D84	D90	D95		
070606	B6S14	0	45	0.153	0.171	0.183	0.204	0.264	0.34	0.375	0.42	0.489	0.54	-0.07
070606	B7S24	-1.5	90	0.123	0.132	0.14	0.151	0.183	0.229	0.264	0.322	0.432	0.53	-0.67
070606	B8S34	-2.5	170	0.109	0.119	0.126	0.136	0.157	0.179	0.196	0.23	0.352	0.44	-0.54
070606	B9S44	-3.5	210	0.118	0.124	0.131	0.137	0.155	0.174	0.19	0.199	0.217	0.28	-0.05
070606	B03M4													
070606	B04M4													
070606	B05M4	-4.8	276	0.111	0.12	0.127	0.135	0.154	0.175	0.184	0.193	0.202	0.28	0.04
070606	B06M4	-5.8	329	0.115	0.125	0.133	0.144	0.17	0.194	0.203	0.22	0.26	0.35	0.00
070606	B08M4	-7.8	428	0.105	0.115	0.122	0.131	0.15	0.168	0.177	0.189	0.196	0.28	0.07
070606	B10M4	-9.8	562	0.094	0.102	0.107	0.115	0.133	0.149	0.158	0.164	0.169	0.28	0.08
160905	C1DU1	+4	0	0.147	0.163	0.171	0.184	0.212	0.239	0.254	0.276	0.327	0.33	-0.04
160905	C2BB1	+3	5	0.199	0.224	0.245	0.268	0.328	0.404	0.444	0.479	0.547	0.46	-0.02
160905	C3BE1	+2	18	0.217	0.236	0.26	0.284	0.356	0.466	0.546	0.621	0.719	0.56	-0.35
160905	C4MI1	+1	30	0.114	0.123	0.131	0.14	0.162	0.184	0.197	0.22	0.252	0.34	-0.07
160905	C5SZ1	0	53	0.109	0.117	0.124	0.137	0.169	0.228	0.324	0.404	0.505	0.72	-1.39
160905	C6S11	-0.85	78	0.103	0.109	0.116	0.124	0.146	0.173	0.215	0.292	0.463	0.58	-1.36
160905	C7S21	-1.35	136	0.126	0.134	0.144	0.152	0.172	0.193	0.203	0.23	0.344	0.37	-0.39
160905	C8S31	-2.35	198	0.124	0.133	0.142	0.15	0.167	0.181	0.188	0.199	0.237	0.26	-0.02
160905	C9S41													
160905	C03M1	-2.4	232	0.113	0.119	0.124	0.131	0.16	0.203	0.287	0.431	0.599	0.70	-1.98
160905	C04M1	-3.4	274	0.11	0.116	0.124	0.131	0.155	0.181	0.207	0.268	0.374	0.48	-0.72
160905	C05M1	-4.4	313	0.11	0.116	0.121	0.129	0.146	0.165	0.176	0.201	0.267	0.35	-0.30
160905	C06M1	-5.4	328	0.11	0.117	0.124	0.132	0.15	0.164	0.171	0.177	0.199	0.26	0.04
160905	C08M1	-7.4	436	0.099	0.104	0.11	0.116	0.132	0.145	0.15	0.154	0.162	0.23	0.06
160905	C10M1	-9.4	531	0.101	0.106	0.109	0.115	0.127	0.138	0.143	0.151	0.161	0.21	0.01
270206	C1DU2	+4.0	0	0.152	0.168	0.182	0.199	0.249	0.303	0.329	0.363	0.459	0.48	-0.11
270206	C2BB2	+3.0	5	0.163	0.186	0.205	0.225	0.285	0.424	0.517	0.608	0.717	0.69	-0.82
270206	C3BE2	+2.0	18	0.135	0.143	0.15	0.162	0.19	0.219	0.231	0.242	0.272	0.32	0.01
270206	C4MI2	+1.0	30	0.124	0.136	0.145	0.155	0.18	0.208	0.226	0.245	0.284	0.36	-0.08
270206	C5SZ2	0.0	53	0.129	0.142	0.153	0.171	0.218	0.394	0.52	0.624	0.795	0.88	-2.11
270206	C6S12	-0.5	83	0.125	0.133	0.138	0.145	0.16	0.178	0.187	0.196	0.262	0.29	-0.19
270206	C7S22	-2.0	143	0.121	0.13	0.137	0.146	0.161	0.177	0.184	0.192	0.225	0.26	-0.02
270206	C8S32	-3.0	223	0.12	0.127	0.134	0.141	0.16	0.183	0.192	0.206	0.306	0.35	-0.35
270206	C9S42													
270206	C03M2													
270206	C04M2	-4.0	306	0.121	0.133	0.143	0.156	0.178	0.208	0.265	0.408	0.641	0.62	-1.67
270206	C05M2	-5.0	313	0.1	0.11	0.118	0.129	0.156	0.184	0.208	0.276	0.462	0.57	-1.03
270206	C06M2	-6.0	328	0.108	0.118	0.127	0.137	0.16	0.184	0.194	0.212	0.281	0.38	-0.15
270206	C08M2	-8.0	436	0.1	0.106	0.11	0.118	0.132	0.147	0.152	0.156	0.164	0.24	0.05
100506	C1DU3	+4	0	0.136	0.146	0.157	0.17	0.202	0.237	0.255	0.272	0.299	0.36	0.01
100506	C2BB3													
100506	C3BE3	+2	18	0.132	0.141	0.15	0.158	0.176	0.194	0.203	0.211	0.23	0.24	0.02

Sampling date	Sample ID	Depth (m to MSL)	Offset from beacon (m)	Grain size (mm)									Sorting	Skew-ness
				D5	D10	D16	D25	D50	D75	D84	D90	D95		
100506	C4MI3	+1	30	0.121	0.131	0.138	0.149	0.17	0.19	0.196	0.202	0.218	0.27	0.08
100506	C5SZ3	0	53	0.129	0.139	0.149	0.163	0.2	0.241	0.265	0.307	0.355	0.45	-0.13
100506	C6S13	-0.5	83	0.126	0.136	0.146	0.157	0.187	0.233	0.267	0.344	0.471	0.53	-0.79
100506	C7S23	-1.5	133	0.126	0.137	0.146	0.159	0.193	0.254	0.298	0.373	0.474	0.58	-0.77
100506	C8S33	-2.5	173	0.124	0.136	0.145	0.158	0.195	0.24	0.325	0.49	0.711	0.71	-1.71
100506	C9S43													
100506	C03M3	-2.6	245	0.124	0.134	0.143	0.155	0.183	0.22	0.284	0.427	0.676	0.66	-1.76
100506	C04M3	-3.6	271	0.125	0.132	0.139	0.15	0.178	0.211	0.227	0.26	0.366	0.44	-0.41
100506	C05M3	-4.6	318	0.118	0.126	0.133	0.142	0.161	0.181	0.189	0.194	0.2	0.25	0.06
100506	C06M3	-5.6	331	0.11	0.118	0.125	0.132	0.149	0.163	0.168	0.174	0.191	0.24	0.05
100506	C08M3	-7.6	434	0.104	0.111	0.118	0.124	0.139	0.151	0.156	0.16	0.163	0.21	0.08
070606	C1DU4	+4	0	0.127	0.141	0.152	0.167	0.199	0.233	0.251	0.264	0.289	0.38	0.08
070606	C2BB4	+3	5											
070606	C3BE4	+2	18	0.124	0.132	0.14	0.149	0.17	0.187	0.194	0.199	0.205	0.24	0.09
070606	C4MI4	+1	30	0.133	0.143	0.151	0.161	0.189	0.226	0.241	0.25	0.265	0.33	0.00
070606	C5SZ4	0	53	0.128	0.137	0.147	0.157	0.183	0.209	0.218	0.224	0.246	0.30	0.06
070606	C6S14	-0.2	73	0.132	0.142	0.151	0.163	0.191	0.222	0.24	0.282	0.381	0.42	-0.35
070606	C7S24	-1.2	103	0.133	0.142	0.149	0.161	0.191	0.229	0.249	0.277	0.39	0.44	-0.40
070606	C8S34	-2.7	153	0.122	0.132	0.141	0.151	0.174	0.206	0.217	0.227	0.285	0.36	-0.13
070606	C9S44	-3.5	203	0.13	0.139	0.145	0.155	0.183	0.222	0.252	0.316	0.426	0.48	-0.67
070606	C03M4													
070606	C04M4													
070606	C05M4	-4.9	282	0.114	0.124	0.132	0.139	0.158	0.174	0.181	0.186	0.197	0.25	0.07
070606	C06M4	-5.9	335	0.107	0.115	0.122	0.131	0.149	0.17	0.174	0.18	0.19	0.27	0.07
070606	C08M4	-7.9	439	0.109	0.113	0.121	0.128	0.144	0.157	0.164	0.169	0.182	0.23	0.04
250606	C1DU5	+4	0	0.159	0.174	0.189	0.207	0.248	0.284	0.294	0.303	0.316	0.32	0.19
250606	C2BB5													
250606	C3BE5	+2	18	0.141	0.157	0.169	0.183	0.219	0.255	0.271	0.288	0.311	0.36	0.10
250606	C4MI5	+1	30	0.138	0.149	0.161	0.174	0.214	0.257	0.275	0.293	0.321	0.40	0.05
250606	C5SZ5	0	53	0.134	0.149	0.162	0.176	0.224	0.314	0.35	0.384	0.424	0.55	-0.25
250606	C6S15	-1	93	0.127	0.135	0.143	0.151	0.177	0.2	0.21	0.233	0.306	0.35	-0.18
250606	C7S25	-2	153	0.135	0.144	0.155	0.173	0.235	0.34	0.421	0.499	0.628	0.73	-0.86
250606	C8S35	-2	178	0.122	0.131	0.139	0.15	0.181	0.224	0.25	0.378	0.527	0.56	-1.06
250606	C9S45	-3.5	203	0.125	0.135	0.141	0.15	0.17	0.189	0.196	0.203	0.225	0.26	0.03
270906	C1DU6	+4	0	0.162	0.18	0.2	0.221	0.276	0.332	0.368	0.412	0.477	0.48	0.01
270906	C2BB6													
270906	C3BE6	+2	18	0.178	0.203	0.221	0.244	0.303	0.386	0.449	0.5	0.596	0.55	-0.24
270906	C4MI6	+1	30	0.328	0.476	0.615	0.758	1.008	1.257	1.372	1.489	1.673	0.68	1.20
270906	C5SZ6													
270906	C6S16	-0.6	68	0.133	0.143	0.15	0.162	0.188	0.232	0.267	0.348	0.559	0.55	-1.19
270906	C7S26	-0.9	103	0.133	0.142	0.152	0.163	0.186	0.213	0.274	0.361	0.485	0.52	-0.95
270906	C8S36	-2.8	173	0.132	0.142	0.152	0.164	0.189	0.217	0.261	0.366	0.652	0.58	-1.52

Sampling date	Sample ID	Depth (m to MSL)	Offset from beacon (m)	Grain size (mm)									Sorting	Skew-ness
				D5	D10	D16	D25	D50	D75	D84	D90	D95		
270906	C9S46	-4.3	213	0.129	0.136	0.142	0.149	0.166	0.183	0.189	0.196	0.222	0.23	-0.01
160905	D1DU1	+2.5	0	0.131	0.139	0.145	0.154	0.175	0.191	0.197	0.204	0.221	0.24	0.05
160905	D2BB1													
160905	D3BE1	+1.8	10	0.136	0.144	0.15	0.159	0.174	0.189	0.199	0.211	0.224	0.22	0.00
160905	D4MI1	+1	27	0.105	0.114	0.12	0.128	0.149	0.166	0.174	0.187	0.209	0.30	0.03
160905	D5SZ1	0	67	0.116	0.128	0.136	0.15	0.195	0.274	0.37	0.485	0.646	0.77	-1.50
160905	D6S11	-0.6	93	0.106	0.111	0.116	0.123	0.144	0.17	0.183	0.218	0.358	0.46	-0.78
160905	D7S21	-1.6	136	0.122	0.131	0.138	0.149	0.177	0.209	0.255	0.38	0.563	0.59	-1.32
160905	D8S31	-3.1	213	0.12	0.13	0.138	0.15	0.176	0.205	0.264	0.378	0.602	0.62	-1.53
160905	D9S41													
160905	D03M1	-2.3	227	0.116	0.122	0.129	0.137	0.154	0.175	0.203	0.274	0.413	0.47	-0.98
160905	D04M1	-3.3	273	0.119	0.125	0.132	0.142	0.168	0.194	0.226	0.268	0.33	0.44	-0.38
160905	D05M1													
160905	D06M1	-5.3	311	0.117	0.122	0.127	0.133	0.148	0.162	0.169	0.182	0.228	0.26	-0.13
160905	D08M1													
160905	D10M1	-9.3	649	0.087	0.089	0.092	0.096	0.107	0.117	0.122	0.127	0.143	0.22	-0.04
270206	D1DU2	+2.5	0	0.128	0.138	0.145	0.152	0.172	0.192	0.201	0.209	0.233	0.26	0.00
270206	D2BB2	+2	5	0.13	0.138	0.144	0.151	0.169	0.191	0.2	0.208	0.223	0.25	-0.01
270206	D3BE2	+1.8	10	0.125	0.133	0.14	0.147	0.163	0.179	0.184	0.188	0.194	0.20	0.05
270206	D4MI2	+1	27	0.121	0.129	0.136	0.143	0.161	0.184	0.192	0.202	0.226	0.27	-0.04
270206	D5SZ2	0	67	0.122	0.132	0.141	0.154	0.195	0.253	0.34	0.437	0.596	0.70	-1.28
270206	D6S12	-0.5	108	0.122	0.132	0.14	0.149	0.174	0.197	0.232	0.311	0.46	0.50	-0.89
270206	D7S22	-1.8	168	0.118	0.128	0.135	0.143	0.169	0.202	0.271	0.385	0.557	0.62	-1.53
270206	D8S32	-3	248	0.123	0.13	0.137	0.146	0.165	0.18	0.186	0.198	0.217	0.25	0.03
270206	D9S42													
270206	D03M2													
270206	D04M2	-4.0	273	0.098	0.104	0.111	0.118	0.135	0.155	0.165	0.176	0.199	0.31	-0.05
270206	D05M2	-5.0	366	0.097	0.107	0.115	0.124	0.148	0.17	0.183	0.219	0.322	0.46	-0.42
270206	D06M2													
270206	D08M2	-8.0	520	0.091	0.099	0.103	0.111	0.127	0.14	0.147	0.153	0.173	0.28	0.04
070606	D04M4	-4	266	0.11	0.118	0.124	0.131	0.148	0.163	0.17	0.175	0.181	0.23	0.06
070606	D05M4	-5	297	0.113	0.121	0.13	0.139	0.159	0.181	0.189	0.194	0.212	0.29	0.05
070606	D06M4	-6	377	0.091	0.104	0.113	0.124	0.14	0.156	0.161	0.165	0.17	0.28	0.18
070606	D08M4	-8	482	0.102	0.109	0.114	0.121	0.139	0.159	0.164	0.17	0.187	0.28	0.02